Chapter I

Introduction

History of mouse adenovirus and relationship to human adenovirus

Mouse adenovirus type 1 (MAV-1) is a member of the *Adenoviridae* family of viruses. It was discovered in 1960 by Hartley and Rowe in their attempt to grow Friend mouse leukemia virus in tissue culture (97). The new virus was identified as an adenovirus based upon seroreactivity (97, 136). MAV-1 infection of suckling mice is typically fatal, even at low infectious doses (97). Infection of adult mice can result in signs of disease and death depending on the dose of virus and strain of mouse used (220, 221).

MAV-1 is similar to human adenovirus and other members of the adenovirus family in both genome and structure (Figure 1.1). The non-enveloped, double stranded DNA genome of MAV-1 is 30,944 bp, similar to the human adenoviruses, which range from 34,125 bp (Ad12) to 36,001 bp (Ad1) (138). MAV-1 shares many open reading frames with Ad2 and Ad5. Among these shared open reading frames there is significant sequence homology, particularly in those for the DNA polymerase and polypeptide III (penton base). However, significant differences in genome sequences are found among the adenoviruses (human and animal) in early region 3 (E3) (63, 76, 190). For MAV-1 E3 there is no significant homology between the MAV-1 sequence and any known

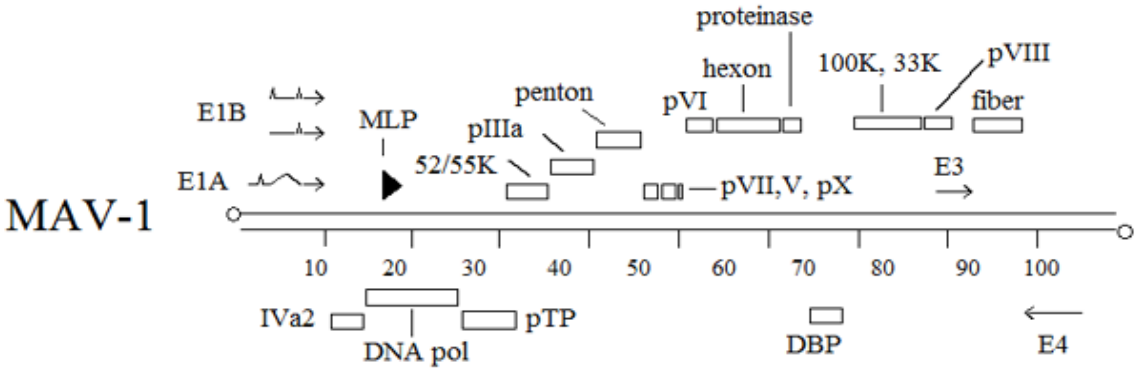

Figure 1.1. Genomic organization of MAV-1. From Spindler et al, 2007 (215).

protein (22, 190). The MAV-1 early region 1A (E1A) protein, an important transcription factor that helps enable viral replication (68), has little overall homology to E1A of human adenoviruses (hAds) but has up to 40% similarity in limited regions (16). Sera from animals exposed to hAd hexon protein recognizes mouse adenovirus particles, indicating that exposed capsid domains are antigenically similar (136).

Mouse adenovirus as an animal model for adenovirus infection

Because adenoviruses cause species-specific infections, it is difficult to study human adenovirus pathogenesis in an animal host. Using MAV-1 infection of mice, we can study virus infection of its natural host in a system that can be manipulated using mutant viruses or mutant mice.

Infection with MAV-1 can result in a range of disease depending on the type and dose of virus given as well as the strain of mouse infected (94, 220). Susceptible mice infected with MAV-1 have highest viral loads in the brain, spinal cord and spleen and succumb to virus infection after developing encephalitis or encephalomyelitis (42, 113, 159). MAV-1 replicates *in vivo* in endothelial cells (113) and macrophages (113) and Spindler et al., unpublished data), and infectious virus is found in tissues throughout the mouse. Positive *in situ* hybridization staining has also been seen in respiratory epithelial cells after intranasal infection (258), suggesting an additional cell type that supports virus replication.

While human adenoviruses primarily infect epithelial cells, causing upper respiratory tract infections, gastroenteritis, and conjunctivitis in immunocompetent patients, infection of immunocompromised patients is much different. Patients who are

undergoing immunosuppressive therapy or who are otherwise immunocompromised can develop severe and disseminated adenovirus infections (117, 197; reviewed in 150) similar to MAV-1 infection. In pediatric bone marrow transplant patients who develop disseminated adenovirus infections, the mortality rate has been reported to be as high as 60% (250). Encephalitis is a rare result of disseminated human adenovirus infection, but it has a high mortality rate (64, 86, 95).

MAV-1 causes a persistent infection, as observed by the shedding of infectious MAV-1 in the urine up to 11 months after infection (195). Similarly, MAV-1 viral DNA can be detected in kidneys, brains, spleens, and prefemoral lymph nodes of infected mice up to 55 weeks after infection (216). Human adenoviruses are also capable of persistent infections. hAd DNA, but rarely infectious virus, was found in 79% of samples analyzed by Garnett in T-lymphocytes from immunocompetent patients isolated from tonsillectomy or adenoidectomy tissue (84). Furthermore, group C adenovirus was found in 76% of lymphocytes from healthy adults including T cells and B cells, and 1-2% of these lymphocytes contained a high number of adenovirus DNA sequences (106). Immunocompromised patients, including transplant recipients and AIDS patients, are at increased risk of adenovirus infection, and their infection status has been studied extensively (108, 129, 278). Adenovirus has been found in the urine of 12% of AIDS patients (109), though it is rarely found in the urine of immunocompetent patients. Virus has also been observed in stool and various tissues of AIDS and other immunocompromised patients (75, 103). Thus despite differences in the site of infection and dissemination between MAV-1 and human adenoviruses, these viruses share the

ability to persist in the infected host and may share strategies for achieving these persistent infections.

Mouse adenovirus and host response to infection

Infection of suckling mice with MAV-1 is fatal, whereas infected adult mice often survive infection (94, 97, 220). Maternal antibodies to MAV-1 are able to protect suckling mice (97). These results indicate that the host immune response is an important contributor to the outcome of MAV-1 infection. C3H/HeJ mice are normally resistant to MAV-1 infection, but upon sublethal exposure to gamma irradiation they become susceptible to infection with a low 50% lethal dose (LD_{50}) (220). This further indicates a role for the host immune response in the control of MAV-1 infection.

Infection of various immunodeficient mice with MAV-1 has revealed a contribution for several immune cell types in responding to and controlling infection. Mice deficient in T cells survive acute infection better than wild type mice, with no clinical signs of disease (159). Furthermore, T cell deficient mice show no inflammation in their brains at 8 days post infection, a time of peak viral replication and maximum inflammatory response (37, 159, 220). Additional studies showed that mice lacking perforin or major histocompatability complex (MHC) class I but not MHC class II genes are also resistant to acute signs of disease while failing to develop inflammation in the brain (159). These data suggest that cytotoxic T cells contribute to the presence of other inflammatory cells in the brain after MAV-1 infection and that antigen presentation and cytolytic T cell activity are important for eventual clearance of virus. Despite the resistance of T cell-deficient mice to acute infection, they fail to clear MAV-1 infection,

and they die with high viral loads 8-12 weeks post infection. The presence of either TCRα T cells, $CD4^+$ or $CD8^+$ T cells is enough to protect from the long term effects of MAV-1 infection.

Humoral immunity is also important for resistance to and survival of MAV-1 infection. SCID mice, which lack functional T cells and B cells, and RAG knockout mice, which are deficient in mature T cells and B cells, are highly susceptible to MAV-1 infection (42, 141, 160). MAV-1 infection of SCID mice results in disease that resembles human Reye syndrome, with hepatic tissue damage (180). Bruton's tyrosine kinase-deficient mice have reduced serum immunoglobulin, conventional B cells, and peritoneal B-1 cells compared to wild type mice (124, 125). These mice normally succumb to MAV-1 infection at early times post-infection (160). Treatment of Bruton's tyrosine kinase-deficient mice with serum from MAV-1-infected wild type mice protects against the lethal effects of infection. Analysis of the protective serum showed that production of early T cell-independent antiviral IgM is important for protection from MAV-1 infection (160).

There is also a role for the innate immune response in MAV-1 infection. MAV-1 infection causes an increase in cytokine and chemokine production (42, 257). MAV-1 is resistant to type I interferon (IFN) *in vitro* (114). However, IFN α/β has been shown to have some role in protecting from MAV-1 infection *in vivo* because mice deficient in the receptor for IFN α/β are more susceptible to MAV-1 infection than wild type controls (Ashley and Spindler, unpublished data). These data indicate that IFN α/β is likely to be important for paracrine signaling in response to MAV-1 infection to activate components of the immune response. hAd E1A is able to prevent activation of IFN-inducible genes

and thus allows infected cells to avoid the antiviral response (115, 142, 192). Similarly, MAV-1 E1A may play a role in protecting MAV-1 from the antiviral effects of IFN-α treatment in both tissue culture and *in vivo* infection (114, Moore and Spindler, unpublished data).

Recent work in our lab suggests that MAV-1 replicates in macrophages, because E3 mRNA is present in peritoneal macrophages of infected mice (Ashley and Spindler, unpublished data). There is also preliminary evidence to suggest that MAV-1 may replicate in dendritic cells. No role is known for either of these cell types in response to MAV-1 infection at this time, but possible roles could include the early response to infection or dissemination of the virus throughout the host. In sum, it is currently known that elements of both innate and adaptive immune responses are involved in control of MAV-1 infection. Furthermore, while T cells are required for clearance of MAV-1 from brain and spleen tissues, they also cause acute immunopathology in infected animals (159).

E3 proteins and immunomodulation by viruses

E3 genes from human and other adenovirus species encode a number of gene products through use of alternative mRNA processing pathways and alternate 3' ends (Figure 1.2). The number and function of the E3 proteins varies among adenovirus species and subspecies, but to date all of them whose function is known play a role in modulating or evading the host immune response. MAV-1 produces three E3 transcripts that share 5' and 3' ends and differ due to alternative splicing between the second and third exons (Figure 1.3). These transcripts are predicted to encode three different

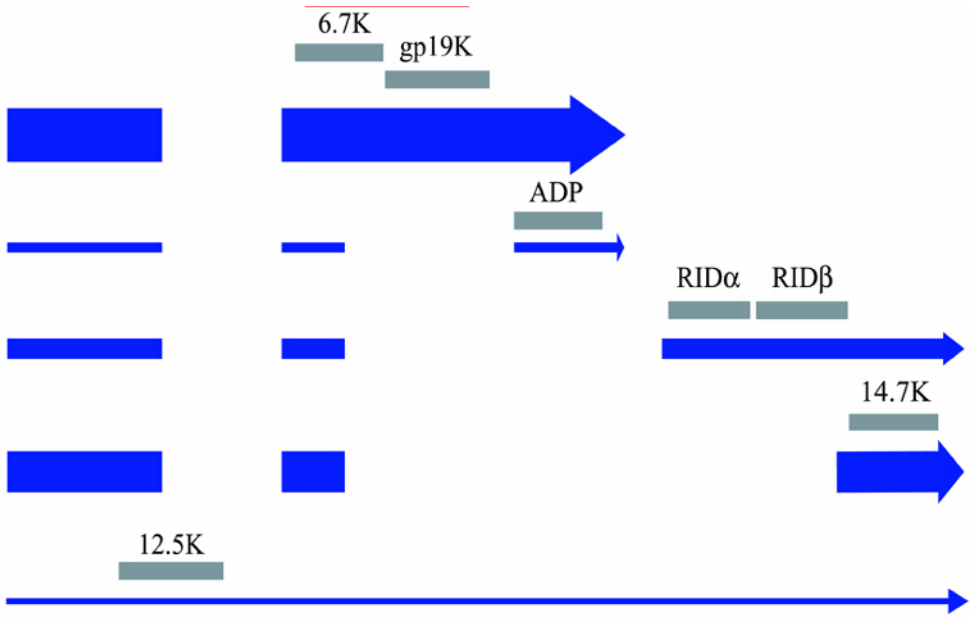

Figure 1.2. Ad5 E3 transcripts. E3 mRNAs are represented by blue lines; width of the line indicates the abundance of the mRNA. Gray bars indicate E3 protein products. Modified from Toth et al., 2003 (236).

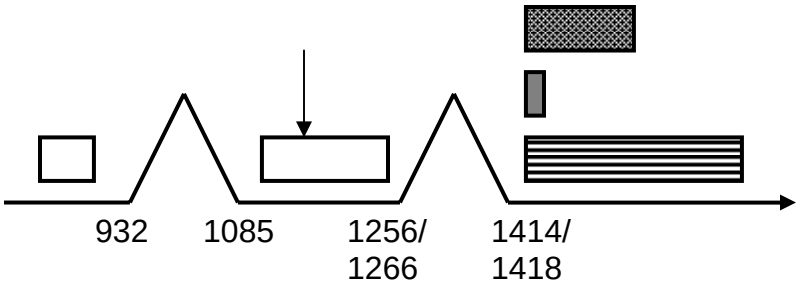

Figure 1.3. MAV-1 E3 transcripts. Alternate third exons are indicated by shading, stripes and stippling. Common coding regions are indicated by white bars. Numbers indicate nucleotides at beginning and end of exons. Modified from Beard and Spindler, 1996 (20).

proteins that are identical at the N terminus and different at the C terminus (21, 22, 37). The MAV-1 E3 proteins are dispensable for viral growth *in vitro* and *in vivo* but contribute to pathogenesis *in vivo* (22, 37). Mutant viruses capable of expressing only one of each of the E3 mRNAs and an E3 null virus have been produced, and they replicate like wild type MAV-1 both *in vitro* and *in vivo* (22, 37). All of the E3-deleted MAV-1 mutants showed reduced pathogenicity compared to wild type virus in an LD_{50} assay, indicating that the MAV-1 E3 transcripts are important for pathogenesis. Mutant virus *dl*E303 expresses only class 1 E3 (also known as E3gp11k) and has an LD_{50} over 100-fold higher than wild type MAV-1 in outbred Swiss mice (22). Viruses *dl*E307 and *dl*E309 express only class 2 or class 3 E3, respectively. The LD_{50}s of these viruses are 1000-10,000 times greater than that of wild type MAV-1. These three viruses (*dl*E303, 307 and 309) were created by replacing the E3 genome sequence with the sequence from a cDNA for each of the three E3 mRNAs. An E3 null virus, *pm*E314, was created by creating stop codons in all three E3 reading frames in the region surrounding the signal sequence cleavage site (37). This virus has an LD_{50} that is 5-6 log units higher than that of wild type MAV-1. In sum, these results indicate that each of the E3 gene products plays a role in pathogenesis because each single E3 mRNA-expressing mutant has reduced pathogenicity compared to wild type infection, and the overall activity of the E3 transcripts may be synergistic.

The function of the MAV-1 E3 proteins has yet to be determined. Investigation has shown that while there are three MAV-1 E3 transcripts, only E3 class 1 or E3gp11k is expressed after infection with wild type virus. E3gp11k is an 11 kDa glycoprotein that

localizes to the endoplasmic reticulum and biochemical analysis shows that it is a peripheral membrane protein (23). E3gp11k has a predicted signal sequence that is cleaved after expression, resulting in a protein with a core molecular weight of 11 kDa, though after glycosylation it migrates at 14 kDa on SDS-PAGE gels.

In vivo infections with an MAV-1 null for E3 expression, *pm*E314, have provided the only evidence regarding the function of the MAV-1 E3 proteins. Mice infected with wild type MAV-1 show inflammation in the brain and spinal cord during acute infection; inflammation is lacking in mice infected with the E3 null virus (37). This difference in inflammatory response is seen despite equal viral loads found in brains of animals infected with wild type or E3 mutant virus. Thus the only clue to the function of the MAV-1 E3 proteins is that they somehow stimulate the host inflammatory response after infection. While it is unusual for a virus to carry the gene for a protein that stimulates inflammation in the infected host, it could be to the virus's advantage in a case like MAV-1 where the virus also replicates in inflammatory cells. By MAV-1 stimulating recruitment of inflammatory cells to the site of infection it could cause increased spread of virus through infected macrophages. Further studies examining the role of MAV-1 E3 in pathogenesis in relation to MAV-1-induced encephalitis are discussed in Chapters 3 and 4 of this thesis.

While the function of the MAV-1 E3 proteins is unknown, extensive research has been performed to determine the role of the human adenovirus E3 proteins. The human adenovirus E3-gp19k protein blocks Major Histocompatability Complex Class I (MHC class I) antigen presentation by retaining the MHC class I heavy chain in the endoplasmic reticulum (33). Through this action, virally infected cells are able to evade detection by

cytotoxic T cells. E3-gp19k is not able to restrict presentation of all MHC class I alleles, but it is able to delay presentation of those alleles that it cannot bind by binding to the transporter associated with antigen processing (TAP) to inhibit tapasin and block peptide loading onto the major histocompatability complex (25). Furthermore, hAd-infected cells are able to evade detection by natural killer cells by decreasing surface expression of NKG2D ligands (157). This occurs by E3-gp19K promoting retention of the MHC class I chain-related proteins A and B in the endoplasmic reticulum. The exact mechanism by which this occurs is not known.

The human adenovirus E3-14.7K protein also functions to block the host immune response to viral infection. It inhibits tumor necrosis factor-α (TNF-α) -mediated apoptosis by interacting with proteins downstream in the TNF-α signaling pathway including FIP-2 (143, 151). Studies have shown that the E3-14.7K protein restricts ligand-mediated internalization of the TNF receptor. TNF-induced apoptosis occurs after the TNF receptor binds to TNF: the TNF receptor-associated death domain (TRADD), Fas-associated death domain (FADD), and caspase-8 all co-localize with the death domain of TNF receptor 1 (TNFR1) and establish the death-inducing signaling complex (DISC) (reviewed in 249). E3-14.7K inhibits apoptosis of infected cells by inhibiting TNFR1 internalization after ligand binding and stopping formation of the DISC complex (205). The E3-14K block of TNFR1 internalization is due to failure of the endocytic machinery to properly assemble, thus preventing endocytosis.

The TNF-α response to adenovirus infection is also blocked by a complex of two proteins, E3-10.4/14.5K, also known as the RID α/β complex, which downregulates surface expression of TNFR1 and Fas ligand receptor (44, 233). This downregulation

occurs through increased clathrin-mediated endocytosis, which results in decreased expression of the TNF receptor, thus allowing infected cells to avoid TNF-mediated apoptosis.

One human adenovirus E3 protein, E3-11.6K, also known as the adenovirus death protein, is synthesized primarily late in infection and promotes apoptosis (62, 234). While this action is opposite in nature to the immune evasion effects mediated by the other adenovirus E3 proteins, it serves a very useful purpose in the viral life cycle. By promoting apoptosis, the adenovirus death protein allows for efficient cell lysis and spread of newly synthesized virus particles. Mutant hAds that lack the adenovirus death protein replicate like wild type virus but have delayed cell lysis and form small plaques.

Study of the E3 proteins from other species of adenovirus has thus far been limited and those studies that have been performed have primarily focused on designing viral vectors (239). Transcription mapping and/or sequence analysis of the bovine, canine, and porcine adenovirus E3 coding regions have revealed that the E3 coding regions of animal adenoviruses contain unique sequences as well as ORFs with homology to known E3 genes (165, 191, 281). Bovine adenovirus-3 has been shown to contain a protein, 121R, with homology to the hAd-E3 14.7K protein (279). Cells infected with hAd5 deleted of E3-14.7K are susceptible to TNF-mediated cytolysis, but cells infected with a recombinant virus containing the bovine adenovirus-3 121R protein are resistant to TNF, indicating that this protein is a functional homolog for human adenovirus E3-14.7K. Analysis of a porcine adenovirus E3 region revealed ORFs with sequence similarity to ORFs of both human and bovine adenoviruses (239), though study of the putative proteins has not yet been reported. While the MAV-1 E3 coding region has been

sequenced and transcription mapped as described above, the MAV-1 E3 coding region has only very minor homology with human E3 genes and MAV-1 E3gp11k has no homology to any known proteins.

Structure and formation of the blood brain barrier

Because MAV-1 causes encephalitis and neurological signs of disease, we investigated the possibility that MAV-1 infection causes changes in the blood brain barrier (BBB). These results are presented in Chapter 3. The BBB is composed of endothelial and supporting cells, and it functions to regulate access from the blood to the tissues of the central nervous system (CNS) (Figure 1.4). Paul Ehrlich first showed experimental evidence of the BBB by observing that dyes injected into the circulatory system are able to stain all organs except the brain and spinal cord (65). Brain microvascular endothelial cells differ from peripheral endothelial cells in their barrier properties. Endothelial cells in the brain have reduced endocytic activity to better regulate access to CNS tissue, and unlike other endothelial cells, they form tight intercellular bonds composed of tight junctions, gap junctions and adhesion junctions (99). The endothelial cells that form the physical barrier of the BBB are supported by astrocytes, pericytes, neurons and the extracellular matrix. Many studies have shown that brain endothelial cells lose their barrier properties in the absence of the support structure found in the brain (228, reviewed in 196). In particular, astrocytes provide critical support, at least partially through secretion of unknown factors, for maintenance of brain endothelial cell barrier properties (268).

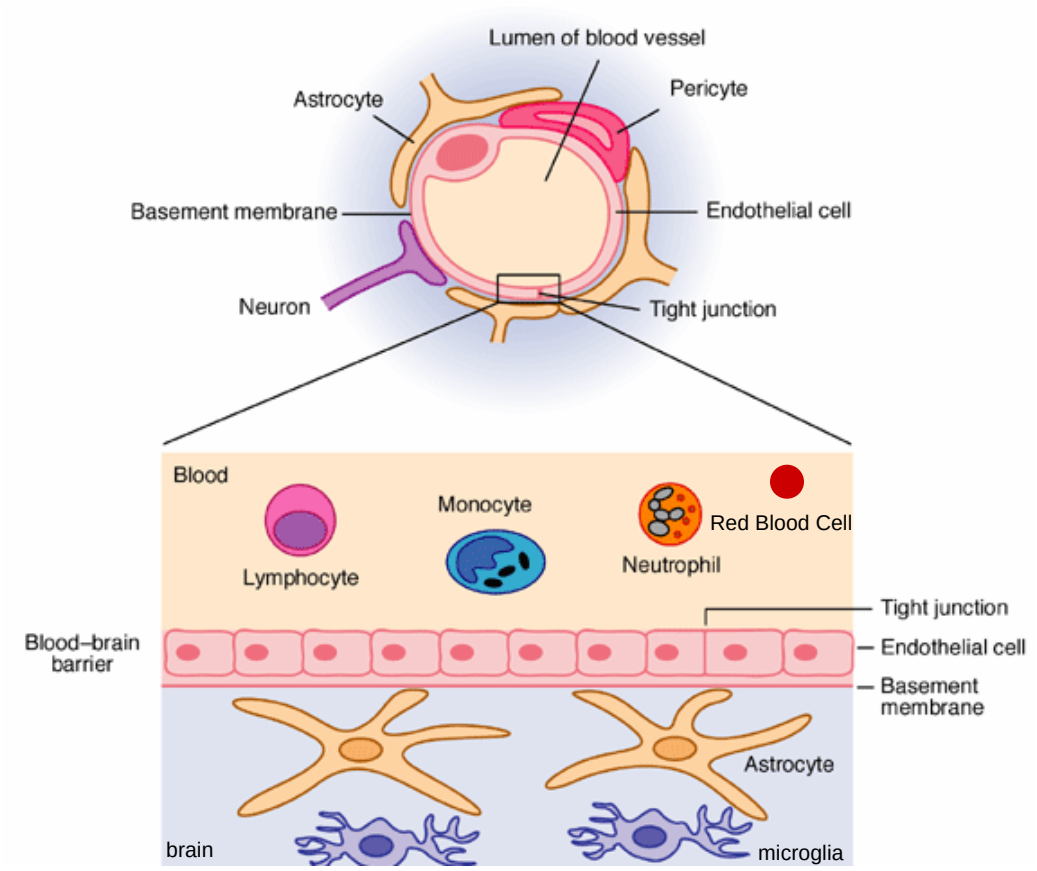

Figure 1.4. The blood–brain barrier (BBB). Cross section of a blood vessel in the brain. Modified from Francis et al, 2003 (78).

Surrogate methods for measuring endothelial cell barrier properties *in vitro* have been developed to aid in studies of the BBB. Fully functioning brain microvascular endothelial cells have a high electrical resistance and impede the ability of current to cross a monolayer of cells (56). Thus measurement of electrical resistance gives an indication of the integrity of the endothelial cell monolayer. A second method of assessing barrier properties is to measure the ability of soluble dyes or inflammatory cells to traffic through an endothelial cell monolayer. Dye permeability is restricted in cell cultures maintaining barrier properties (26). *In vivo*, BBB permeability can be measured by the ability of certain dyes to access and stain brain tissues. Evans blue dye (269) and sodium fluorescein can be used to determine BBB permeability, though they have different sensitivities. Sodium fluorescein is a very small marker (376 daltons) and is largely unbound when injected into mice. In contrast, Evans blue dye is somewhat larger (960 daltons), and after injection it is almost completely bound to albumin. The amount of dye in the brain can be quantitated using either Evans blue or sodium fluorescein (179, 273), though sodium fluorescein is more sensitive.

Proper formation of tight junctions between endothelial cells is essential for maintaining the endothelial cell barrier properties of the BBB. Tight junction (TJ) proteins include members of the claudin family, occludin, junctional adhesion molecules (JAMs) and members of the membrane-associated guanylate kinase-like (MAGUK) homolog family such as zonula occludens protein 1 (ZO-1) (Figure 1.5). The JAMS, claudins and occludin are transmembrane proteins found at the plasma membrane. These proteins work together to form a tight network of endothelial cells to seal the BBB (144). The zonula occludens proteins are peripheral membrane proteins that connect the

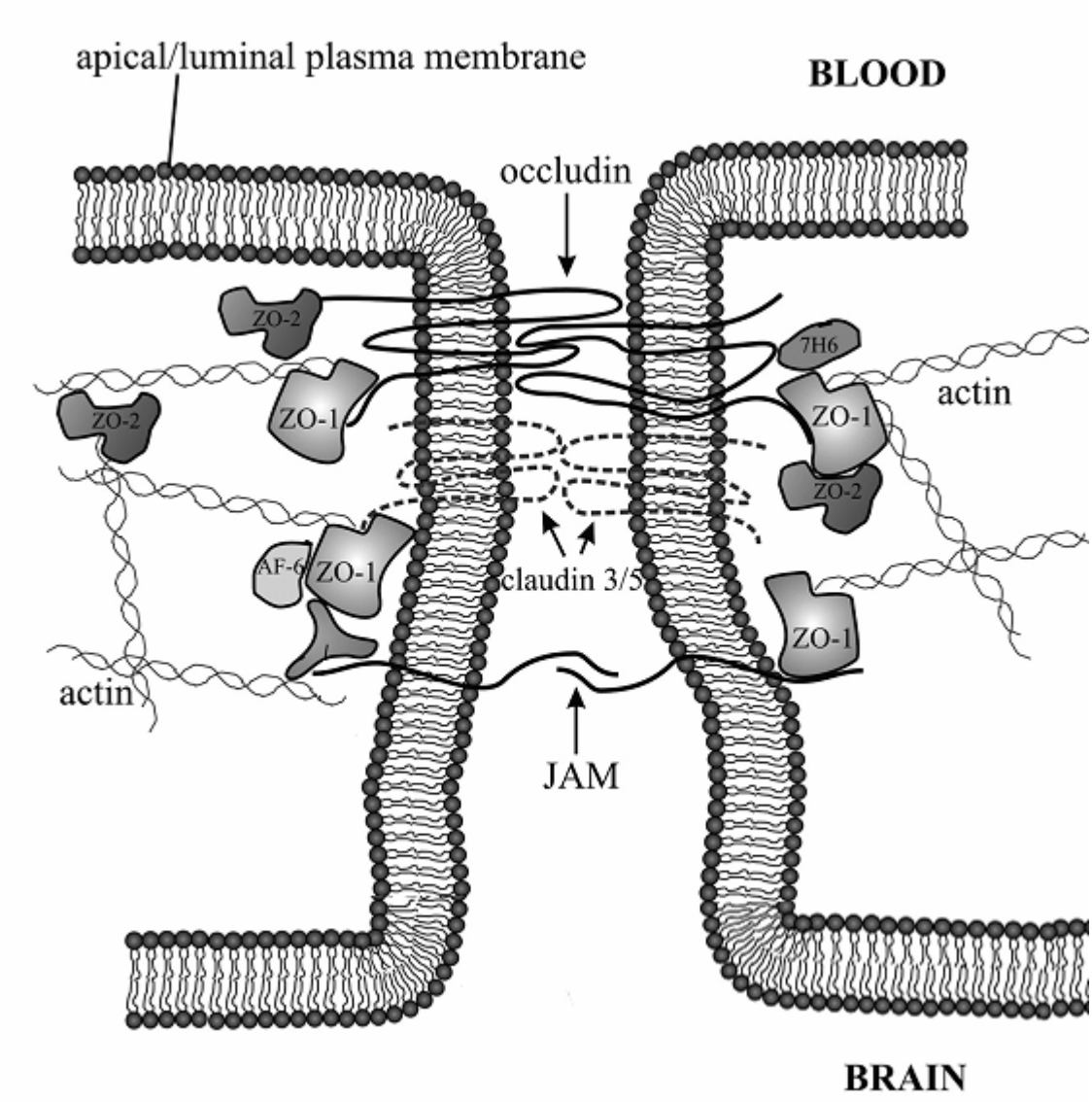

Figure 1.5. Molecular organization of blood-brain barrier tight junctions.
Modified from Hawkins and Davis, 2005 (94).

transmembrane tight junction proteins to the actin cytoskeleton (70). ZO-1 and ZO-2 co-localize at the peripheral cell membrane and they are thought to have overlapping functions (240).

Localization changes and biochemical modifications have been shown to correlate with altered functions of tight junction proteins. For example, when cells are stressed or in states of depleted calcium, ZO-1 and ZO-2 localize in the nucleus instead of their normal location at the periphery of the cell (90, 237). Occludin has been shown to be phosphorylated at many residues, and this may regulate its localization at the cell periphery (200). Rho kinase (RhoK) phosphorylation of occludin and claudin-5 is associated with an increase in monocyte migration across the BBB in patients with HIV-1 encephalitis (271).

BBB in disease and infection

In healthy individuals the BBB functions to regulate nutrient flow to the brain and restrict access by toxic metabolites and cells or molecules that might cause damage to the sensitive CNS tissue (reviewed in 18). Viral and parasite infections, injuries such as stroke or head trauma, and diseases such as multiple sclerosis and Alzheimer's have all been shown to impact the function of the BBB (4, 7, 162, 199). Breakdown of the BBB caused by infection may occur as a result of a pathogen invading brain microvascular endothelial cells in order to infect CNS tissues (111), as a result of the host's inflammatory response to the infection (139).

HIV-1 infection can result in CNS complications including human immunodeficiency virus-related encephalitis (HIVE), commonly associated with

breakdown of the BBB. While HIV-1 does not infect the brain endothelium itself, HIV-1 infection causes alterations in the expression of endothelial cell tight junction proteins (55, 118). HIV-1-infected leukocytes have increased expression of the chemokine receptor CCR2 and show increased migration across an endothelial cell monolayer in response to CCL2 (67). CCL2 itself causes a decrease in expression of tight junction proteins and a loss of barrier properties in brain endothelial cells (218, 222) and functions through activation of RhoK to down-regulate occludin and claudin expression (222). RhoK is also responsible for the increased phosphorylation of occludin and claudin 5 at specific residues in the brains of HIVE patients as observed by immunofluorescent staining specific for the phosphorylated forms of the tight junction proteins (271). These data indicate that there is a common mechanism involving RhoK for decreasing TJ protein expression and tight junction function in HIVE patients and in models that use chemokine-induced signaling to disrupt the BBB. Both systems involve the disruption of tight junction proteins and involve aspects of the Rho signaling pathway. Although all of the effects of CCL2 signaling in the brain are not yet understood, this molecule clearly plays a major role in recruiting inflammatory cells to the brain as well as directly modulating expression of tight junction proteins to alter the permeability of the BBB (153, 219, 259).

Other viruses shown to transit or cause breakdown of the BBB include dengue virus, West Nile virus, lymphocytic choriomeningitis virus and herpes simplex virus-1 (5, 10, 140, 254). While dengue-induced reduction in endothelial cell barrier properties is partially neutralized by antibody to CCL2, the mechanism by which other viruses cause disruption of tight junctions and breakdown of the BBB is not yet understood. West Nile

virus induces BBB permeability by signaling through toll like receptor 3 and TNF-α (254). Recent data suggests that matrix metalloproteinase 9 (MMP9) is also involved in the disruption the BBB in WNV infections (253). MMP9 is already known to be important in focal ischemia models of BBB breakdown (12, 13) and involved in the breakdown of the TJ protein ZO-1 after brain injury.

Natural killer cells and function during viral infection

Because viruses replicate using host cell machinery, viral antigens are normally presented by MHC class I along with host peptides. Thus viral infected cells are at risk for detection by CD8 T cells unless they somehow block this MHC class I presentation. Many viruses, including human adenoviruses, decrease MHC class I expression in order to avoid this detection by host T cells (6). While this lack of MHC class I expression allows virus-infected cells to evade detection by CD8 T cells, it has the consequence of creating targets for recognition by natural killer (NK) cells.

NK cells are an important part of the innate immune response to viral infection. NK cells are lymphocytes that function to lyse their targets without requiring a prior signal or sensitization to a specific antigen (148). In the immune response to viral infections, NK cells have an important role in recognizing and destroying infected cells before other arms of the immune system have been primed and activated. NK cells express inhibitory receptors that are specific for MHC class I and their function is inhibited when MHC class I molecules bind to such receptors. When NK cells bind to cells lacking surface MHC class I, the NK cell inhibitory receptor is not engaged and NK cells function to lyse the target cell (30) (Figure 1.6). Thus NK cells serve as a line of

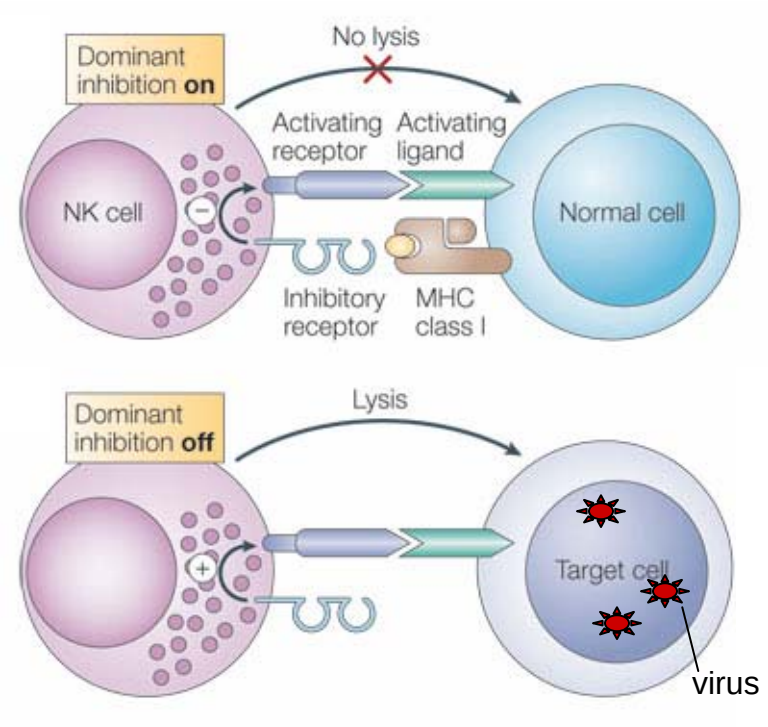

Figure 1.6. Target-cell recognition by natural killer cells. Modified from Fauci et al, 2005 (72).

defense against pathogens that downregulate antigen presentation by MHC class I as a strategy to evade the host immune system. NK cells also have activation receptors that can be stimulated by mechanisms that are still being determined (31); these function in conjunction with the inhibitory receptors to regulate target cell killing.

Viruses have varying susceptibility to NK cells. Mouse cytomegalovirus (MCMV) infection is very sensitive to NK cells, while lymphocytic choriomeningitis virus and herpes simplex virus-1 are resistant (reviewed in 32, 267). MCMV susceptibility to NK cells has been studied extensively and found to rely on factors from both the host and virus (reviewed in 275). Mice that are resistant to MCMV infection such as C57BL/6 carry the *Ly49h* gene which encodes an NK cell activation receptor. Ly49H recognizes the MCMV protein M157 allowing for host recognition and killing of MCMV-infected cells.

The role of NK cells in MAV-1 infection was of interest because previous results have shown that the innate immune response likely plays a part in successful control of infection (41, 42, Ashley and Spindler, unpublished). SJL mice are known to be susceptible to MAV-1 infection (220) and they have a "low NK cell phenotype," defined as having low levels of NK cell killing (116). MAV-1 has not been shown to down-regulate any of the mouse MHC class I allotypes examined (132), but that does not exclude the possibility that MAV-1 infection alters the expression of MHC class I on cell types that were not examined. Given these data it was of interest to determine whether NK cells have a role in protecting the host from MAV-1 infection. The role of NK cells following MAV-1 infection is described in recently published work (265) and in Chapter 2 of this thesis.

Tandem affinity purification

Unknown protein binding partners can be purified for identification through a number of means including co-immunoprecipitation and GST-pulldown assays. Tandem affinity purification (TAP) is a more recently developed method that uses a similar approach to isolate proteins and complexes that interact with a known protein (186). The TAP tag consists of the calmodulin binding peptide domain, a tobacco etch virus cleavage site and a *Staphylococcus aureus* protein A domain (Figure 1.7). Expression of the tagged protein of interest can be performed by transient transfection or through infection with retrovirus to allow for stable expression. To perform a TAP isolation of interacting proteins, cell lysates are incubated with IgG-labeled sepharose beads in a column (186). The protein A domain of the tagged protein binds to these beads, allowing both the tagged protein and any interacting proteins to be retained in the column. After eluting with tobacco etch virus protease, the tagged protein and interacting proteins can be analyzed immediately or run through a second purification step that takes advantage of the calmodulin binding domain in the TAP tag. The second purification is performed by adding calmodulin-labeled sepharose beads and the first column eluate to a new column. The final product is eluted using EGTA to release the tagged protein along with any proteins that it binds to. The ability to select for appropriate expression levels of that tagged protein in the TAP purification system is a distinct advantage compared to using traditional techniques such as overexpressing a tagged protein for purification assays. The tagged protein is expressed in a bicistronic promoter construct in which expression of green fluorescent protein (GFP) can then be measured to monitor expression levels

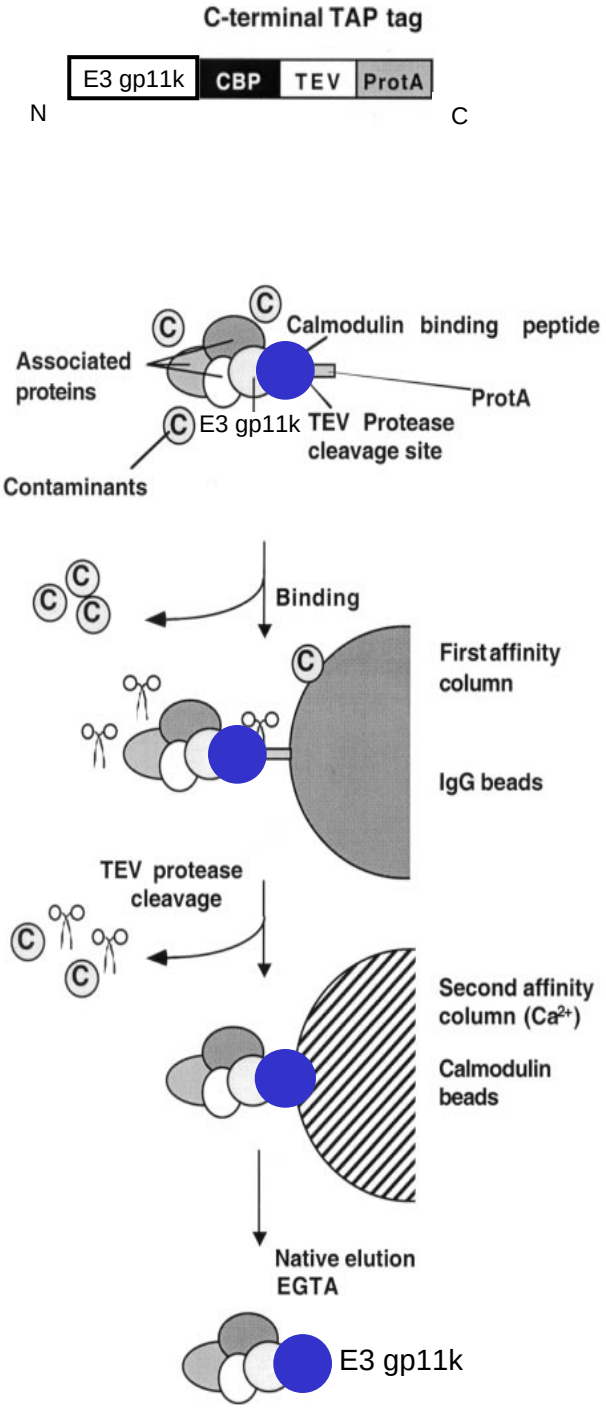

Figure 1.7. Tandem affinity purification method. (A) E3 gp11k with C-terminal TAP tag. (B) Overview of the TAP purification method. Modified from Puig et al, 2001 (180).

from the construct (128). An internal ribosome entry site follows the tagged protein sequence, and it is followed by the gene for GFP. By performing pulldown assays using samples with endogenous protein levels, the likelihood of non-specific interactions and mislocalized protein expression is decreased and the ability to identify a true protein interaction is increased (128, 193, 283). Two cell lines expressing TAP-tagged MAV-1 E3 gp11k were constructed and used in experiments to begin identifying cellular proteins that interact with E3 gp11k. These experiments are described in Chapter 4.

Studies performed in this work

In this work we examine the pathogenesis of MAV-1 infection in the natural host. The role of NK cells in responding to wild type MAV-1 infection is examined in Chapter 2 (265). NK cells were depleted by antibody injection in two inbred strains of mice and the course of MAV-1 infection was examined. Short-term control of viral replication was also analyzed in mice genetically deficient in NK cells and T cells and compared to wild type mice. Long-term survival of MAV-1 infection in mice genetically deficient in NK cells and T cells was also measured and was compared to virus control and survival in wild type mice as well as survival of mice deficient only in T cells.

The immune response to infection with both wild type and an E3 null mutant virus was examined during acute infection by analysis of inflammatory cells in the brain as well as analysis of the chemokine response to infection of endothelial cells. The mechanism by which wild type and E3 mutant MAV-1 infection cause disease in the CNS was investigated in Chapter 3. These studies included the determination of the ability of wild type or mutant MAV-1 to cause breakdown of the blood brain barrier.

BBB integrity was also examined in MAV-1 infection models genetically deficient in aspects of the host immune response. Primary brain endothelial cells were isolated and analyzed for barrier properties after infection with wild type MAV-1 or an E3 null virus, *pm*E314. Tight junction protein expression was measured after infection with wild type or mutant virus and the ability of the chemokine CCL2 to cause tight junction protein changes was assayed.

In Chapter 4 we describe the creation and characterization of two cell lines that stably express MAV-1 E3 gp11 with a C-terminal TAP tag. Preliminary studies to identify cellular proteins that interact with E3 gp11k were performed and the results are discussed. The purpose of these studies is to gain insight into the function of E3 gp11k by identifying cellular proteins that bind to E3 gp11k.

Chapter II

Mouse adenovirus type I infection of natural killer cell-deficient mice

ABSTRACT

Natural killer (NK) cells contribute to the initial nonspecific response to viral infection, and viruses exhibit a range of sensitivities to NK cells in vivo. We investigated the role of NK cells in infection of mice by mouse adenovirus type 1 (MAV-1) using antibody-mediated depletion and knockout mice. MAV-1 causes encephalomyelitis and replicates to highest levels in brains. NK cell-depleted mice infected with MAV-1 showed brain viral loads 8-20 days p.i. that were similar to wild-type control non-depleted mice. Mice genetically deficient for NK cells behaved similarly to wild-type control mice with respect to brain viral loads and survival. We conclude that NK cells are not required to control virus replication in the brains of MAV-1-infected mice.

INTRODUCTION

Mouse adenovirus type 1 (MAV-1) infects monocytes and endothelial cells throughout the animal (42, 113, 159). In acute infection, the highest viral loads are found in the brain, spinal cord, and spleen, and the virus causes encephalomyelitis (94, 113, 131, 216). Adaptive immune responses to MAV-1 infection have been investigated using immunodeficient mice. T lymphocytes contribute to pathology during the acute phase of MAV-1 infection, since T cell-deficient mice display fewer signs of immunopathology

than do control mice (159). Mice deficient in α/β T cells succumb to MAV-1 infection 9-12 weeks after infection with high viral loads, either because MAV-1 replication is not limited during the acute phase or because T cells are needed to suppress persistent MAV-1 replication, or both. Mice deficient in B cells or B cell functions succumb to low dose MAV-1 infection 6-9 days after infection (160). These mice have high viral loads and disseminated infections; early T cell-independent IgM and neutralizing antibody are critical for protection from disseminated MAV-1 infection.

The role of innate immune response components in MAV-1 infection has not been well studied. NK cells are a key effector of the innate response to viral infection, and two major functions of NK cells are cytotoxicity and secretion of interferon (IFN)-γ (reviewed in 27). However, NK cells are not required for defense against all viruses. For example, in infections of mice, mouse cytomegalovirus is sensitive to NK cells (32) while lymphocytic choriomeningitis virus and murine gammaherpesvirus 68 are relatively resistant (241, 260, 262, 263). Little is known about the importance of NK cells in controlling adenovirus infections in their natural hosts. The adenoviruses are species-specific, and human adenoviruses do not complete the full virus replication cycle in mice (reviewed in 85). Nonetheless, mice infected with high doses of human adenovirus develop pneumonia and have been used to evaluate early immune responses. NK cells are activated in response to injection with adenovirus vectors with and without transgenes in C57BL/6 mice, showing increased IFN-γ expression and cytotoxic killing (198). This response is independent of viral gene expression but requires intact viral particles. Mice depleted of their NK cells express transgenes longer than nondepleted mice (176). There are mouse strain differences in NK cell responses to infection with human adenovirus

vectors, with higher NK cell activation, cytotoxicity, and IFN-γ production in BALB/c mice compared to C57BL/6 mice (176). Mouse NK cell cytotoxicity for tumor cells expressing the human adenovirus gene early region 1A is higher than for cells not expressing the gene, indicating that there are also NK cell responses elicited by adenoviral gene expression (47).

There is one report of the role of NK cells in MAV-1 infection. MAV-1 infection of CB.17/scid and CB.17/scid/beige mice was compared (42); *beige*$^{-/-}$ (*Lyst*$^{-/-}$) mice are deficient in NK and other cell activity (194, 203). The two strains of mice succumbed to MAV-1 with similar kinetics and were resistant to neurologic disease (42). The results suggest that the presence of NK cell activity offered no survival advantage to the SCID mice.

The role for B cell function (production of early antiviral IgM) in MAV-1 infection overlaps the time when typical innate immune responses occur (160), and could reduce the need for an NK cell response. NK cell killing is regulated by a balance of positive and negative signaling through activating and inhibitory cell receptors (reviewed in 27, 148). Net activation of NK cell killing can occur when NK cells have received positive activation signaling greater than inhibitory signaling. Reduced inhibitory signaling can occur when NK cells encounter cells with low levels of major histocompatibility complex (MHC) class I antigens, which are ligands for some NK cell inhibitory receptors. Many viruses have mechanisms to downregulate MHC class I, thus protecting them from $CD8^+$ T cell killing, but making them potentially susceptible to NK cell killing. However, MAV-1 does not downregulate MHC class I during infection (132). This suggests that the cytotoxic function of NK cells might not be necessary for

control of MAV-1 infection. On the other hand, SJL mice, which are highly susceptible to MAV-1 infection (220), display a "low NK" phenotype, defined as low endogenous levels of NK cell killing that increase only minimally upon poly-I:C treatment (116). Thus MAV-1 resistance may depend on functional NK cell responses.

To examine more thoroughly whether NK cells are necessary for control of MAV-1 infection, we infected mice that had undergone antibody-mediated depletion of NK cells and mice genetically deficient for NK cells. Depletion of NK cells in two MAV-1-resistant mouse strains, C57BL/6 and BALB/c, with anti-NK1.1 and anti-asialo GM1 antibodies, respectively, had no effect on control of replication of MAV-1 in the brain at early and late times post infection (p.i.). Mice genetically deficient in NK cells or a combination of NK and T cells did not differ from control mice in viral loads or survival. We conclude that NK cells are not required for control of MAV-1 replication in brains of resistant BALB/c and C57BL/6 mice.

MATERIALS AND METHODS

Mice, virus, infections, and statistics. BALB/cAnNCr and C57BL/6NCr mice were obtained from the National Cancer Institute (Bethesda, MD). CD3εtg mice were a kind gift of E. Szomolanyi-Tsuda. These mice express human CD3ε in high copy and are defective in T cells and NK cells, but not B cells (105, 230, 251). These mice had been backcrossed onto a C57BL/6 background for 10 generations by Dr. Szomolanyi-Tsuda. C57BL/6NTac-*IL15*^{tm1Imx} mice and C57BL/6NTac background controls were obtained from Taconic (Germantown, NY), originally generated in the laboratory of Dr. Jacques Peschon of the Immunex Corporation (Seattle, WA). IL15$^{-/-}$ mice lack NK cells and have

reductions in memory CD8 T cells, NK1.1 T cells and Thy1$^-$ CD8α intraepithelial lymphocytes (122). C57BL/6NCR.129P2-*Tcrb*^{tm1Mom} *Tcrd*^{tm1Mom}/J (βxδ) were obtained from The Jackson Laboratory (Bar Harbor, ME). These mice had been backcrossed onto a C57BL/6 background for an unknown number of generations, and C57BL/6NCr mice were used as background controls. These βxδ mice do not express αβ T-cell receptor or any γδ T-cell receptor and are thus deficient in both αβ and γδ T lymphocytes. Mice were infected i.p. with 10^2 or 10^3 PFU of MAV-1 in 100 μl phosphate-buffered saline or mock-infected with conditioned media (media from uninfected cells 3-5 days post confluence) similarly diluted. Mice were euthanized at 8, 14 or 20 days p.i. or when moribund in the long-term survival experiment by CO_2 asphyxiation, and their organs were harvested. All mice were maintained in microisolator housing with food and water ad libitum. All animal work complied with relevant federal and institutional policies. MAV-1 was grown and titrated in NIH 3T6 cells, a mouse fibroblast cell line (39). A log rank (Mantel-Cox) test of the null hypothesis that the survival curves (based on Kaplan-Meier estimates) were equivalent was performed using SPSS software. Student's *t* test analyses were performed using Microsoft Excel.

Depletion of NK cells. To deplete NK cells in BALB/cAnNCr mice, 1.07 mg anti-asialo GM1 antibody (Wako Chemicals USA, Inc., Richmond, VA) was administered i.p. on days -1, 1, 3, 5, 7 relative to infection (day 0). Control animals were given the same dose of rabbit γ-globulin (Jackson ImmunoResearch Laboratories, Inc., West Grove, PA). To deplete NK cells in C57BL/6NCr mice, an i.p. injection of 100 μg of PK136, a rat monoclonal against mouse NK1.1 antigen (purified by University of Virginia

Lymphocyte Culture Center), was administered on days 0 and 1 relative to infection (day 0) for a total dose of 200 μg. The same dose of rat IgG antibody (Jackson ImmunoResearch Laboratories, Inc., West Grove, PA) was given to control mice. For long-term NK cell depletion in C57BL/6NCr mice, animals were given 100 μg doses of PK136 on days -1, 0, 7, 8, 15 and 16 relative to infection. NK cell depletion was confirmed by flow cytometry in every experiment. Depletion with PK136 and anti-asialo GM1 antibody reduced NK cell numbers to a mean of 6 or 16% of non-depleted levels of NK cells, respectively.

Flow cytometry analysis. C57BL/6NCr splenocytes were stained with antibodies to NK1.1, TCRβ and DX5 (BD Biosciences, San Jose, CA). BALB/cAnNCr splenocytes were stained with antibodies to TCRβ and DX5 (BD Biosciences, San Jose, CA). Analysis was conducted on 150,000 cells per sample in C57BL/6NCr experiments and 200,000 cells per sample in BALB/cAnNCr experiments. Stained samples were analyzed by flow cytometry with a FACScan™ or FACSCaliber flow cytometer and CellQuest™ (BD Biosciences, San Jose, CA) or FlowJo (Tree Start Inc, Ashland, OR) software. Efficient NK cell depletion was confirmed by identifying NK cells as $NK1.1^{+}TCR\beta^{-}$ and $DX5^{+}$ $TCR\beta^{-}$ in the case of C57BL/6NCr mice or $DX5^{+}$ $TCR\beta^{-}$ in the case of BALB/cAnNCr mice.

Quantitation of virus. Brain homogenates were prepared using the Mini-Beadbeater-96 (BioSpec Products, Bartlesville, OK) as previously described (264, 266). Briefly, the ~100 mg samples were mechanically disrupted with sterile glass beads in phosphate-

buffered saline and assayed via plaque assay (39) or by antigen capture ELISA (264, 266). These two methods of virus quantitation have been shown by regression analysis to have a high correlation coefficient (264).

RESULTS

Effects of NK cell depletion on early replication of MAV-1 in the brains of BALB/c and C57BL/6 mice.

BALB/c mice were depleted of NK cells using anti-asialo GM1 to examine the ability of depleted mice to control MAV-1 infection at early times post infection. This antibody depletes NK cells and Ag-specific T cells when administered in vivo (215). Mice were treated every two days with intraperitoneal (i.p.) injections of anti-asialo GM1 or control antibody; injections began one day before i.p. infection with 10^2 plaque-forming units (PFU) of MAV-1, a dose more than 2 log units below the LD_{50} for BALB/c mice (94, 220). Eight days after infection, splenocytes were analyzed by flow cytometry to measure the level of NK cell depletion (Fig. 2.1). NK cells were identified by $DX5^+$ $TCR\beta^-$ staining and therefore fall in the upper left quadrant of the dot plots. In mock-infected mice treated with control antibody, 2.75% of the splenocytes were $DX5^+$ $TCR\beta^-$, whereas in anti-asialo GM1 antibody-treated mice the $DX5^+$ $TCR\beta^-$ cells were reduced to 0.45%, indicating a significant depletion of the NK cells. Upon MAV-1 infection alone we observed a reduction in the percentage of NK cells (Fig. 2.1A, compare top panels), but because there were increased numbers of total splenocytes in the infected mice, the absolute number of NK cells did not differ between mock and infected control antibody-treated mice (data not shown). There was no significant difference in percentage of NK

cells between the antibody-depleted mock-infected and antibody-depleted MAV-1-infected groups (Fig. 2.1A, lower panels, 0.45% and 0.51%**)**. We analyzed the brain viral loads from all of the infected mice to determine the effects of NK cell depletion on viral replication. The brain viral titers were measured by enzyme linked immunosorbent assay (ELISA); there were no significant differences between control mice and NK cell-depleted mice (Fig. 2.1B). There were also no clinical signs of disease observed in infected NK cell-depleted or control mice. The finding that NK cell depletion did not lead to increased viral replication suggests that BALB/c mice do not require NK cells for control of MAV-1 in the brain at early times after infection.

We tested the effect of NK cell depletion in C57BL/6 mice, a strain in which NK cells can be depleted with the anti-NK1.1 antibody (PK136). Mice were treated with PK136 i.p. on days -1 and 0 and infected i.p. on day 0 with 10^3 PFU of MAV-1, a dose more than 1.4 log units below the LD_{50} for C57BL/6 mice (94, 220). Mice were euthanized on day 8, and flow cytometric analysis of their splenocytes revealed that treatment with PK136 effectively depleted NK cells while treatment with control antibody had no effect (Fig. 2.2A). The upper left quadrant of the dot plots indicates NK cells ($DX5^+$ $TCR\beta^-$). The upper plots illustrate that 3.30% of the splenocytes in mock-depleted, mock-infected animals were $DX5^+$ $TCR\beta^-$, whereas the lower plots show that only 0.52% of splenocytes in PK136-treated, mock-infected animals were $NK1.1^+$ $TCR\beta^-$, indicating a significant depletion of NK cells. The PK136 antibody also depletes NK1.1 T cells (166), and a reduction in this cell population can be seen in these experiments (upper right quadrants of the dot plots). MAV-1 infection alone (in the absence of NK cell depletion) of C57BL/6 mice resulted in a reduction in the percentage of splenic NK

cells (Fig. 2.2A, compare upper left and right panels), but because of increased numbers of splenocytes in the infected mice, the number of NK cells was similar between mock- and virus-infected control antibody-treated mice (data not shown). Brain titers of NK cell-depleted and mock-depleted animals were measured by plaque assay and capture ELISA; we have previously shown that ELISA and plaque assay measurements of viral load correlate (264). A similar correlation is seen here (Fig. 2.2B, 2.2C). There were no significant differences in viral load between NK cell-depleted mice and mock-depleted mice (Fig. 2.2B, $P = 0.12$; Fig. 2.2C, $P = 0.46$). There were also no observable clinical signs of disease in NK-cell depleted or control mice. These results indicate that the absence of NK and NK1.1 T cells did not alter viral replication in the brains of C57BL/6 mice at early times after MAV-1 infection.

To examine the role of NK cells at other times in infection, we depleted C57BL/6 mice of their NK cells for 4, 14 or 20 days. Mice were injected with either PK136 or a control antibody on days -1, 0, 7, 8, 15 and 16 and infected with 10^3 PFU of MAV-1 on day 0. At 4 days p.i. in NK cell-depleted and mock-depleted mice, brain viral loads were below the limit of detection (data not shown). At 14 or 20 days p.i., groups of mice were euthanized, and the effectiveness of the NK cell depletion was examined by flow cytometry of splenocytes. NK cells were depleted in mice treated with PK136 at both 14 and 20 days p.i. (Fig. 2.3A and data not shown). NK cells comprised 2-4% of the splenocytes in control antibody-treated mice but <0.9% of splenocytes in PK136-treated mice. This indicates that the long-term treatment schedule effectively depleted NK cells. Although there was a lower percentage of NK cells in virus-infected γ-globulin-treated mice compared to mock-infected mice (compare Fig. 2.3A upper left and right panels),

the number of NK cells was similar because there were more splenocytes in the infected mice (data not shown). At 14 days p.i., NK cell-depleted mice had a low level of detectable virus in their brains, whereas mice that were mock-depleted had viral loads that were below the limit of reliable detection by plaque assay (Fig. 2.3B). This suggests that there may have been a slower rate of clearance of virus in the absence of NK cells. However, by 20 days p.i., mice in both the NK cell-depleted and control groups had cleared MAV-1, with brain viral titers below the limit of reliable detection by plaque assay, indicating that the overall result was clearance of the virus in both the absence and presence of NK cells. No clinical signs of disease were observed for NK cell-depleted or control mice at any time point. Despite the difference in viral load at 14 days p.i. between the mock- and NK cell-depleted mice, the ability of all animals to control the infection by day 20 is consistent with results described above that NK and NK1.1 T cells were not required for the control of acute MAV-1 infection.

Virus loads in MAV-1 infected IL-15$^{-/-}$ mice are similar to those in control mice.

To test if mice genetically deficient in NK cells retain the ability to control MAV-1 at early times post infection, we tested interleukin (IL)-15$^{-/-}$ (C57BL/6NTac-*IL15*^{tm1Imx}) mice, which lack NK cells and also have reductions in memory CD8 T cells, NK1.1 T cells and Thy1^{-} CD8α intraepithelial lymphocytes (122). IL-15$^{-/-}$ and control C57BL/6NTac mice were infected i.p. with 10^2 PFU of MAV-1 and euthanized 8 days p.i. Brain viral titers were analyzed by capture ELISA. IL-15$^{-/-}$ mice did not show increased viral titers compared to the control mice (Fig. 2.4). Neither NK cell-deficient nor control mice showed any signs of clinical disease. This result suggests that IL-15, NK cells,

memory CD8 T cells, NK1.1 T cells and Thy1$^-$ CD8α intraepithelial lymphocytes were not required to control MAV-1 infection. These data are consistent with the data in Figs. 2.1 - 3 that neither NK cells nor NK1.1 T cells played a major role in the control of MAV-1 infection in the brain.

Effects of the combined lack of NK cells and T cells on replication of MAV-1 in the brains of CD3εtg mice.

We further tested the importance of NK cells using a strain of mice lacking both NK and T cells. T cell-deficient mice are able to control MAV-1 infection at early times but succumb 10-12 weeks p.i. (159). CD3εtg mice lack NK cells and T cells (251) and provide another genetically deficient model in which to test the importance of NK cells for control of MAV-1 at early and late times of infection, albeit in the background of T cell deficiency. CD3εtg and C57BL/6 control mice were infected i.p. with 10^2 PFU of MAV-1 and euthanized 8 days p.i. Brain viral titers were analyzed by plaque assay. Titers were similar for both C57BL/6 and CD3εtg infected mice (Fig. 2.5), indicating that CD3εtg mice did not differ from C57BL/6 controls in their ability to control MAV-1 infection at 8 days p.i. Mice were also analyzed at 4 and 6 days p.i. Viral loads were below the limit of detection in both CD3εtg and C57BL/6 mice at 4 days p.i., but at 6 days p.i. viral loads were detectable and also did not differ between the two strains (data not shown). To examine a role for NK cells in long-term MAV-1 infections, CD3εtg mice (deficient in NK and T cells) were compared to B6.129P2-*Tcrb*^{tm1Mom} *Tcrd*^{tm1Mom}/J (βxδ) mice (deficient in αβ and γδ T cells). These two strains and C57BL/6 control mice were infected with 10^2 PFU of MAV-1, and survival was measured over the course of 10

weeks. The results indicate there was not a significant difference in the ability to control and survive MAV-1 infection in mice lacking NK and T cells compared to mice lacking only T cells (Figure 2.6). These data are consistent with the findings above that NK cells were not critical for control of MAV-1 infection of BALB/c and C57BL/6 mice.

DISCUSSION

We hypothesized that NK cells may be important for MAV-1 infection because SJL mice, which are susceptible to MAV-1 (220), have a "low NK" phenotype (116). That is, they have low endogenous levels of NK cell activity that are not increased by treatment with IFN-γ or IFN inducers. The corollary is that NK cells of MAV-1-resistant mouse strains contribute to this resistance to infection. To test this, we depleted resistant mouse strains of their NK cells in order to mimic the low NK phenotype of SJL mice. BALB/c mice are considered to be resistant to MAV-1 and C57BL/6 mice are relatively resistant, with a 1-2 log unit lower 50% lethal dose (LD_{50}) than BALB/c (94, 220). Despite this lower LD_{50}, C57BL/6 mice are able to survive and clear virus doses used in these experiments (159, 160). In the experiments reported here, mice of these two inbred strains were efficiently depleted of NK cells by administration of anti-asialo GM1 antibody (BALB/c) or anti-NK1.1 antibody (C57BL/6). Mice depleted of NK cells by antibody injection showed no clinical signs of disease, and brain viral loads were similar in NK cell-depleted and mock-depleted mice 8-20 days post infection (Figs. 2.1-3). These results indicate that a lack of NK cells did not result in altered levels of MAV-1 replication in the brain in the acute phase of infection and suggest that NK cell depletions did not increase the ability of MAV-1 to traffic to the brain. The data do not support the

hypothesis that MAV-1-susceptible mouse strains are susceptible because of functional NK cell deficiency.

The antibody depletion strategies used in these studies deplete NK1.1 T cells as well as the larger NK cell population. IL-15$^{-/-}$ mice also lack NK1.1 T cells, allowing for the possibility that an absence of this cell population played a role in these results. While not yet fully understood, the role of NK1.1 T cells in fighting infection is believed to occur primarily through their rapid release of IFN-γ and ability to activate other immune cells (244). NK1.1 T cells have been reported to confer protection or partial protection from various viral and bacterial infections including HSV-1 and HSV-2 (14, 93) and *Streptococcus pneumoniae* (121). The simultaneous depletion of NK and NK1.1 T cells had no effect on pathogenesis or brain viral loads in MAV-1-infected mice. Given these results we conclude that NK1.1 T cells are unlikely to play a role in controlling MAV-1 infection.

Depletions of NK cells by anti-asialoGM1 and PK136 antibody treatment have been widely demonstrated to functionally deplete NK cell activity in vivo (252, 261). Furthermore, use of mice genetically deficient for NK cells confirmed the results obtained by NK cell-depletion, i.e., lack of NK cells did not make BALB/c or C57BL/6 mice more susceptible to MAV-1 infection in the brain. IL-15 induces the activation and increases the cytotoxicity of mature NK cells, and it is crucial for NK cell development and maintenance of memory CD8^{+} T cells (36, 87, 122, reviewed in 182). Due to these roles, mice deficient in IL-15 lack NK cells and have reductions in memory CD8^{+} T cells, NK1.1 T cells and Thy1^{-} CD8α intraepithelial lymphocytes (122). Despite these defects, IL-15$^{-/-}$ mice mount effective virus-specific primary CD8^{+} T cell responses and control

some experimental viral infections (24, 87, 170, 284) but not others (122, 204). We found that IL-15$^{-/-}$ mice showed no increase in susceptibility to MAV-1 upon infection relative to control mice on the same strain background. These data support our findings that NK cells are not required for control of MAV-1 infection. Furthermore they indicate that IL-15, memory CD8^{+} T cells, NK1.1 T cells and Thy1^{-} CD8α intraepithelial lymphocytes also do not play a significant role in the acute phase of infection.

CD3εtg mice are another genetically NK cell-deficient mouse model. These mice are deficient in T cells and NK cells and showed no differences in MAV-1 brain viral titers from control mice at 6 and 8 days p.i. We compared long-term survival of these CD3εtg mice that lack both NK and T cells to mice that lack only T cells (βxδ) (Figure 2.6). Previous work using T cell-deficient mice (βxδ and others) showed that T cells are required for long-term control of viral infection (159). In the experiments reported here, CD3εtg mice succumbed to MAV-1 infection before all of the βxδ mice, suggesting that the NK cell deficiency in the CD3εtg mice may have an effect on long-term survival. However, statistical analysis revealed that the difference was not significant at the 5% level. We note that the genetic cause of the T cell deficiency is different in the βxδ and CD3εtg mice, and that there are inevitable minor strain background differences arising from backcrossing the T cell mutations to the C57BL/6J background. Thus there are caveats to making comparisons of mice with the two T cell deficiencies. However, the long-term survival data for the CD3εtg mice are consistent with only a modest role (if any) for NK cells late in MAV-1 infection. Our data suggest that the role of T cells in controlling MAV-1 infection is greater than that of NK cells.

Although we were initially surprised that a lack of NK cells did not alter disease signs, survival, and brain viral loads in MAV-1 infection, our data are consistent with the results of Charles et al. (42), who examined MAV-1 infection of mice carrying a mutation of the *Lyst* (*beige*) gene. *Lyst*$^{-/-}$ mice (knocked out for the lysosomal trafficking regulator) have reduced NK cell activity (194, 203). However these mice do not lack all NK cell function, particularly in viral infections (120, 194, 263). In addition, *Lyst*$^{-/-}$ mice have granulocyte defects (83); thus NK cells are not the only cells affected. Charles et al. (42) found that whether mice carried the *Lyst*$^{-/-}$ mutation or not, they were equally susceptible to MAV-1 infection at lethal doses and lacked neurologic dissemination and signs of central nervous system hemorrhage. Despite the caveats about the pleiotropic effects of the *Lyst*$^{-/-}$ gene mutation, the data suggest that the NK cell defects (and other defects) of the *Lyst*$^{-/-}$ mice do not make mice more susceptible to MAV-1 infection.

In addition, in agreement with our findings for MAV-1, there are other viruses known to be relatively resistant in vivo to the effects of NK cells. These include lymphocytic choriomeningitis virus and murine gammaherpesvirus 68 (241, 260, 262, 263). We consider here reasons why control of MAV-1 replication in the brain is not dependent on NK cells. Alteration of MHC class I expression is a common tactic viruses employ to evade detection and activation by immune cells (173). The balance of NK cell activation vs. inhibition can be shifted toward activation of cytotoxicity when NK cells detect target cells expressing reduced levels of MHC class I (reviewed in 27). A previous finding suggests that NK cell recognition of "low MHC class I" cells may not be important for control of MAV-1 infection: MAV-1 infection does not decrease MHC class I expression (132). This may reduce the need for NK cell-mediated cytolysis of

cells lacking MHC class I. NK cells in mice deficient for MHC class I are defective in target killing (276). Mice genetically deficient for MHC class I expression ($\beta 2m^{-/-}$) survive infection with MAV-1 and are able to clear virus nearly as well as control mice (159), despite having functionally defective NK cells. Another reason why NK cells may not be critical for response to MAV-1 infection is that they may not be needed for production of IFN-γ. Antigen-presenting cells produce large amounts of IFN-γ in response to IL-12, and the amounts of IFN-γ produced in vitro by dendritic cells and macrophages are substantially larger than those produced by NK cells (80, 81, 171, 185). MAV-1 infection induces transient IL-12 expression in splenocytes and peritoneal cells, which should thus induce IFN-γ (49). IFN-γ likely plays a role in control of MAV-1 infection, because mice deficient for IFN-γ are more susceptible than control mice to MAV-1 infection (M. Moore and K. Spindler, unpublished). However we postulate that T cells and antigen presenting cells produce enough IFN-γ to control the MAV-1 infection in the absence of NK cells.

The data presented in this report indicate that NK cells are not required for control of MAV-1 infection at early or late times post infection, as measured by brain viral loads. This suggests that neither cytotoxic effects nor IFN-γ secretory functions of NK cells are critical to the control of MAV-1 replication. These studies also suggest that the "low NK" phenotype of MAV-1-susceptible SJL mice is not responsible for their inability to control MAV-1 replication. This is consistent with our susceptibility mapping studies (264), which indicate that a major quantitative trait locus on mouse Chromosome 15 is involved in susceptibility to MAV-1, whereas we found no quantitative trait loci for susceptibility on Chromosome 6, where the mouse natural killer complex locus maps.

Combined, these data indicate that in mouse strains with a range of susceptibilities to MAV-1 infection, NK and NKT cells are unimportant for control of replication of virus in the brain.

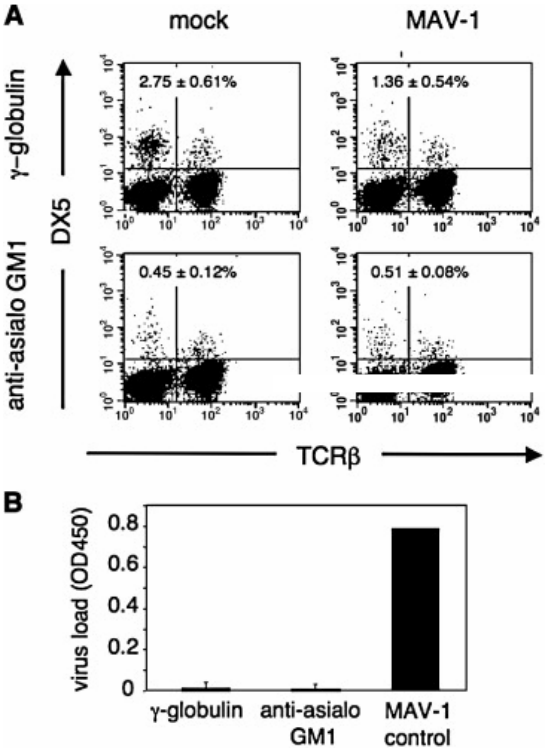

Figure 2.1. Effects of NK cell depletion on BALB/c mice. A. Representative example of flow cytometric confirmation of depletion. BALB/cAnNCr mice were injected i.p. at day -1, 1, 3, 5, 7 relative to infection with 1.07 mg of anti-asialo GM1 or rabbit γ-globulin as control antibody. Animals were given a dose of 10^2 PFU of MAV-1 i.p. and euthanizes at 8 days p.i. Splenocytes were analyzed for individual mice, and dot plots for one representative mouse of each treatment group are shown. Percentages of $DX5^+$ $TCR\beta^-$ cells are indicated in the top left quadrants; values are the mean and standard deviation for all the mice in each treatment group (n= 3-4 per group). Mice were analyzed individually for both NK cell depletion and brain viral titer. B. Brain titers following NK cell depletion and MAV-1 infection of BALB/cAnNCr mice 8 days p.i., assayed by capture ELISA. Each bar represents the background-subtracted average of the group, with standard deviation indicated. The MAV-1 control is an internal standard run in each assay as a positive control for the ELISA. A and B are representative examples of three depletion experiments of BALB/cAnNCr mice that all had similar results.

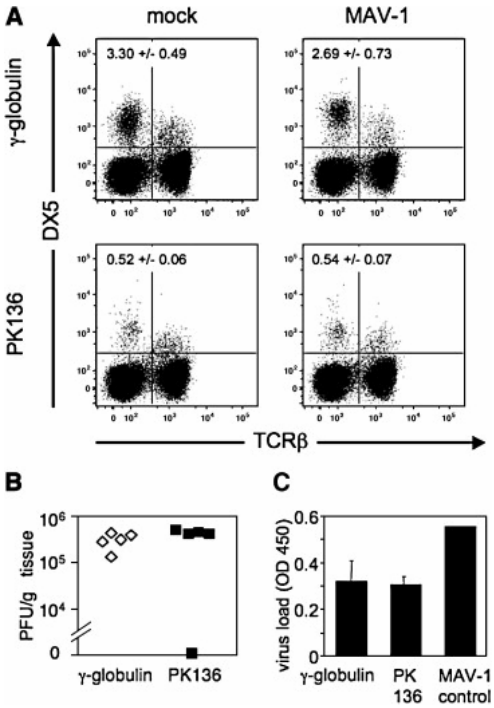

Figure 2.2. NK cell depletion and infection in C57BL/6NCr mice. A. Representative example of flow cytometric confirmation of depletion. C57BL/6NCr mice were mock depleted using a γ-globulin control antibody (upper panels) or were depleted of NK cells using PK136 (lower panels). On days -1 and 0 animals were injected i.p. with 100 μg of antibody. Intraperitoneal infection with 10^3 PFU of MAV-1 or mock infection also occurred on day 0. Splenocytes isolated from mice 8 days p.i. were analyzed individually and one mouse of each treatment group is shown. Percentages of NK cells in the spleen are indicated in the upper left quadrant ($DX5^+$, $TCR\beta^-$) for the four treatment groups; values are the mean and standard deviation for all the mice in each treatment group (n = 4-5 per group). Depletion results were confirmed by staining for NK1.1 instead of DX5 (data not shown). B. Viral loads in the brain were determined by plaque assay for each animal, treated either with control γ-globulin or PK136, as indicated. Serially diluted MAV-1 was concurrently titrated as a positive control (data not shown). Results are one example of three replicate experiments performed. C. Viral loads were also determined for the same animals as in B using capture ELISA. The MAV-1 control is an internal standard run in each assay as a positive control for the ELISA.

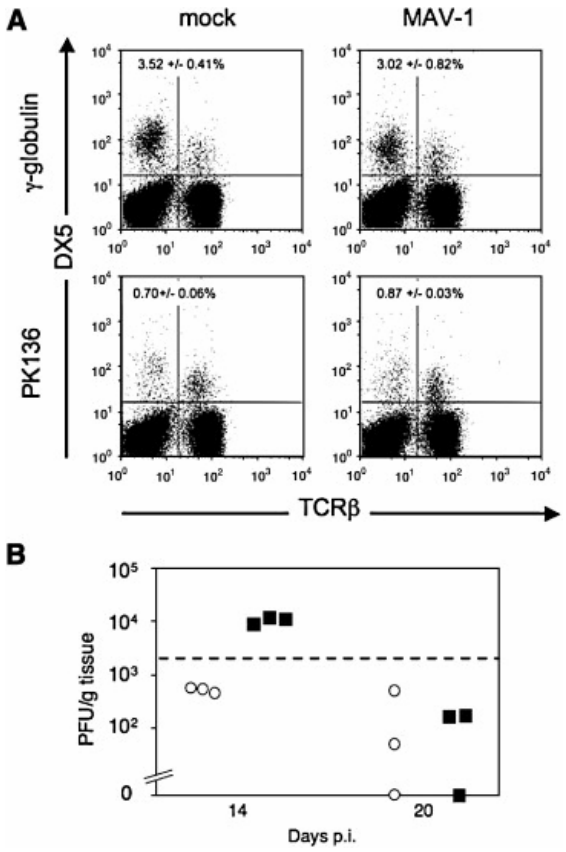

Figure 2.3. Effect of NK cell depletion and infection in C57BL/6NCr mice at 14-20 dpi. A. Mice were given γ-globulin or PK136 on days -1, 0, 6 and 7 for 14-day infections and on days -1, 0, 6, 7, 13 and 14 for 20-day infections. Mice were infected i.p. with 10^3 PFU of MAV-1 on day 0. NK cell depletion was confirmed by flow cytometry as shown in this representative example from 14 days p.i. in which one mouse of each treatment group is shown. Percentages of NK cells in the spleen are indicated in the upper left quadrant ($DX5^+$, $TCR\beta^-$) for each of the four groups; values are the mean and standard deviation for all the mice in each group (n = 3). For the 20-day samples the depletions were comparable (data not shown). Depletion results were confirmed by staining for NK1.1 instead of DX5 (data not shown). B. Viral loads in the brain as determined by plaque assay in mock depleted (circles) or NK cell-depleted (squares) mice 14 or 20 days p.i. Dotted line indicates the limit of reliable detection in the plaque assay (2 x 10^3 PFU/g).

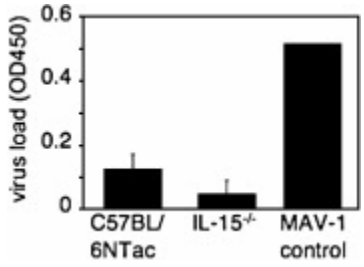

Figure 2.4. Capture ELISA quantitation of brain viral titers in MAV-1-infected C57BL/6NTac (control) and IL-15 $^{-/-}$ mice. Animals were infected for 8 days with 10^2 PFU of MAV-1. Each bar represents the background subtracted averages per group; n= 5 for each group. The MAV-1 control is an internal standard run in each assay as a positive control.

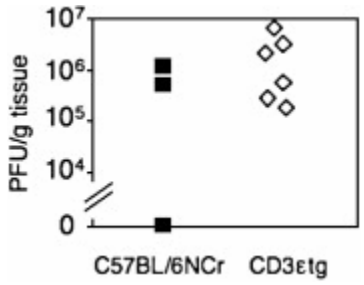

Figure 2.5. Infection of CD3εtg and C57BL/6NCr mice. Animals were infected for 8 days with 10^2 PFU of MAV-1. Viral loads in the brain were determined by plaque assay and were not significantly different ($P = 0.76$).

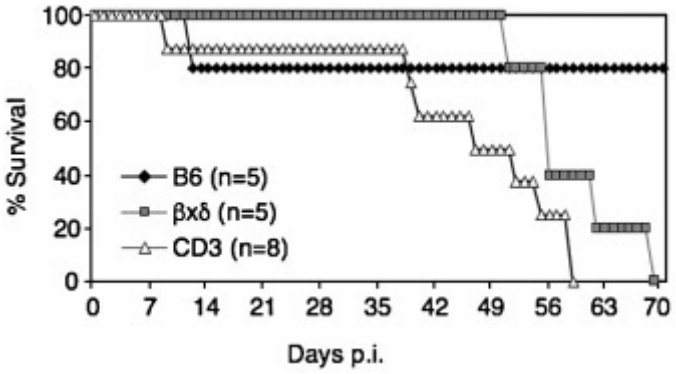

Figure 2.6. Survival curve of infected C57BL/6NCr (B6), CD3εtg (CD3) and βxδ mice. Mice were infected with 10^2 PFU of MAV-1 and monitored daily for survival. Comparison of the survival curves of βxδ and CD3εtg mice indicated that the log rank (Mantel-Cox) chi-square statistic was 3.06, on one degree of freedom ($P = 0.08$) and the survival curves were not significantly different at the 5% level.

Chapter III

Mouse adenovirus type 1-induced breakdown of the blood brain barrier

ABSTRACT

Infection with mouse adenovirus type 1 (MAV-1) results in acute encephalomyelitis that is fatal in susceptible mouse strains. In the brain, MAV-1 only infects endothelial cells. Brains of C57BL/6 mice showed a significant increase in leukocytes, including CD8 T cells after MAV-1 infection. Mouse brain microvascular endothelial cells infected *in vitro* with MAV-1 showed an increase in expression of the pro-inflammatory chemokines CCL2 and CCL5. MAV-1 infection of C57BL/6 mice caused a dose-dependent breakdown of the blood brain barrier (BBB) as seen by Evans blue dye or sodium fluorescein staining of brain tissues. This breakdown of the BBB was primarily due to direct effects of virus infection, because brains were permeable to dye even in the absence of inflammation. A primary mouse brain endothelial cell (pmBEC) culture was developed to measure direct effects of virus infection in the absence of an inflammatory response. MAV-1 infection caused a loss of transendothelial electrical resistance (necessary for maintaining the BBB). The tight junction proteins claudin-5 and occludin are required for the integrity of the BBB as well as transendothelial electrical resistance, and both proteins showed reduced expression on pmBECs following MAV-1 infection. Taken together, these results demonstrate that MAV-1 causes

breakdown of the BBB and decreased barrier properties in infected endothelial cells, due to reduced cell viability and altered expression of tight junction proteins.

INTRODUCTION

Adenoviruses are host restricted in their replication, so study of pathogenesis must occur in the natural host. Human adenovirus infections are typically mild and self-limiting in immunocompetent hosts; however disease can be much more severe in patients who are immunocompromised. Disseminated human adenovirus infection in transplant or other immunosuppressed patients can result in encephalitis and has a mortality rate up to 60% (250). Mouse adenovirus type 1 (MAV-1) infection has been shown to cause dose-dependent encephalitis in susceptible mouse strains (42, 94, 220). MAV-1 is similar to human adenovirus in genome and structure, and both viruses cause persistent infections, making MAV-1 a good model for adenovirus-based disease in the natural host. While signs of disease and lethality of MAV-1 infection are positively associated with the presence of inflammatory cells in the brain (37, 159), the precise manner in which MAV-1 infection causes inflammation and disease is not yet understood.

Integrity of the blood brain barrier (BBB) is important for regulating the flow of nutrients from the blood to the brain and restricting access by toxins and other substances that are harmful to the CNS. The BBB also functions to restrict access of inflammatory cells to the CNS as protection from both swelling and damage to cells such as neurons that cannot be replaced. The BBB is composed of microvascular endothelial cells, astrocytes, pericytes, neurons and basement membrane, connected by a network of tight junctions, adherens junctions and gap junctions (99, 178). Many diseases that affect the

CNS also alter the function of the BBB (5, 118, 161), often through disruption of tight junctions (55, 118). HIV-1 encephalitis results in increased permeability of the BBB and studies have shown that HIV-1 infection causes a CCL2-dependent reduction in expression of tight junction proteins (67). West Nile virus infection in a mouse model causes breakdown of the BBB mediated by Toll-like receptor 3 and tumor necrosis factor-α signaling (254). Treatment of human umbilical vein endothelial cells with supernatant from dengue virus infected cells resulted in a decrease in expression of ZO-1, a tight junction protein important for vascular integrity (140). Thus, human viruses can alter the BBB and tight junctions through a variety of mechanisms, none of which is fully understood or able to be studied in infection of the natural host.

Here we investigate how MAV-1 infection of the natural host results in fatal encephalitis. We show that BBB integrity is compromised after infection with MAV-1 and that infection results in recruitment of inflammatory cells, including cytotoxic T lymphocytes, to the brain. Although inflammation contributes to MAV-1 pathogenicity (38, 159), breakdown of the BBB was shown to be independent of the presence of inflammatory cells. Infection with MAV-1 resulted in reduced expression of tight junction proteins and loss of barrier properties in primary brain microvascular endothelial cells.

MATERIALS AND METHODS

Cells and viruses. Mouse brain microvascular endothelial cells (MBMECs) were originally obtained from Howard Fox, Scripps Research Institute, and were maintained in MBMEC growth medium (Cell Applications, Inc., San Diego). Isolation of primary

mouse brain endothelial cells (pmBECs) is described below. Wild-type MAV-1 comes from the original stock obtained from S. Larsen (17). *pm*E101 is the wild type parental virus used to construct mutant virus *pm*E314 which has stop codons in all three reading frames encoding E3 sequences (37). *pm*E101 was used as the wt virus throughout this work as a control in experiments using *pm*E314.

Mice and infections. Male C57BL6 mice were obtained from Charles River (C57BL6/NCI) or Jackson Laboratories (C57BL6/J). Perforin deficient ($pfp^{-/-}$) mice (C57BL/6-*Prf1*^{tm1Sdz}/J) were obtained from Jackson Laboratories. 3-5 week old mice were infected via intraperitoneal injection with 10^3 or 10^4 PFU of virus diluted in PBS in a total volume of 100 μL. Mock-infected mice were injected with conditioned media diluted in PBS. Organs for histological studies were harvested from mice 8 days after infection and either snap-frozen or fixed in 3.7% formaldehyde in PBS. Sections were stained with hematoxylin and eosin for histopathological analysis. All animal experiments complied with relevant university and federal guidelines for humane use and care. Animals were housed in microisolator cages and provided with food and water *ad libitum*.

Preparation of cells and staining for flow cytometry. C57BL6/NCI mice in groups of five were mock-infected or infected with 10^3 PFU of wt MAV-1 or *pm*E314 for 8 days. Mice were euthanized and immediately perfused with 30 mL of PBS before organ collection. CNS cells were isolated similarly to the method of Campanella et al, 2002

(35). Briefly, brains from each infection condition were pooled and homogenized in DMEM with 10% heat inactivated calf serum to create a single cell suspension. A step gradient was used to isolate cells for staining. Cells were suspended in a 15 mL conical tube in 70% percoll in DMEM in a final volume of 5 mL and then overlaid with 37% percoll in PBS (4 mL) followed by 30% percoll in DMEM (4 mL). After a 20 minute spin at 1500g the cells at the 37:70% interphase were collected. Cells were treated with fluorescently labeled antibodies to CD8, CD4, CD19, CD45 and CD69 or Ly6 G/C, F4/80, CD45 and CD69 (F4/80 from Invitrogen, Carlsbad, CA; all other antibodies from BD, San Jose, CA). Cells were analyzed using a FACSCanto machine (BD, San Jose, CA) and FlowJo software (Tree Star Inc, Ashland, OR).

Primary cell isolation. Primary mouse brain endothelial cells were isolated by a combination of methods described previously (218, 222). Briefly, cortexes from 30 3-4 week old C57BL6/NCI mouse brains were isolated and cleaned of blood vessels. Tissue was minced, then homogenized and suspended in a solution of 18% dextran (USB, Cleveland, Ohio) with 50 mM HEPES and antibiotic/antimycotic. The dextran solution was spun at 12,000 x g for 10 minutes to remove myelin. Cell pellets were digested for 90 minutes in 1 mg/mL collagenase/dispase (Roche, Indianapolis, Indiana) made in Hanks' balanced salt solution (Gibco) at 37ºC. After digestion, microvessels were isolated by positive selection using sheep anti-rat Dynabeads (Invitrogen, Carlsbad, CA) labeled with a rat anti-CD31 antibody (BD, San Jose, CA). Dynabeads were labeled by overnight incubation at 4ºC with 0.1 volume of antibody. Microvessels were grown on collagen-IV coated plates (BD, San Jose, CA) in DMEM (Gibco) containing 10% fetal

bovine serum, 10% newborn calf serum, 0.1 mg/mL endothelial cell growth supplement (BD, San Jose, CA), 0.1 mg/mL heparin (Sigma), 2 mM glutamine, Pen/Strep (Gibco), antimycotic/antibiotic (Gibco), non-essential amino acids (Sigma) and 20 mM HEPES (Sigma). After isolation, cells were passaged one time with trypsin/EDTA before use. The cells are designated primary mouse brain endothelial cells (pmBECs) throughout this work.

pmBEC characterization. pmBECs were incubated for two hours at 37ºC with DiI-labeled acetylated LDL (Biomedical Technologies Inc), rinsed with PBS and visualized using an Olympus BX60 upright fluorescent microscope. J774 macrophages were used as a positive control with the same conditions. pmBECs were tested for CD31, ICAM and VCAM expression levels by flow cytometry. Cells were trypsinized and incubated with anti-mouse CD16/CD32 monoclonal antibody (Fc Block, BD, San Jose, CA) prior to staining. Primary hamster anti-ICAM and rat anti-VCAM and anti-CD31 antibodies were from BD (San Jose, CA) and were detected with anti-rat PE secondary (Sigma) and anti-hamster FITC labeled secondary antibody from Rockland (Gilbertsville, PA). Cells were analyzed as in identification of brain inflammatory cells above.

Growth curve/plaque assay. pmBECs were grown on a 24 well plate coated with collagen IV and infected at an MOI of 5. Virus was allowed to adsorb for 1 hour at 37ºC before the addition of media. At 1, 2, 3, 4 and 5 days post infection (dpi) cells were scraped off the plate and collected along with supernatants. Input virus plus conditioned

media was used for the 0 dpi time point. After three rounds of freeze/thawing to release any intracellular virus, infectious virus was quantified by plaque assay on 3T6 cells (39).

Quantitation of MAV-1 by capture ELISA. Brain homogenates were prepared as previously described (264) and assayed by capture ELISA (266). Briefly, microtiter plates were coated overnight with a rabbit polyclonal anti-MAV-1 antiserum. After washing the plate was blocked with 1% BSA, washed again and then incubated with brain homogenates diluted to 9% in PBS. The plates were then washed and incubated with a pool of mouse polyclonal anti-MAV antiserum. After washing, a horseradish peroxidase-conjugated secondary antibody was used to detect the anti-MAV antiserum. Horseradish peroxidase detection was measured using Turbo-TMB (Pierce, Rockford, IL) on a microtiter plate reader detecting an optical density of 450 nm. All samples were assayed in triplicate, and ELISA values were calculated after subtracting the value for mock-infected samples. A MAV-1 virus stock, PBS and conditioned media were included as positive and two negative controls, respectively, in each assay performed.

Sodium fluorescein injection and quantification. A 10% sodium fluorescein (Sigma) solution in PBS was sterile filtered. Ten minutes before the desired time of euthanasia, mice were i.p. injected with 100 μL of sodium fluorescein solution. Immediately after euthanasia, blood was collected and then the mice were perfused with 30 mL of PBS. Brains were isolated and snap-frozen until used for quantitation. To quantify sodium fluorescein in the brain, the method of Phares et al. (179) was used. Briefly, brain tissue

was homogenized in 7.5% trichloroacetic acid (TCA), centrifuged and acid neutralized with 5 N NaOH. Fluorescence was measured with a microplate reader with excitation of 485 nm and emission at 530 nm and amount of fluorescein for each sample was determined by comparing to standards ranging from 4 μg/mL to 0.125 μg/mL. Brain values were normalized to serum dye concentrations for each mouse to allow comparisons between mice. Serum was isolated from the blood, and serum dye levels were measured by mixing equal parts serum and 15% TCA, centrifuging and mixing the supernatant with 1:1 7.5% TCA:5 N NaOH. Fluorescence was measured as above.

Immunofluorescence. pmBECs were grown on collagen IV-coated Lab-Tek chamber slides (Nalge Nunc, Rochester, NY). Cells were infected for 48 hours at an MOI of 5 and then stained for tight junction protein expression. Cells were washed, fixed with 3.7% formaldehyde for 15 minutes at room temperature (RT) and then permeabilized with ice-cold methanol for 1 minute. All remaining steps took place in a humid chamber. To block, cells were incubated for 1 hour at RT with 1% BSA in TBS-TX (25 mM Tris-HCl pH 8.0, 150 mM NaCl, 0.1% Triton X-100). Antibodies to ZO-2 (BD, San Jose, CA), occludin or claudin-5 (Invitrogen, Carlsbad, CA) were all used at a 1:50 dilution in 1% BSA in TBS-TX for 1 hour at RT. To stain for virus, the AKO-1-103 antibody to the MAV-1 capsid (264) was used at a 1:5000 dilution. After washing, cells were incubated for 1 hour at RT with Alexa-Fluor 594-conjugated anti-mouse secondary antibody (Invitrogen, Carlsbad, CA) and anti-rabbit FITC (Vector Labs) at a 1:200 dilutions. Samples were mounted with coverslips using ProLong Gold antifade reagent with DAPI

(Invitrogen, Carlsbad, CA), and visualized with an Olympus BX60 upright fluorescent microscope.

CCL2 ELISA. pmBECs were mock-infected or infected with wt MAV-1 or *pm*E314 at an MOI of 5. Supernatants were collected at 0, 6, 12, 24, 48 and 72 hours after infection and assayed for CCL2 expression by ELISA by the University of Michigan Cellular Immunology Core Facility.

Reverse Transcriptase Quantitative PCR. RNA was isolated from cells using Tri Reagent (Molecular Research Center, Inc., Cincinnati, OH) according to the manufacturer's instructions. cDNA was synthesized from total pmBEC RNA using random hexamers and MMLV reverse transcriptase (Invitrogen, Carlsbad, CA). Quantitative PCR was performed using primers to amplify claudin-5 (Mm00727012_s1) on a 7300 RealTime PCR machine from Applied Biosystems (Foster City, CA). All reactions were run in duplex with GAPDH primers as an internal control for normalization of chemokine signals. Briefly, one μL of cDNA was added to reactions containing 2X TaqMan Universal PCR Mix (Applied Biosystems) and 1.25 μL each of 20x primer/probe for the target cytokine and GAPDH. All reactions were for 40 cycles of 15 seconds at 90ºC and 60 seconds at 60ºC. Target gene expression was calculated by normalization to GAPDH and expressed as fold change from control groups (mock infection) using the comparative C_T method.

Ribonuclease protection assay. Total RNA was isolated as above and analyzed by RPA as described previously (257). Chemokine expression was measured using the mCK-5c riboprobe template (Pharmingen), and MAV-1 hexon expression was measured with a custom probe set and normalized to L32 levels as described (68, 258). All reactions used α-^{32}P UTP (Amersham) as the labeling nucleotide. Bands were detected by autoradiography and quantified using a Storm or Typhoon PhosphoImager (GE Healthcare) and ImageQuant software (GE Healthcare).

Measurement of transendothelial electrical resistance. pmBECs were grown on a collagen-IV coated 12-well Transwell® Plate (Corning, Corning, NY) with a 0.4 μm pore size. Cells were grown in the presence of 20% conditioned astrocyte media (a kind gift from A. Andjelkovic) to promote tight junction formation. After 7-10 days of growth on the Transwell plate, cells were mock-infected or infected with either wt MAV-1 or *pm*E314 at an MOI of 5. Transendothelial electrical resistance was measured with an Endohom-12 electrical resistance apparatus (World Precision Instruments Inc., Sarasota, FL) before infection and every 24 hours following infection. Resistance of a blank transwell insert was measured as a background reading and subtracted from all experimental values. Recombinant CCL2 (Protech) was added as indicated to a final concentration of 100 nM. Neutralizing CCL2 antibody (119) or naïve rabbit serum control were added to cultures at a 1:50 dilution to the indicated cells.

MTT assay. To assess pmBEC viability, cells were treated with 3 mg/mL of MTT (Invitrogen, Carlsbad, CA). After two hours the solution was aspirated and 0.05 N acetic

acid in isopropanol was added to solubilize dye crystals. The optical density of a 1:1 mixture of dye and water was measured at 570 nm to determine cell viability. Sample values were normalized to mock-infected values that were set at 100%.

RESULTS

MAV-1 induced inflammation in the brain is reduced in the absence of E3.

Since MAV-1 infection causes fatal encephalitis in susceptible mouse strains (94, 220) we wanted to understand how and why this occurs. To study MAV-1 induced disease we used C57BL/6 mice infected for 8 days, corresponding to a time of acute infection and maximum inflammation in the brain (159). A virus null for E3 expression, *pm*E314, has been previously shown to cause low levels of inflammation in outbred mice despite replicating to titers similar to wt MAV-1 (37; L. Gralinski, unpublished). To test whether this was true in inbred mice, C57BL6/NCI mice were infected with 10^3 or 10^4 PFU of wt MAV-1 or *pm*E314. Hematoxylin and eosin stained brain sections showed the presence of inflammatory cells and significant perivascular edema surrounding blood vessels in wt infected mice (Fig. 3.1A). Fewer inflammatory cells were seen surrounding the blood vessels of mice infected with *pm*E314 than in mice infected with wt virus. In all infected animals the endothelium in the brain was thickened compared to that of mock-infected animals. These results were consistent with those seen previously in outbred mice (37).

To identify the inflammatory cells seen histologically in MAV-1 infected mouse brains, groups of C57BL/6 were mock infected or infected with wt MAV-1 or *pm*E314. Five brains were pooled from each group and analyzed by flow cytometry for the

presence of inflammatory cells eight days post infection. Total leukocytes, as measured by CD45 staining, were significantly increased in the brains of mice infected with wt virus (Fig. 3.1B). Specifically CD4 and CD8 positive T cells, B cells, neutrophils and macrophages were present at higher levels in mice infected with wt MAV-1 compared to mock-infected mice. Mice infected with *pm*E314 showed an intermediate phenotype, with more CD45 positive cells than mock-infected mice but fewer than wt MAV-1 infected mice, consistent with the phenotype seen histologically in both outbred and inbred mice. Mice infected with *pm*E314 virus had fewer CD8 T cells and B cells in their brains than mice infected with wt MAV-1, but equivalent numbers of CD4 T cells, macrophages and neutrophils.

Chemokine and cytokine transcript levels were analyzed to determine the signals recruiting inflammatory cells to the brain. Mouse brain microvascular endothelial cells (MBMECs) were infected for 48 hours and RNA was collected for analysis by ribonuclease protection assay (RPA). CCL1, CCL2, CCL5 and CXCL10 all showed significantly increased levels of expression in cells infected with wt MAV-1 compared to cells that were mock-infected (Fig. 3.1C). These chemokines function to recruit macrophages (CCL1, CCL2, CXCL10), B cells (CCL1) and T cells (CCL5, CXCL10) (reviewed in 43, 172), and CXCL10 also promotes T cell adhesion to endothelial cells (202). MBMEC expression of CCL1, CXCL10 and CCL5 was increased after infection with *pm*E314 compared to mock infection but was lower than in cells infected with wt MAV-1. CCL2 expression in *pm*E314-infected cells was also lower than that measured in wt MAV-1-infected cells and equivalent to levels measured in mock-infected cells.

Minimal expression of RNA for nonchemotactic cytokines was seen following wt MAV-1 or *pm*E314 infection (data not shown).

MAV-1-induces breakdown of the blood brain barrier.

In addition to its ability to recruit monocytes to its site of expression, the chemokine CCL2 has also been shown to mediate disruption of the BBB. Addition of CCL2 to cultured brain endothelial cells causes a decrease in expression of tight junction proteins as well as a loss of the barrier properties necessary for function of the BBB (218, 222). Furthermore, intracerebral injection of CCL2 was shown to be sufficient to cause leakage of peripherally-injected FITC-albumin into the brain, a measure of BBB breakdown (223). Because MAV-1 causes fatal encephalitis in susceptible mouse strains (94, 220) and because we saw increased expression of CCL2 in MAV-1 infected MBMECs, we investigated the ability of MAV-1 to cause breakdown of the BBB in infected mice. C57BL6/NCI mice were infected with 10^3 or 10^4 PFU of wt MAV-1 or mock infected for eight days. Mice were injected with 10% sodium fluorescein dye prior to euthanasia. This dye is only able to access and stain brain tissue when the blood brain barrier is compromised (179). Infection with both doses of virus resulted in high viral loads in the brain as measured by capture ELISA (Fig. 3.2A). Levels of sodium fluorescein in the brain, normalized to levels in the serum, were increased in mice infected with MAV-1, indicating that MAV-1 infection caused a breakdown of the BBB (Fig 3.2B). We observed that the amount of sodium fluorescein staining in the brain correlated with the amount of virus measured in brain tissue: the Pearson correlation coefficient between sodium fluorescein levels and virus loads (as measured by ELISA

values) in mouse brains was 0.871, and this was statistically significant ($P < 0.001$, data not shown).

MAV-1-induced breakdown of the BBB is not dependent on inflammation.

To determine whether MAV-1-induced breakdown of the BBB is mediated by the inflammation resulting from infection or due to direct effects of viral infection of brain endothelial cells, various infection models were employed that lacked an inflammatory response. The first model was to use an E3 null mutant virus, *pm*E314, because infection with *pm*E314 results in a lower level of inflammation in the brain than infection with wt MAV-1 (37, Fig 3.1), despite similar levels of virus in the brain with both infections. C57BL6/NCI mice were infected with 10^3 PFU of wt MAV-1 or *pm*E314 for 8 days and injected with sodium fluorescein. Viral loads were equivalent for wt- and *pm*E314-infected mice (Fig. 3.3A). All infected mice showed breakdown of the BBB as measured by an increase in sodium fluorescein levels compared to mock-infected mice (Fig. 3.3B). Perforin deficient ($pfp^{-/-}$) mice do not have visible inflammation in the brain after infection with MAV-1 (159). Furthermore, these knockout mice do not show any signs of disease during acute MAV-1 infection, a phenotype that is associated with a lack of inflammatory cell response to MAV-1 infection. $Pfp^{-/-}$ and C57BL6/J mice were infected with 10^4 PFU of wt MAV-1 for seven days and injected with sodium fluorescein and viral load and dye were quantitated from the brain tissue. While only C57BL6/J mice showed signs of disease, $pfp^{-/-}$ and C57BL6/J mice showed similar viral loads as measured by capture ELISA (Fig. 3.3C). High levels of sodium fluorescein were measured in the brains of infected C57BL6/J and $pfp^{-/-}$ mice compared to mock infected mice (Fig. 3.3D).

Thus BBB breakdown was equivalent in wt and pfp$^{-/-}$ mice despite the lack of inflammation in pfp$^{-/-}$ mice. T cell deficient mice (α/β and γ/δ T cells) also lack inflammation after MAV-1 infection (159), and MAV-1 infection of these mice resulted in the in the breakdown of the BBB (data not shown). Combined, these results indicate that breakdown of the BBB after MAV-1 infection was not dependent on inflammatory cells as mediators. Furthermore, since mice infected with *pm*E314 had significant sodium fluorescein staining in the brain, these data indicates that the E3-specific induction of chemokines was not necessary for breakdown of the BBB.

Infection of pmBECs with MAV-1.

Based on the results that MAV-1-induced breakdown of the BBB is due to direct effects of viral infection, we further examined MAV-1 infection of brain endothelial cells. We established a primary mouse brain microvascular endothelial cell (pmBEC) culture system to enable infection of brain endothelial cells in an isolated and controlled environment. Culture and infection of primary cells is preferable to use of established brain endothelial cell lines, such as bEnd.3 cells, because several functional features and characteristics of endothelial cell lines are unlike those of primary cells. For example, in bEnd.3 cells several tight junction proteins are aberrantly expressed in the cytoplasm instead of the cell membrane, and VCAM expression is lost with increased passage (212, 218). We used fluorescence microscopy to show that pmBECs took up DiI-labeled acetylated LDL, an important functional characteristic of endothelial cells (Figure 3.4A) (245). Flow cytometric analysis was used to show that the pmBECs uniformly expressed high levels of CD31, ICAM and VCAM, markers that should be expressed by

endothelial cells (91), after one passage (Figure 3.4B, data not shown). The cells used in the subsequent experiments were all passed one time before use. To establish that pmBECs could be infected by MAV-1, we added wt virus at an MOI of 5 and analyzed virus yield at different times post infection. MAV-1 productively replicated in pmBECs (Fig. 3.4C) as demonstrated by the increase over input virus measured in infected cells at two to five days post infection. Because MAV-1 infection caused breakdown of the BBB and CCL2 can itself cause a breakdown of the BBB, we determined whether MAV-1 infection induces increased levels of CCL2 in primary cells. We infected pmBECs with wt MAV-1 or *pm*E314 at an MOI of 5 and assayed supernatants for the presence of CCL2 by ELISA. At 48 hours post infection pmBECs infected with wt MAV-1 but not *pm*E314 showed a large increase in CCL2 expression compared to mock infected cells (Fig. 3.4D).

Tight junction protein localization after MAV-1 infection.

Tight junction (TJ) formation is important for maintaining the function of the BBB (247), and viral-induced disruption of TJs is associated with breakdown of the BBB (55). To determine whether infection with MAV-1 results in loss of tight junction formation, we infected pmBECs with MAV-1 and then immunofluorescently stained them to determine the location of their TJ proteins. ZO-2 is an intracellular peripheral membrane protein and binds to transmembrane proteins of the tight junction such as occludin and claudins; connecting them to the actin cytoskeleton (70, 135, 177, 271). Occludin and the claudins are transmembrane proteins with extracellular domains that work in conjunction to form tight junctions (104, 163; reviewed in 55, 99, and 140). Disruption of these proteins is associated with vascular leakiness and has been observed

in CNS diseases such as HIV-1 encephalitis and also in dengue infection (55, 140). ZO-2 staining of mock-infected cells was localized to the periphery of the cells, creating a cobblestone-like appearance, consistent with the expected staining pattern (223). This staining pattern and the level of peripheral staining were unchanged 48 hours after infection with either wt MAV-1 or *pm*E314 (Fig. 3.5A), even in cells that showed significant staining for the MAV-1 capsid. ZO-2 expression appeared to be increased in the cytoplasm of some infected cells. Results were similar for timepoints up to 5 days post infection (data not shown). Occludin protein levels were also analyzed at 48 hours post-infection and mock-infected cells showed the expected occludin staining pattern at the peripheral cell membrane. Despite the presence of intact nuclei and a healthy cell monolayer (data not shown), occludin staining was decreased at the periphery of cells that showed positive staining for the MAV-1 capsid (Fig. 3.5B). This decrease in occludin at the cell membrane occurred in cells infected with both wt MAV-1 and *pm*E314. Some changes in intracellular occludin staining were also observed in infected cells. Another TJ protein, claudin-5, also showed decreased expression at the peripheral membrane in cells infected with either wt MAV-1 or *pm*E314 (Fig. 3.5C) compared to mock-infected cells. Infected cells appeared to show an overall decrease in claudin-5 staining compared to mock-infected cells which was further examined below. Combined, these results indicate that MAV-1 infection resulted in a loss of surface expression of some tight junction proteins; furthermore, this was not dependent on the presence of E3.

We examined whether transcriptional or post-transcriptional changes were responsible for the decreased TJ protein expression seen at the cell membrane. Steady-state claudin-5 transcript levels were analyzed by RT-qPCR using RNA isolated from

pmBECs 48 hours after infection. Claudin-5 mRNA levels, relative to GAPDH expression, were unchanged in cells infected with wt MAV-1 or *pm*E314 compared to mock-infected cells (Fig 3.5D). This indicates that the decrease in cell surface expression of claudin-5 protein observed in the immunofluorescence analysis did not occur at a transcriptional level. GAPDH signals reached threshold levels at similar cycle times in both mock-infected and virus-infected RNA samples indicating that MAV-1 infection did not cause a global decrease in transcription.

Barrier properties in pmBECs after MAV-1 infection.

Because MAV-1 infection resulted in a decrease in expression of some tight junction proteins at cell junctions (Fig. 3.5A, B, C), it was possible that infection could decrease the barrier properties of endothelial cells. Fully functioning brain endothelial cells should have a high transendothelial electrical resistance (TEER) (56, 82). To determine whether MAV-1 infection results in a loss of barrier properties in brain endothelial cells, pmBECs were grown on transwell plates so their electrical resistance could be measured. Cells were either mock-infected or infected with wt MAV-1 or *pm*E314 at an MOI of 5. There was no drop in TEER after cells were mock-infected (Fig. 3.6A). After 48 hours of infection with either wt MAV-1 or *pm*E314, there was a dramatic decrease in TEER, reducing resistance to nearly background levels. Although *pm*E314-infected cells showed a slight lag in their TEER decrease compared to wt MAV-1-infected cells, all infected cells showed a substantial loss of resistance by 72 hours post infection.

To determine how MAV-1 infection caused this drop in the barrier properties of pmBECs, cell metabolic activity was assessed by MTT assay at both 48 and 72 hours post infection as a measure of viability. At 48 hours post infection, pmBECs infected with either wt MAV-1 or *pm*E314 showed viability that was 50% that of mock-infected cells (Fig. 3.6B), although only cells infected with wild type virus showed a decrease in barrier properties as measured by TEER. At 72 hours post infection, MTT assay showed that infection with wt MAV-1 reduced pmBEC metabolic activity to 34% while cells infected with *pm*E314 remained at 50% metabolic activity (Fig. 3.6C). Although cells infected with *pm*E314 showed the same viability as that measured at 48 hours post infection, the TEER of these cells decreased to almost background levels by 72 hours post infection. Thus although MAV-1 infection resulted in a drop in the metabolic activity of infected cells, this change did not correlate with the loss of electrical resistance.

A second possible mechanism for MAV-1 infection-induced decrease in barrier properties of pmBECs is through the effects of CCL2 expressed by infected cells. As noted previously, CCL2 added to primary brain endothelial cultures causes a decreased expression of tight junction proteins at cell borders and a loss of electrical resistance (222). To determine the role of CCL2 in mediating MAV-1-induced changes in TEER, cells were mock infected, infected with wt MAV-1 or *pm*E314, and a CCL2 neutralizing antibody was added to the samples at 72 hours post infection. Mock infected cells had a high TEER that was decreased after the addition of recombinant CCL2 (Fig 3.6D). Addition of a CCL2 neutralizing antibody to CCL2-treated, mock infected samples restored their TEER to pre-treatment levels. In contrast, addition of the neutralizing CCL2 antibody had no effect on the TEER of pmBECs infected for 72 hours with either

wt MAV-1 or *pm*E314, indicating that CCL2 was not responsible for the decrease in TEER caused by MAV-1 infection at this timepoint.

DISCUSSION

We demonstrate here that MAV-1 infection, in addition to causing fatal encephalitis in susceptible mouse strains, causes breakdown of the BBB. Characterization of the inflammatory response to MAV-1 infection in C57BL6 mice showed increased numbers of T cells, B cells, neutrophils and macrophages in infected mouse brains (Fig. 3.1A). MAV-1 induced inflammation in inbred mice is partially dependent on the presence of the E3 proteins, as shown by an intermediate inflammatory phenotype. Previous experiments with MAV-1 have shown that mice lacking $CD8^+$ T cells do not develop acute signs of disease after infection (159). Interestingly, cytotoxic $CD8^+$ T lymphocytes were present in significantly higher numbers in the brains of animals infected with wt MAV-1 than animals infected with *pm*E314, correlating with the reduced pathogenesis of the E3 null virus. Breakdown of the BBB occurred in animals deficient in T cells (Fig. 3, data not shown) indicating that CD8 T cells are not necessary for this process.

Pathogenic viruses such as HIV-1, dengue, LCMV and West Nile virus have all been shown to cause breakdown of the BBB and/or disruption of endothelial junctions through a variety of means (1, 5, 140, 232, 254). We found that MAV-1 infection caused breakdown of the blood brain barrier as assayed by sodium fluorescein dye penetration of brain tissues (Fig. 3.2). Use of various infection models deficient in inflammation in the brain revealed that MAV-1 induced breakdown of the BBB was largely independent of

the presence of inflammatory cells (Fig. 3.3). Combined, these data indicate that MAV-1 infection causes breakdown of the BBB during acute infection; however, signs of disease and lethality of infection depend on inflammatory cells being recruited to the site of infection and crossing into the brain parenchyma (37, 159; Fig. 3).

MAV-1 infects endothelial cells throughout the mouse, and the highest viral loads are found in the brain and spinal cord (42, 113). Thus, given that endothelial cells are the major structural component of the BBB (reviewed in 196), it is not entirely surprising that MAV-1 infection can cause disruptions in the BBB. MAV-1 infection of pmBECs caused a loss of barrier properties in the endothelial cells as measured by decreased tight junction staining and a drop in transendothelial electrical resistance (Fig. 3.5 and Fig. 3.6). Loss of tight junction protein staining was observed 48 hours after MAV infection despite levels of RNA transcription equivalent to those seen in mock-infected cells. Also at 48 hours post infection wt MAV-1 caused a substantial decrease in TEER while infection with *pm*E314 did not cause a decrease in barrier properties. This occurred despite infection with either virus causing a 50% decrease in cell metabolic activity, measured as a surrogate for cell viability, compared to mock-infected cells (Fig. 3.6A and B). Thus loss of cell metabolic activity did not completely correlate with loss of barrier properties in infected pmBECs. Despite these results, a decrease in cell viability is consistent with causing loss of functional properties in infected endothelial cells (282), and decreased pmBEC cell metabolic activity and viability may contribute to the decrease in TEER seen after MAV-1 infection.

Although some other viruses that cause CNS disease do not primarily infect endothelial cells (1, 54, 232), they still cause breakdown of the BBB by disrupting tight

junction formation and altering adhesion molecule expression on brain endothelial cells. CCL2 expression is often induced by virus infection, and CCL2 has been shown to be sufficient for disruption of tight junctions in endothelial cell culture and also for BBB breakdown in mice (219, 222, 223). Studies have shown that HIV-1 and dengue virus mediate disruption of tight junctions through CCL2 signaling (67, 140). MAV-1 infection of pmBECs also stimulates secretion of CCL2 (Fig. 3.4D). However, infection of pmBECs with the MAV-1 mutant *pm*E314 did not induce CCL2 production although *pm*E314 infection of C57BL/6 mice did cause breakdown of the BBB (Fig. 3.4D, Fig. 3.3A) and a loss of TJ protein expression at cell junctions (Figs. 5 B and C). Furthermore, addition of CCL2 neutralizing antibody did not restore the TEER of MAV-1-infected pmBECs (Fig 3.6D). Together these results combine to suggest that MAV-1 infection can cause a decrease in tight junction protein expression at cell borders and breakdown of the BBB in a CCL2-independent manner. However, it is likely that CCL2 contributes to BBB disruption after wt MAV-1 infection, because CCL2 expression is induced during these infections.

While these data indicate that CCL2 expression is non-essential for loss of pmBEC barrier properties following MAV-1 infection at 3 days post infection, it would be useful to examine the role of CCL2 at additional timepoints and in *in vivo* infections. It is possible that breakdown of the BBB would be delayed in CCL2-deficient mice, allowing inflammatory cells to aid in viral clearance without resulting in CNS pathology. Such studies would allow for a more complete understanding of how MAV-1 infection causes breakdown of the BBB.

The mechanism by which MAV-1 infection alters TJ protein expression is not yet clear. The studies presented here indicate TJ transcript levels for one TJ protein, claudin-5, were unaltered after MAV-1 infection and that occludin and claudin-5 protein levels were similar between mock and infected pmBEC samples. These data are consistent with the increase in occludin and claudin-5 cytoplasmic staining coincident with decreased junctional staining seen in infected cells compared to mock infected cells. That is, the low level of peripheral staining of two TJ proteins observed in wt MAV-1 and *pm*E314 infected cells appears to be balanced by the increased cytoplasmic staining levels in these samples.

Numerous studies have examined the function and expression of tight junction proteins in maintaining the BBB or epithelial barriers (61, 134, 226). One important molecule controlling TJ protein localization is Rho kinase. Rho kinase signaling is often triggered in cells that detect CCL2 and this signal causes a decrease in cell surface expression of TJ proteins after viral infections (88, 177, 271) . Nonetheless, Rho kinase is unlikely to be the primary determinant of MAV-1-induced alteration of TJ protein expression because infection with *pm*E314 causes breakdown of the BBB and loss of peripheral membrane localization of tight junction proteins despite failing to induce CCL2 production in infected cells. One possible way RhoK could be involved in the MAV-1-induced decrease in peripheral membrane expression of TJ proteins is if MAV-1 infection causes a non-CCL2 dependent increase in Rho kinase signaling.

Cytokines other than CCL2 have also been shown to cause breakdown of the BBB. Primary bovine brain microvessel endothelial cells treated with low concentrations of TNF-α show an increase in permeability as measured by dye migration across cell

monolayers (155). TNF-α signaling is necessary for West Nile virus-induced breakdown of the BBB (254). Recent studies of West Nile virus showed that TNF-α is necessary for clearance of virus in the brain, a process that is dependent on T cells and macrophages and their ability to access CNS tissues (211). TNF-α also mediates BBB permeability during sepsis induced by *E. coli* and *S. pneumoniae* infection (238). Other cytokines including IL-1beta and interferon gamma have also been shown to decrease the barrier properties of brain endothelial cells (270). These cytokines have not yet been measured MAV-1 infection of pmBECs and could contribute to MAV-1-induced breakdown of the BBB.

Other stimuli that alter TJ protein function and localization include protein kinase C (PKC) signaling, which is related to intracellular calcium levels, cAMP levels, TJ protein phosphorylation states and mitogen-activated protein kinase (MAPK) signaling (reviewed in 88). Low levels of intracellular cAMP can result in low TEER values in brain endothelial cells, and high cAMP levels help to stabilize tight junction formation and promote high TEER values (110, 189). Phosphorylation levels on TJ proteins are important for the barrier properties of tight junctions (207, 271), and specific phosphorylation and dephosphorylation events are associated with changes in paracellular permeability. The RhoA signaling pathway is also involved in the assembly and disassembly of tight junctions (112). RhoA signaling pathways include proteins such as Rho kinase that are involved in post-translational modifications of myosin light chain and other proteins that are important for control of actin and microtubule cytoskeletal networks (89, 169). These networks interact directly with TJ proteins such as ZO-1 and ZO-2. Thus altered Rho signaling can lead to cytoskeletal contractions that are able to

disrupt intercellular junctions. MAP kinases are activated in response to extracellular signals including stress and growth factors. Oxidative stress results in increased ERK1/2 signaling that ultimately causes decreased expression of occludin, ZO-1 and ZO-2 at the borders of brain endothelial cells (74, 134). A similar decrease in TJ protein expression is observed after ERK1/2 activation by the HIV-1 Tat protein (7, 183). While there is a precedent for viral-induced CCL2-independent disruptions in TJs (183), it remains to be determined what pathways are involved in regulation of TJ protein expression after MAV-1 infection.

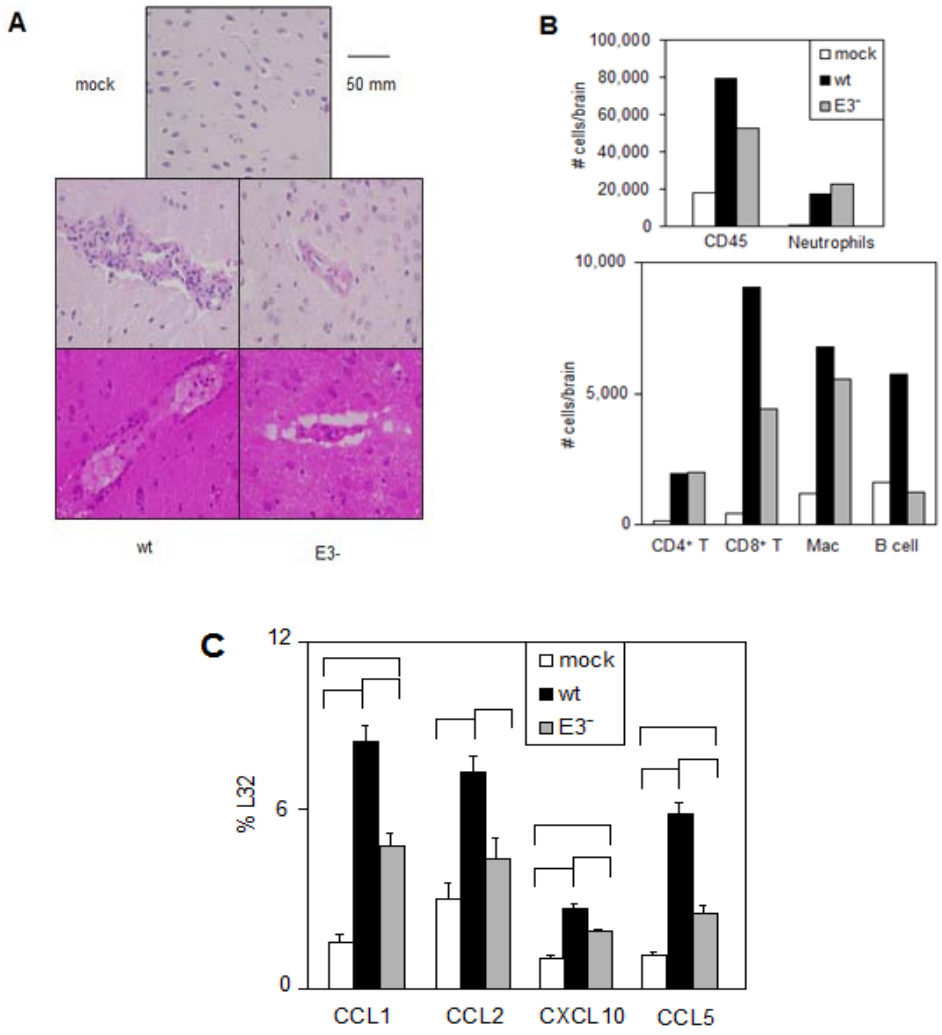

Figure 3.1. Inflammation in the brains of mice infected with MAV-1. A. Mice were infected with 10^3 or 10^4 PFU of the wt MAV-1 or *pm*E314 ($E3^-$) virus or mock-infected for 8 days. Brain sections were mounted on slides and stained with hematoxylin and eosin and examined by microscopy. B. C57BL6/NCI mice were mock infected or infected with 10^3 PFU of wt MAV-1 or *pm*E314. Eight days post infection, brains were analyzed for the presence of inflammatory cells by flow cytometry. Cell types are indicated on the graph: Mac, macrophages. Each group represents the number of cells per brain from analysis of five brains that were pooled for staining and is representative of three experiments for wt MAV-1 and mock samples and two experiments for the *pm*E314 samples. C. MBMECs were infected at an MOI of 5 with wt MAV-1 or *pm*E314 as indicated for 48 hours and RNA analyzed for chemokine expression using the mck-5c probe set (Pharmingen). Values are shown as percentage expression relative to expression of RNA for the ribosomal protein L32. Brackets indicate a P value ≤ 0.01 for the Student's t test. Transcript levels shown are the mean of triplicate infections and are representative of three experiments.

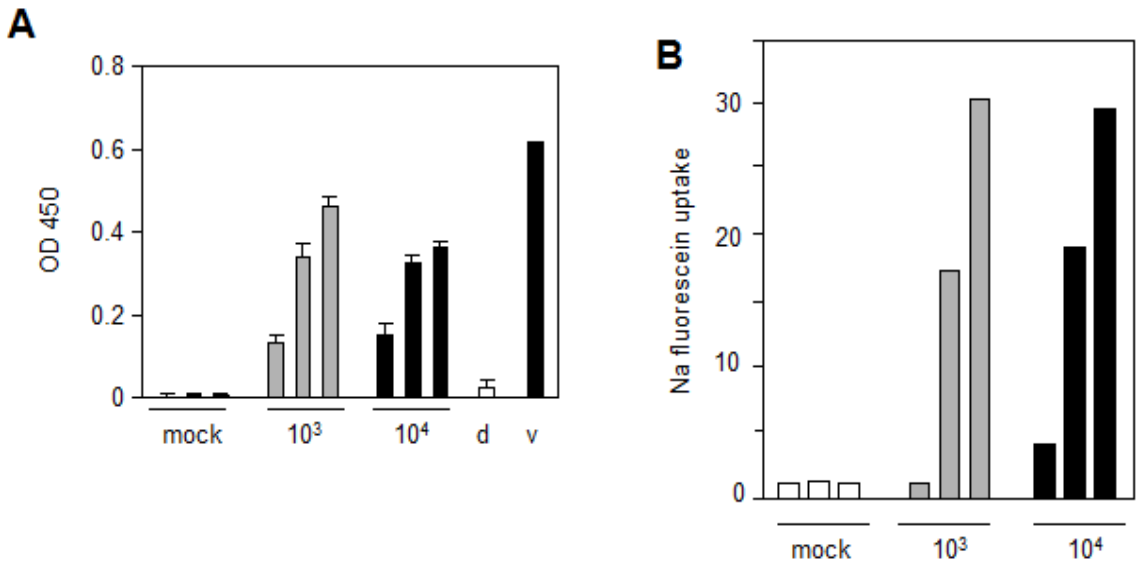

Figure 3.2. MAV-1-induced breakdown of the blood brain barrier. C57BL6/NCI mice were infected with 10^3 or 10^4 PFU of MAV-1 for eight days. Ten minutes before euthanasia, mice were injected with sodium fluorescein dye to measure the permeability of the blood brain barrier. Bars in A and B are representative of individual mice and are presented in the same order in each figure. A. Viral load was measured by capture ELISA, including a tissue with dye control (d) to insure that Na fluorescein did not interfere with virus detection in the ELISA. A positive control of virus stock (v) was included and each individual mouse was assayed in triplicate. B. Levels of sodium fluorescein in the brain were quantified and are presented normalized to dye levels in serum. Results shown are representative of three experiments.

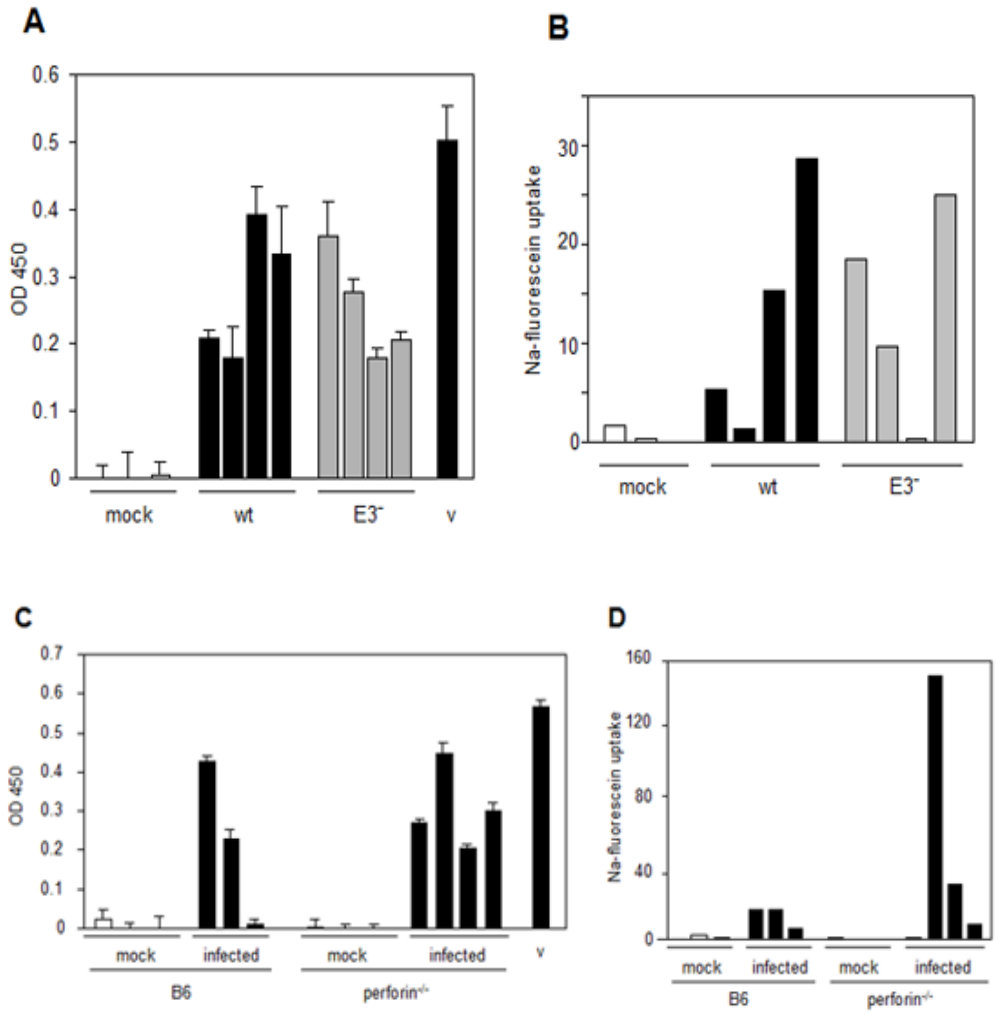

Figure 3.3. MAV-1-induced breakdown of the BBB is not dependent on inflammation. A and B. C56BL/6J and perforin deficient mice were infected with 10^4 PFU of wt MAV-1 for 7 days. Before euthanasia, mice were injected with sodium fluorescein dye to measure the permeability of the blood brain barrier. Bars in A and B represent individual mice and are presented in the same order in each figure. A. Viral load was assayed by capture ELISA with virus stock (v) used as a positive control. Each individual mouse was assayed in triplicate. B. Sodium fluorescein levels in the brain were quantitated relative to levels in the serum. A and B are representative of two experiments. C and D. Mice were infected for 8 days with wt MAV-1 or *pm*E314 and injected with sodium fluorescein before euthanasia. Bars in C and D represent individual mice and are presented in the same order in each figure. C. Viral load in the brain was measured in individual mice in triplicate by capture ELISA. MAV-1 viral stock (v) was assayed as a positive control. D. Na fluorescein in the brain of each mouse was quantitated and normalized to the amount of dye present in the serum. C and D are representative of three experiments performed.

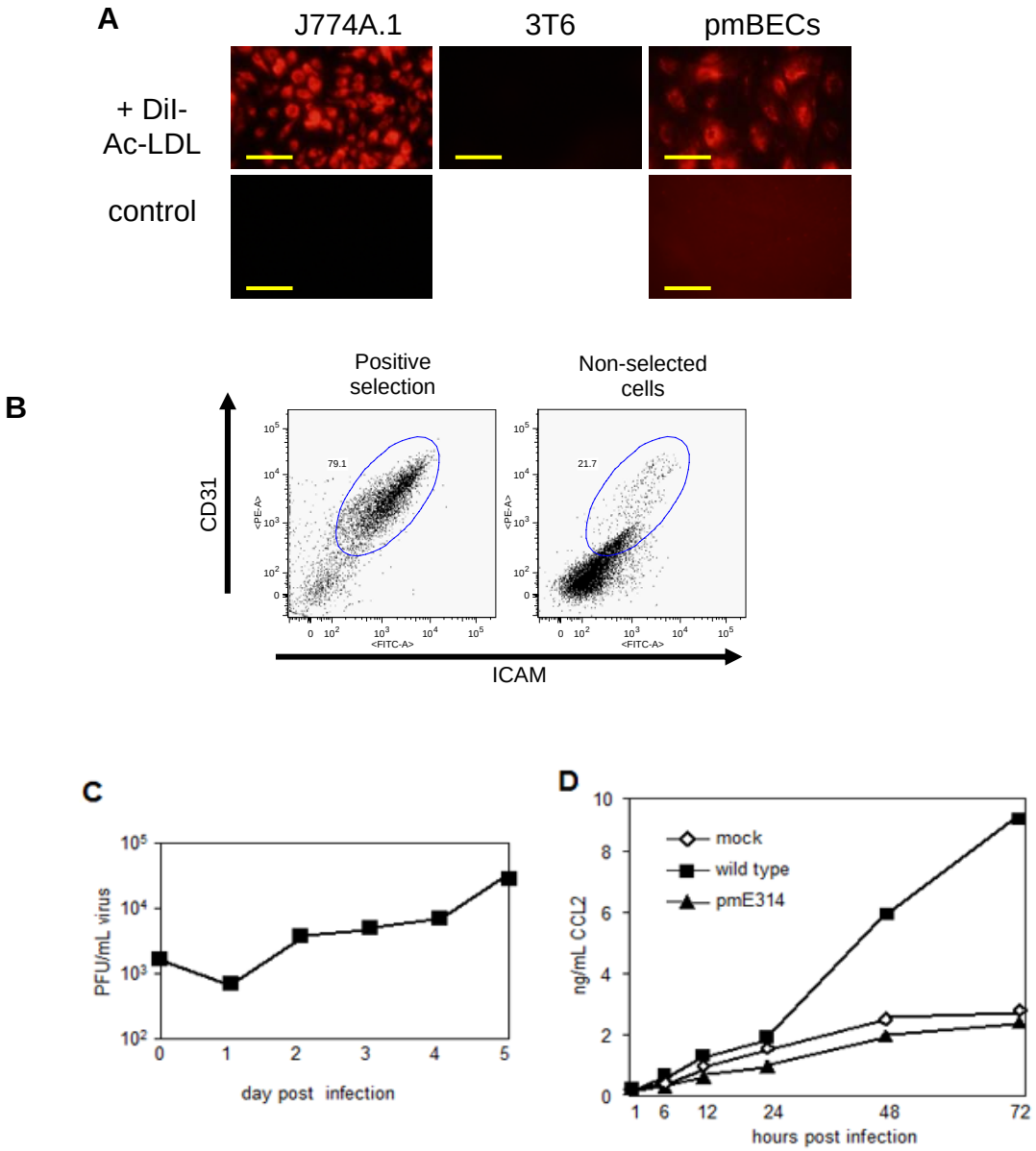

Figure 3.4. Infection of pmBECs with MAV-1. A. pmBECs, mouse 3T6 cells (negative control) or mouse J774A.1 macrophages (positive control) were incubated with DiI-labeled acetylated LDL and examined by fluorescence microscopy. Untreated cells were also imaged. Bars indicate 100µm. B. ICAM and CD31 expression were measured on first passage pmBECs by flow cytometry. Cells that were not selected by the anti-CD31-labeled beads were also analyzed. Circled cells represent a double positive population, gating is based on unstained controls. The number given is the percentage of cells falling within the double positive gate. C. pmBECs were infected with wt MAV-1 at an MOI of 5. Cells and supernatants were harvested on the days indicated and assayed for infectious virus by plaque assay. Results are representative of two experiments. C. pmBECs were infected with wt MAV-1 or *pm*E314 at a MOI of 5 or were mock infected. Supernatants were collected at the indicated time points and assayed in duplicate for CCL2 by ELISA. Results are representative of two experiments.

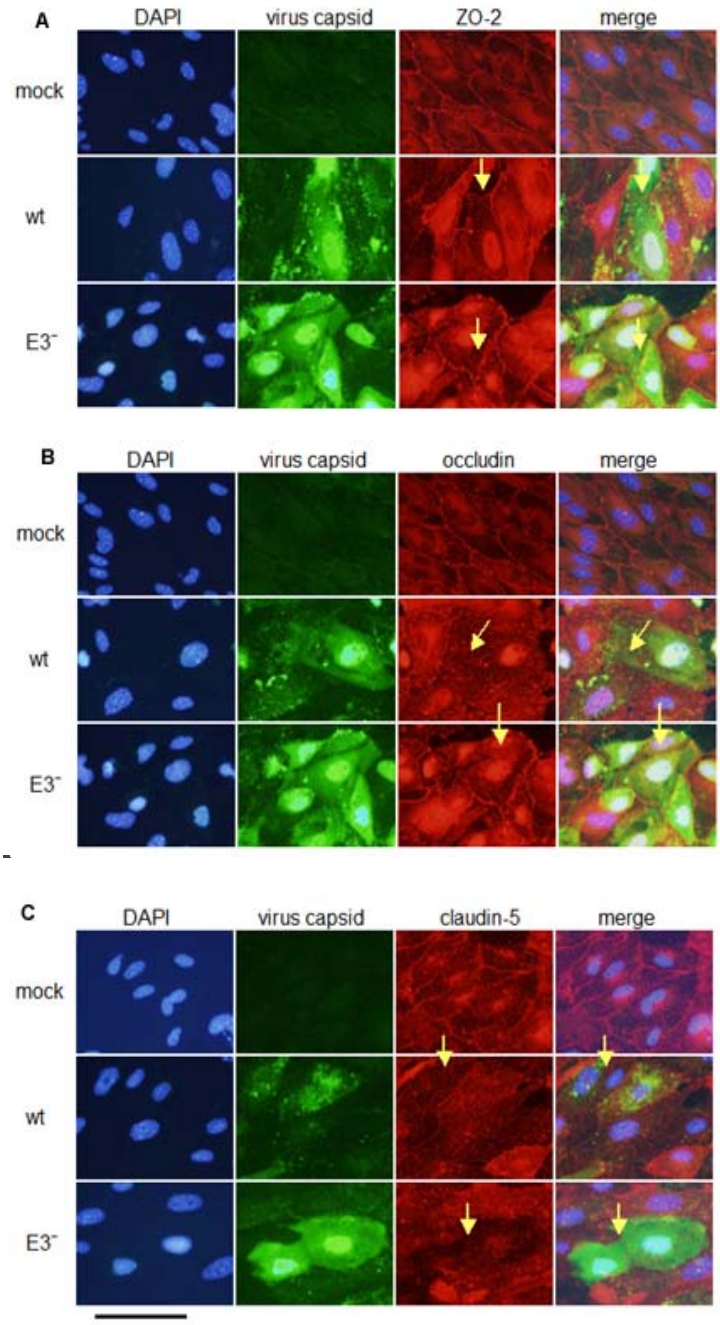

Figure 3.5. Tight junction protein localization after MAV-1 infection. pmBECs were mock-infected or infected with wt MAV-1 or *pm*E314 at an MOI of 5 for 48 hours and tight junction proteins were visualized by immunofluorescence. A. ZO-2 expression B. occludin expression, and C. claudin-5 expression. Images are all representative of at least three experiments each from separate primary cell preparations. Image exposure time was constant between the mock, wt and *pm*E314 pictures for each protein assayed and all magnifications were identical. D. claudin-5 steady-state mRNA levels 48 hours after mock infection, infection with wt MAV-1 or *pm*E314.

Figure 3.5D

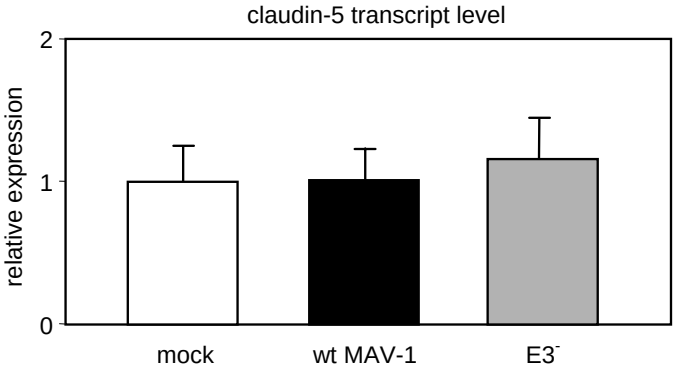
claudin-5 transcript level
relative expression
2
1
0
mock
wt MAV-1
E3-

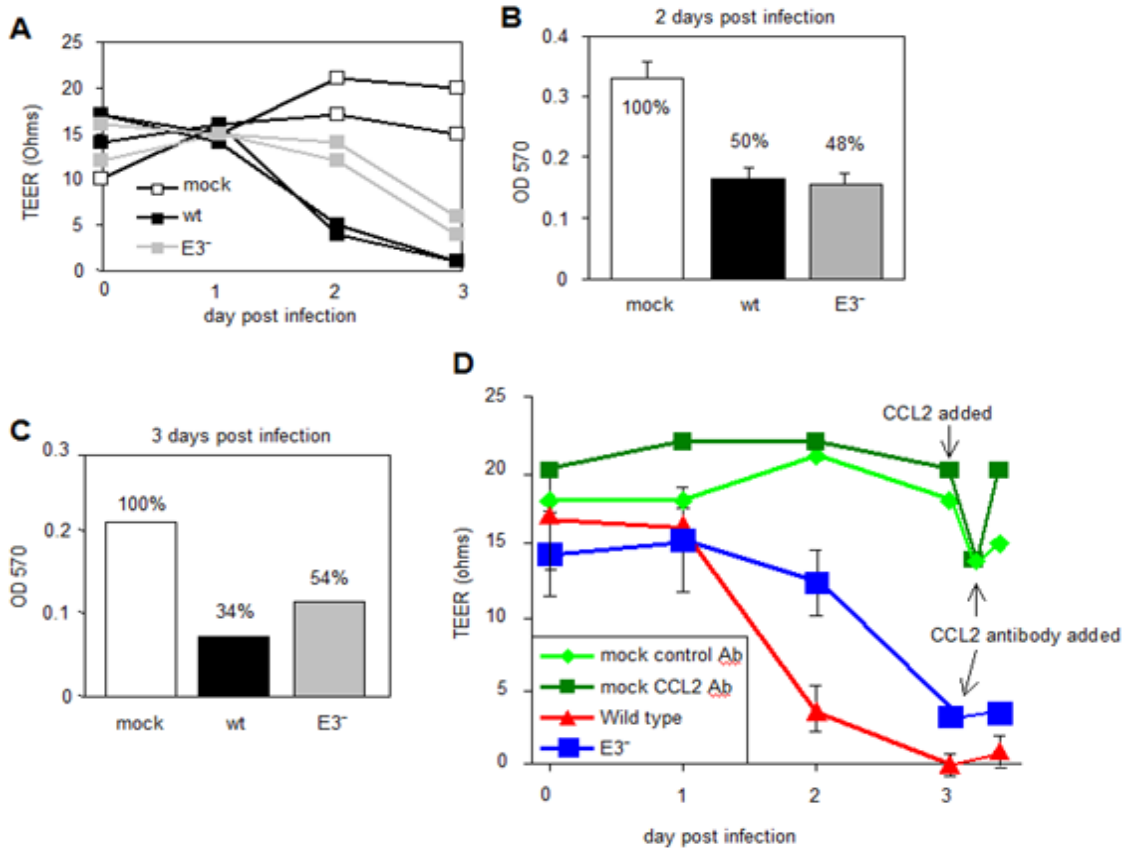

Figure 3.6. Barrier properties in pmBECs after MAV-1 infection. A. pmBECs were grown to confluency on 0.4 mm pore size transwell plates with astrocytes grown in the lower chamber to promote tight junction formation. Cells were infected with wt MAV-1 or *pm*E314 at an MOI of 5 or mock infected. Resistance was measured at 24-hour intervals. Mitochondrial metabolic activity as a surrogate for cell viability was measured by MTT assay two days post infection (B) in a replicate experiment and at 72 hours post infection (C) on the same cells as in A. Results are representative of four experiments for A, three experiments for B and two experiments for C. D. TEER was measured in cells infected with wt MAV-1 or *pm*E314 for three days. Recombinant CCL2 was added to mock infected cells after three days, and one hour later CCL2 neutralizing antibody or naïve rabbit serum was added to all cells. Note that after 3 dpi the x-axis is on a different scale.

Chapter IV

Cellular protein interactions with MAV-1 E3 gp11k

ABSTRACT

While the human adenovirus E3 gene products have immunoregulatory functions, the function of the MAV-1 E3 proteins is currently unknown. An E3 null virus, *pm*E314, is less pathogenic than wild type MAV-1 in infection of outbred Swiss mice (37), indicating that the E3 proteins play a role in pathogenesis. We generated stable cell lines expressing MAV-1 E3 gp11k (the only E3 protein detected after wild type infection of cultured cells (22) with a C-terminal tandem affinity purification (TAP) tag in order to isolate cellular proteins that interact with E3 gp11k. E3 gp11k expression was confirmed by Western blot, and proper E3 gp11k location was observed by immunofluorescence. Preliminary mass spectrometry results identified several proteins that may interact with E3 gp11k; these results will need to be independently confirmed by immunoprecipitation or other means.

INTRODUCTION

The E3 regions of adenoviruses code for protein products that help the virus evade the host immune response (107). The function of the MAV-1 E3 gene products is currently unknown, though previous studies have given some clues as to their function.

Only one E3 protein is observed after wild type MAV-1 infection, although three mRNA transcripts have been detected (23). Infection with mutant viruses expressing any one of the three E3 transcripts is less lethal than infection with wild type MAV-1, as demonstrated by LD_{50} experiments (22). Similarly, *pm*E314, an E3 null virus, has an LD_{50} 5-6 log units higher than wild type virus (37), indicating that E3 plays an important role in the pathogenesis of MAV-1. The difference in LD_{50} between wild type and *pm*E314-infected mice is not due to a growth defect in the mutant virus, because they have identical growth curves *in vitro* and replicate to similar titers *in vivo* (37; unpublished data).

Histological studies have shown that infection with MAV-1 causes significant inflammation in the brain and spinal cord of infected animals (131). The endothelium is activated and perivascular edema is seen around blood vessels in the brain in mice infected with MAV-1 (113, 159). Infection with *pm*E314 results in less inflammation in the brain and spinal cord than infection with wild type MAV-1 (37). Thus, in contrast to the human adenovirus E3 proteins, which are involved in evasion of the host immune response, this evidence indicates that the MAV-1 E3 products are involved in stimulating the host immune response. One reason for a virus to stimulate an inflammatory response to infection is to promote the presence of inflammatory cells that the virus replicates in to enhance viral spread. It is possible that MAV-1 E3 exists to promote this function, or that the E3-dependent recruitment of inflammatory cells serves to promote viral persistence in these cells similar to Theiler's murine encephalomyelitis virus (225). The only E3 product to be detected after wild type MAV-1 infection, gp11k, has been characterized *in vitro* (23). MAV-1 E3 gp11k is a glycoprotein with a core molecular

weight of 11 kDa that migrates at 14 kDa on an SDS-PAGE gel. The protein can be detected starting 16 hours post infection, and immunofluorescence studies demonstrated that E3 gp11k localizes to the endoplasmic reticulum after infection. Further biochemical studies indicated that E3 gp11k is a peripheral membrane protein, likely localized to the endoplasmic reticulum by binding to another, integral membrane protein. Despite these studies, the function of E3 gp11k is still unknown.

One common method used to discover the function of an uncharacterized protein is to search for proteins with which it has biochemical interactions (213). If two proteins are in a complex together, then it is probable that they will have a common or related function, or influence each others' function. Thus by identifying known proteins that interact with the uncharacterized protein of interest, one can begin to discern the role played by the uncharacterized protein. Potentially interacting proteins can be isolated by several affinity purification methods including immunoprecipitation, glutathione S-transferase (GST) pulldown, yeast two-hybrid, and TAP (128, 208, 210). After isolation of protein complexes, identification of interacting proteins can be achieved by mass spectrometry analysis. Then the interaction should be confirmed by co-immunoprecipitation or other studies.

Given the demonstrated role for E3 in the pathogenesis of MAV-1 (37), we sought to determine the function of E3 gp11k by determining what cellular proteins it binds. TAP was selected as a method to isolate interacting proteins because of the dual isolation and gentle wash conditions (193) used in this technique. Previous studies (a GST pulldown and a yeast two-hybrid screen) attempting to isolate E3 gp11k-interacting proteins had failed to yield consistent and reliable results (Spindler et al, unpublished).

We hoped that the advantages of the TAP system and the creation of cell lines that stably expressed E3 gp11k with the TAP tag would enable us to isolate true interacting proteins.

METHODS

Cloning. The MAV-1 E3 gp11k sequence was mutated to include a full or partial Kozak sequence (130) and inserted into the pFG9 vector, a kind gift from Colin Duckett. pFG9 contains the TAP sequence under control of the EF1α promoter and GFP under the control of the UbiC promoter and is based on the replication defective lentiviral vector FUGW (149) which was modified to pFG12, (187). The E3 gp11k sequence was PCR amplified from the cDNA plasmid ZU14 (22) using primers that introduced a BamHI site at the 5' end and a full Kozak initiation sequence or a shortened Kozak sequence, and a NotI site at the 3' end (Fig. 4.1 A and B). The PCR product was digested with BamHI and NotI and was ligated with BamHI- and NotI-digested pFG9. In the resulting constructs the TAP tag coding sequence is fused in frame downstream of the C terminus coding sequence of gp11k. The final constructs were named pFG9-MAVE3A and pFG9-MAVE3B (having the full and shortened Kozak sequences respectively), and the DNA was sequenced to confirm proper construction.

Generation of the E3 TAP lentiviruses and stable cell lines. Human 293 cells were transfected with the lentivirus E3-TAP plasmids (pFG9-MAVE3A or B), pRSSREV and pRRE plasmids containing the HIV packaging sequence (127), and pHCMVG containing the vesicular stomatitis virus G protein (34), using calcium phosphate precipitation. Briefly, 5 μg of each plasmid was mixed with 250 mM $CaCl_2$ and 25 mM HEPES

containing sodium phosphate, pH 7.9. The solution was then added to the 293 cells along with media (Dulbecco's modified Eagle media (DMEM with 10% serum) containing 25 μM chloroquinone to aid with transfection efficiency. After 8 hours the media was changed to DMEM with 10% serum (no chloroquinone). 40 hours after transfection, 293 cell supernatant containing the replication-deficient, E3-TAP containing lentivirus was filtered through a 0.45 μm Millex-HV filter (Millipore # SLHV R25 LS) and added to mouse NIH 3T6 fibroblasts at a high MOI. (3 mL of supernatant was added per 35 mm well of cells.) The resulting cell lines obtained after lentivirus infection (and integration of the retroviral constructs) were named 3T6-E3-TAPA and 3T6-E3-TAPB and grown as described below. 3T6-E3-TAPA and 3T6-E3-TAPB were visualized by fluorescence microscopy using an Olympus BX60 upright microscope to detect GFP expression 3 days post infection. The parental NIH 3T6 cells and 3T6-E3-TAPA and 3T6-E3-TAPB cell lines were grown in DMEM media (Gibco) with 2 mM glutamine and 5% heat-inactivated calf serum (Gibco).

Western blotting. Cells were lysed in 1% Triton X-100 in 100 mM NaCl, 25 mM HEPES, 10% glycerol, 10 mM EDTA buffer with protease inhibitors: 10 μg/mL aprotinin, 1 mM PMSF, 2.6 mM benzamidine, 5 μg/mL leupeptin and 1.4 μg/mL pepstatin. Cells were lysed with 1 mL of lysis buffer per 150 mm plate of cells. Cell lysates were electrophoresed on a 10% SDS-PAGE gel with Rainbow Marker (Amersham, RPN 756) as a size standard. Proteins were transferred to a nitrocellulose membrane and blocked with 5% nonfat dry milk in TBS-Tween (20 mM Tris pH 8.0, 135 mM NaCl, 0.1% Tween-20) for 2 hours. A monoclonal anti-E3 antibody, 11H9 (69) was

used to detect MAV-1 E3 gp11k expression. The membrane was washed with TBS-Tween. The secondary antibody was HRP-conjugated sheep anti-mouse (Amersham, NA931V) and visualization occurred after incubation with Pierce SuperSignal West Pico Chemiluminescent Substrate (Pierce, Rockford, IL).

Tandem affinity purification. 3T6 cells or 3T6-E3-TAPA and B cells were grown in bulk (30 150 mm plates) and lysed as above. Cell lysates were incubated for 2 hours at 4°C with 400 mL of IgG sepharose beads (Amersham, #17-0969-01) in IPP150 buffer (0.1% NP-40, 150 mM NaCl, 10 mM Tris-Cl pH 8.0). After incubation, the beads were washed twice with IPP150 buffer and incubated at 16°C for 2 hours with 20 units of AcTEV Protease (Invitrogen, Carlsbad, CA) in IPP150 buffer with 0.5 mM EDTA and 1 mM DTT. Eluate from the IgG beads was collected and added to calmodulin 4B beads (Amersham, #17-0529-01) with buffer (IPP150 with 10 mM β-mercaptoethanol, 1 mM Mg-acetate and 2 mM $CaCl_2$). After incubation at 4°C for 1 hour, the E3-TAP protein and any associated proteins were eluted at room temperature with IPP150 with 10 mM β-mercaptoethanol, 1 mM Mg-acetate, 1 mM imidazole and 2 mM EGTA (total elution volume of 2.5 mL) for 10 minutes. The final eluate was analyzed as below.

Coomassie and silver staining. Purified proteins were concentrated approximately 10X using Amicon Ultra spin columns before gel analysis (Millipore, Billerica, MA). Cell lysates and proteins purified through tandem affinity purification were electrophoresed on a 10% SDS-PAGE gel. For Coomassie staining the gel was fixed with 45% acetic acid and 45% methanol. Staining was in the same solution with 2.5g/L of Coomassie Brilliant

Blue R (Sigma), and destaining was in 10% acetic acid and 10% methanol. Alternatively, gels were silver stained using the OWL Silver Stain Kit from (Fisher Healthcare, Houston, TX) using the recommended protocol. For mass spectrometry analysis, proteins were visualized by Coomassie staining. Bands of interest were cut out and analyzed by LC-MS/MS at the University of Victoria Proteomics Centre.

Unless otherwise noted all chemicals were obtained from Sigma.

RESULTS

Generation of stable E3-TAP-expressing cells: cloning, transfection, infection

To generate MAV-1 E3 gp11k with the TAP tag on the C-terminus, the restriction sites BamHI and NotI were engineered into 5' and 3' ends respectively of the gp11k coding sequence from the pZU14 plasmid (Fig 4.1) (22). A full or partial Kozak sequence was engineered upstream of the E3 gp11k initiation sequence in order to achieve efficient mRNA translation (130). The E3 gp11k fragment was subcloned into pFG9, which contains the TAP tag and a replication defective lentivirus genome (187). Two plasmids were obtained and named pFG9-MAV1E3A or B, having a full and partial Kozak sequences respectively. The constructs were confirmed by DNA sequencing. pFG9-MAV1E3 and plasmids encoding the lentiviral packaging constructs and the VSV G protein were co-transfected into 293 cells to produce replication defective lentiviruses encoding MAV-1 E3 gp11k with a C-terminal TAP tag. Forty hours after transfection, supernatant from the transfected 293 cells was added to mouse 3T6 fibroblasts. Stable

cell lines 3T6-E3-TAPA and 3T6-E3-TAPB resulted, expressing the E3-TAP containing integrated retroviral construct.

Confirmation of E3-TAP expressing cells

Lentivirus-infected 3T6 cells were first examined for GFP expression to determine if cells were successfully infected; the pFG9-based plasmid containing E3-TAP also encoded GFP. All 3T6 cells treated with supernatant from transfected 293 cells showed GFP expression (Figure 4.2), indicating that the lentivirus was produced and that it successfully infected the mouse cells. Cell lysates from the 3T6-E3-TAP cell lines were analyzed by Western blot for expression of E3 using a monoclonal antibody specific to the unique portion of MAV-1 E3 gp11k. Lentivirus-infected cells, but not control 3T6 cells, showed a band of the appropriate size for the E3-TAP construct (Figure 4.3). To ensure that the E3-TAP construct localized like wild type E3 gp11k, the E3-TAP cells lines were examined by immunofluorescence. Wild type E3 gp11k localizes to the endoplasmic reticulum (23) and 3T6 cells expressing E3-TAP showed a staining pattern consistent with an endoplasmic reticulum location for the E3 TAP protein (Figure 4.4).

Tandem affinity purification of E3 interacting proteins

Large preparations of 3T6-E3-TAP cells were grown in bulk and E3 gp11k-interacting proteins isolated by tandem affinity purification. After the dual purification steps the final eluates were concentrated and electrophoresed on SDS-PAGE gels. Proteins were visualized by Coomassie staining, and bands specific to the E3-TAP-containing cell lines were analyzed by mass spectrometry (Figure 4.5 A and B). Mass

spectrometry results from the bands in Figure 4.5B returned several proteins of interest (Table 1) in addition to the typical heat shock protein and keratin contamination. Proteins shown in Table 1 were identified in both the 3T6-E3-TAPA and 3T6-E3-TAPB cell lines in multiple experiments. Verification of the interaction of E3 gp11k with the identified proteins has not yet been undertaken but will be the first step in future studies of E3 gp11k.

DISCUSSION

These studies have provided a system for the discovery of proteins that interact with MAV-1 E3 gp11k. The generation of mouse cell lines stably expressing E3-TAP will be a useful tool in studying the function of E3 gp11k, allowing for easy immunoprecipitation (multiple antibody recognition targets) to confirm protein interactions and avoiding the difficulty of transient transfection in mouse cells (128). Furthermore, the function of TAP-tagged E3 gp11k can be studied in the context of viral infection in these cell lines by infection with an E3 null mutant virus, *pm*E314. By studying the TAP-tagged E3 gp11k in the context of an E3 null virus we will avoid the complications of interpreting results from cells containing two versions of E3 gp11k.

In the studies performed to date, a protein of approximately 80 kDa has been repeatedly isolated as interacting with E3-TAP. Mass spectrometry analysis to identify this unknown protein has revealed several possibilities for interacting proteins that have yet to be confirmed by Western blot or another means. These proteins are considered here.

Rufy1 (also known as Rabip4) is a recently identified Rab4 effector protein that is associated with early endosomes and cell mobility (248). Rufy1 is notable for containing a FYVE finger domain. This domain binds specifically to phosphatidylinositol 3-phosphate. When the FYVE finger domain of Rabip4 was expressed alone, it localized to the plasma membrane (272). Rabip4 has also been shown to control early endosomal trafficking (48, 77).

p140 is another protein identified by the mass spectrometry analysis. An interaction of E3 gp11k and this protein is somewhat less likely, because only a fragment of p140 could have migrated at the size of approximately 80 kDa, the size of the band analyzed. Despite this, p140 would be an interesting binding partner for E3 gp11k, because p140 localizes with elements of the actin cytoskeleton and may negatively regulate cell adhesion (59). p140 was discovered through its interaction with p130Cas in human cell lines. p130 is a scaffolding molecule involved with cell adhesion, indicating that p140 may also play a role in cell adhesion. It is intriguing to consider E3 interacting with proteins involved in cell adhesion because cells infected with wt MAV-1 recruit more inflammatory cells than do cells infected with *pm*E314, suggesting the possibility of differential expression of cellular adhesion molecules in cells infected with the two viruses.

Another potential E3 gp11k-interacting protein that is of interest is development and differentiation factor 2 (Ddef2), a cytoplasmic protein of relatively unknown function. Ddef 2 is also known as PAP and binds to Pyk2, a tyrosine kinase (8). Ddef2 may be involved in vesicular transport and has been shown to have GTPase-activating protein

activity towards several of the small Arf GTPases that are involved in vesicular trafficking pathways in eukaryotes.

To confirm the interaction of these proteins with E3 gp11k, standard techniques such as immunoprecipitation followed by Western blotting or colocalization will need to be used. There are commercially available antibodies to Rufy1 and Ddef 2 and published work details the use of lab-generated antibodies to p140 (59). Once protein interaction has been confirmed, the functional significance of this binding can be investigated by disrupting the protein binding by mutating either E3 gp11k or the interacting protein. After MAV-1 infection in a system in which E3 gp11k and its newly discovered binding partner could not interact, one would assay for a phenotype compared to wild type infection and infection with the E3 null virus *pm*E314. *In vitro* a possible phenotype to analyze is an absence of the E3-specific induction of chemokine expression reported in Chapter 3. *In vivo* analysis could include examination of inflammation in the brain after infection, because *pm*E314-infected mice show fewer inflammatory cells than do mice infected with wild type virus (Chapter 3).

In searching for proteins that interact with E3 gp11k, it is important to consider that E3 gp11k is predicted to be a peripheral membrane protein and thus may bind to integral membrane proteins. Integral membrane proteins are often insoluble and hard to purify, and thus it may be difficult to isolate proteins that interact with E3 gp11k. However, Western blot analysis of 3T6-E3 TAP lysates showed that the proteins calnexin and calreticulum (integral and resident endoplasmic reticulum membrane proteins) are present (data not shown), indicating that that some membrane proteins found in the endoplasmic reticulum were present in the cell lysates used for the TAP assay. This is

promising evidence that an endoplasmic reticulum integral membrane protein could be identified by TAP. In addition, optimization of detergent conditions used in lysate preparations could result in a better yield of membrane proteins. Tandem affinity purification has been successfully used to isolate membrane proteins by others, but with slightly modified lysis buffer (246).

A

ATGTCCGAA***A*** ***TG*****AGCGGGGC** **GCCCAG**AATC CCGCGCAGCG GAGATCGGCT
GCGCTTCCTG TGCCTGCTTC TACTCGTATT GGGTTGGTGT TTGCCCGTGA
CCGGTCATCC TCTCAAAGGG GTTCAACCAT CGCAGTGTCA GTGCCCTGCT
AGTCCCCCGT GGACTAATTC TTCTGTTACT TCCTTCGCCC AGAAAACAAA
ATGGGAAAAC TCACGGTATG TACAACCAGT ATTGCCCTGT ACCTTCTGAG
TCCTCAACTC GGGGCAAGAA TGCTGTTCGA ACTGGT**GCAG** **GCCCGGACGA**
CGAGTGTTTC TAA

B

5′ end
full kozak:
ATA GGATCC GCCACC ATG GCC GAA ***ATG*** **AGC GGG GCG CCC AG**

short kozak
ATA GGATCC ATG GCC GAA ***ATG*** **AGC GGG GCG CCC AG**

3′ end
AAT **GCGGCCGC** **GAA ACA CTC GTC GTC CGG GCC TGC**

C

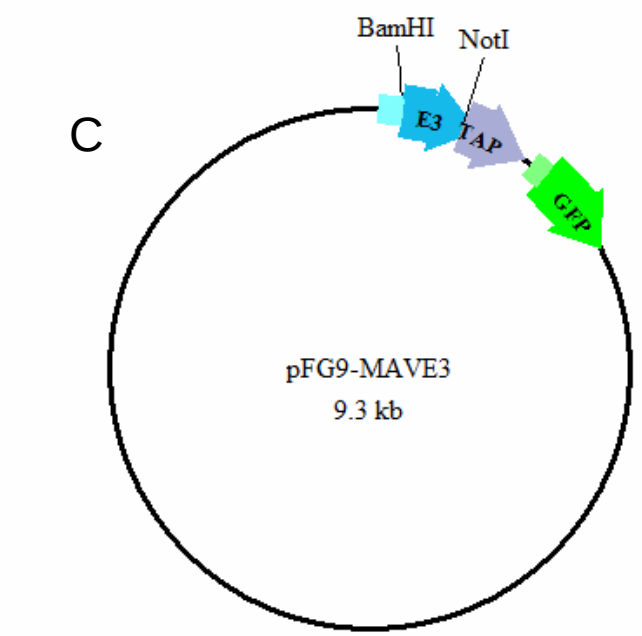

Figure 4.1. Cloning of E3-TAP. A. cDNA sequence of E3 gp11k with residues matching primers in bold. Italics indicates the E3 gp11k initiator codon. B. Primers used to generate E3 gp11k with full or partial Kozak sequence, residues in bold match the E3 gp11k cDNA indicated in bold in part A. Underlined residues indicate BamHI, bold and underlined indicates NotI restriction enzyme recognition site. C. pFG9-MAVE3 plasmid with E3-TAP sequence.

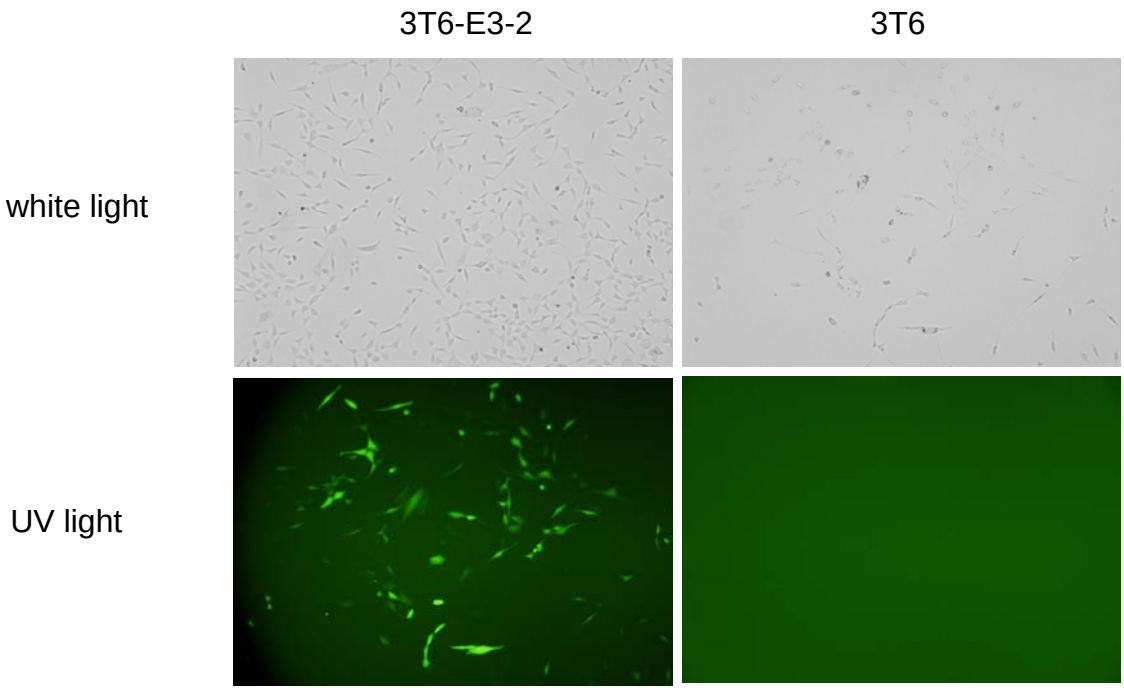

Figure 4.2. Lentivirus infected cells express GFP. 3T6-E3-TAPA cells (left panels) and 3T6 cells (right panels) were exposed to UV light (lower panels) to detect GFP expression. Upper panels show cells under white light. While light images were adjusted for brightness and contrast using Adobe Photoshop. Similar results are obtained for 3T6-E3-TAPB cells (data not shown).

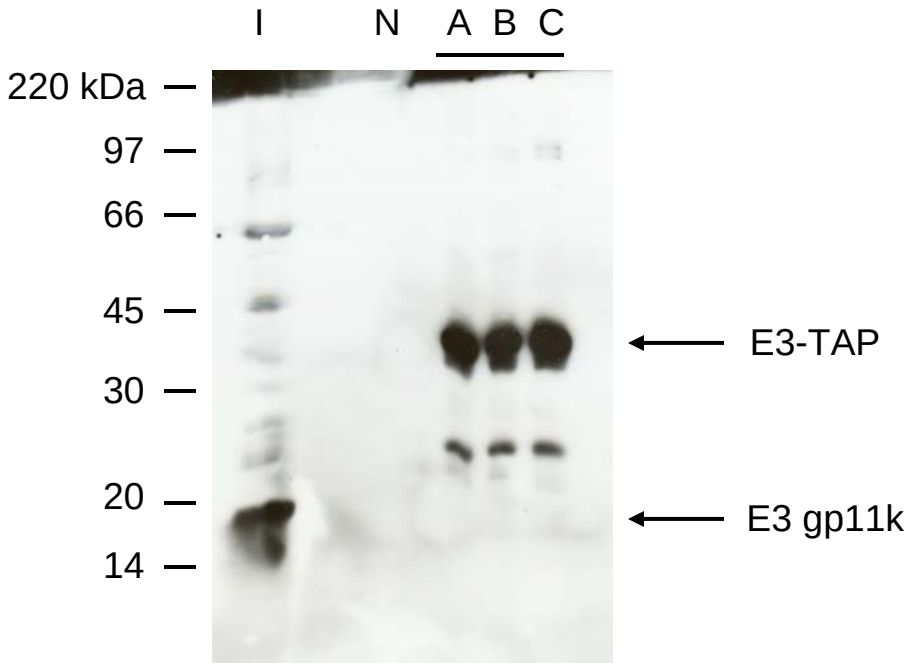

Figure 4.3. E3 expression in E3-TAP cell lines by Western blot. 3T6 cells (N) and three E3-TAP-containing cell lines (A, B and C) were examined for E3 expression by Western blot. Marker size standards are shown on the left. Lane I shows MAV-1-infected NIH 3T6 cell lysates (prepared 36 hours post infection) as a positive control for E3 staining.

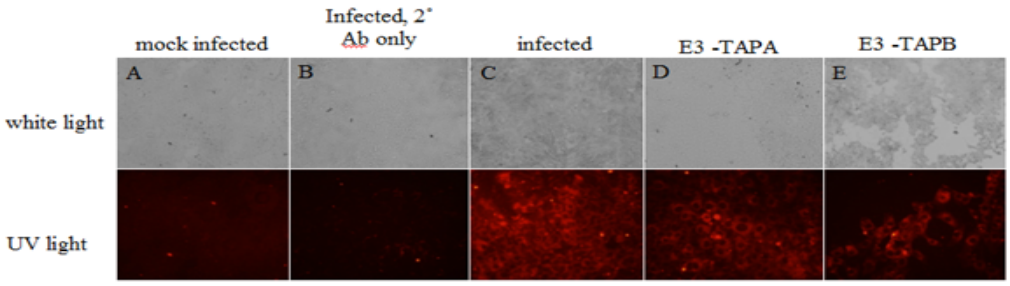

Figure 4.4. E3-TAP localizes like wild type E3. Anti-E3 immunofluorescent staining of A) mock infected cells, B) infected cells stained with only secondary antibody, C) infected cells, D and E) 3T6-E3-TAPA and B cell lines respectively. The upper panel shows cells under white light (images were adjusted for brightness and contrast as in Fig. 2), in the lower panels cells were exposed to UV light.

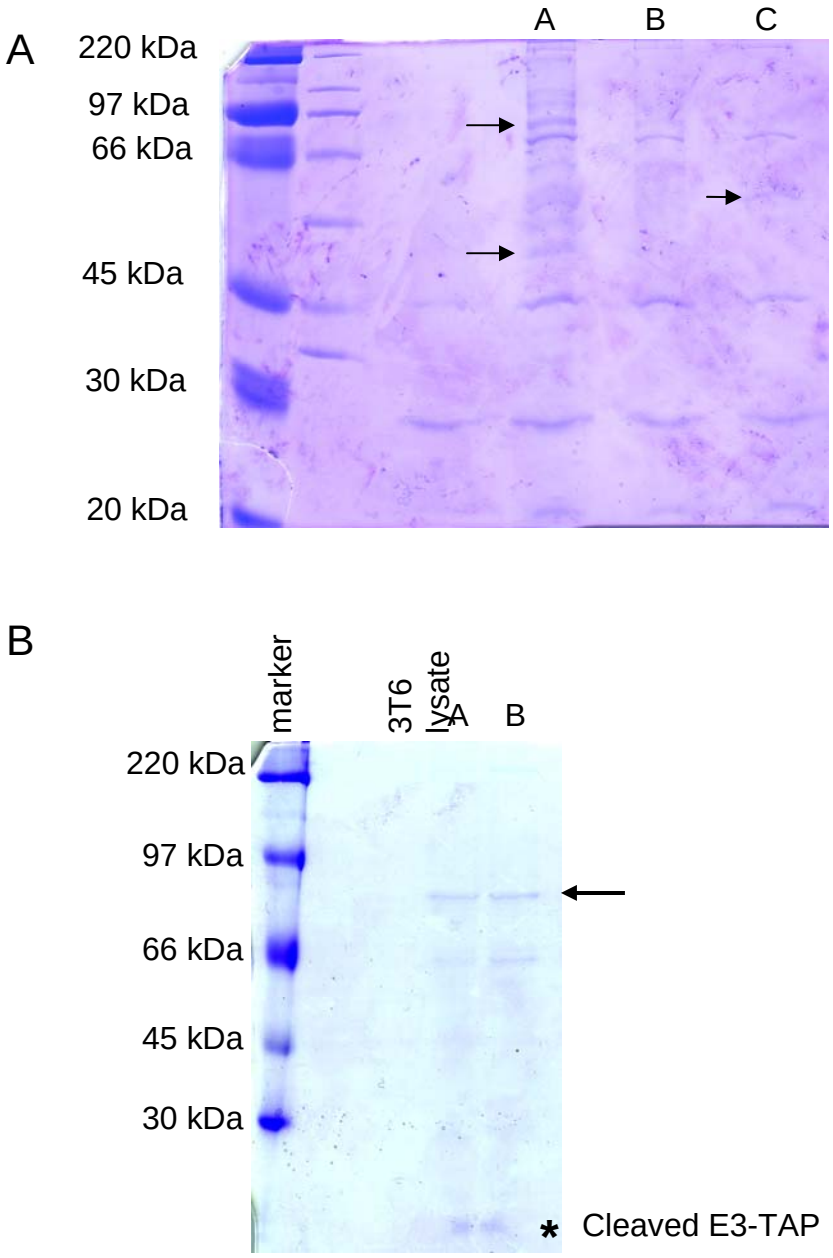

Figure 4.5. Tandem affinity purification results. TAP purified cell lysates from 3T6 cells (negative control) or the two E3-TAP-containing cell lines were electrophoresed on 10% SDS-PAGE gels and Coomassie stained to show proteins. The results of two independent purifications are shown in A and B. Results from B are discussed in the text. Results from A were obtained after only the first purification step of the TAP method. Upper arrow in A indicates a protein band of the same rough size as those analyzed in B. Mass spectrometry analysis of this band identified many of the same proteins as shown in Table 1. Arrows indicate the bands of interest that were analyzed by mass spectrometry, star indicates the cleaved E3-TAP protein.

Table 1.

Protein	Function
Rufy1/rabip4	role in endocytic trafficking
p140	cell adhesion
Ddef2/PAP	GTPase-activating protein

Mass Spectrometry Results. Peptides present in the ~80 kDa band excised in Figure 5 B were identified in the mass spectrometry analysis and matched in a mouse protein database to the indicated proteins. Each protein listed was identified in two independent TAP purifications.

Chapter V

Discussion

The experiments described in this dissertation examine MAV-1-induced pathogenesis. Previous studies examined the role of the adaptive immune response to MAV-1 infection (159, 160) and revealed a role for T cells in mediating MAV-1-induced pathogenesis. This work focuses on the innate immune response to MAV-1 infection and the effects of MAV-1 infection of brain endothelial cells, a major site of infection (113). Natural killer (NK) cells were examined for a role in protecting the host from MAV-1 infection (Chapter 2, 265). Mice deficient in NK cells had viral loads in their brains similar to those measured in the brains of wild type mice at early and late times after infection. Flow cytometric analysis revealed that NK cells are present only in very low numbers in the mouse brain and that this number is unchanged in mice infected with MAV-1. In studies of MAV-1-induced encephalitis, we have shown that MAV-1 infection causes breakdown of the blood brain barrier (BBB) that is independent of the presence of inflammatory cells in the brain (Chapter 3). Mutant mice that fail to develop inflammation in the brain after infection with MAV-1 likewise fail to show signs of disease during acute infection; however these mice show BBB permeability like wild type mice after infection with MAV-1. Thus it is not the insult to the BBB that causes MAV-1-induced disease but the presence of inflammatory cells in the brain. The MAV-1

E3 gene products are important for MAV-1-induced inflammation as well as pathogenesis. We investigated the mechanism by which MAV-1 E3 causes disease and inflammation by searching for cellular proteins that interact with MAV-1 E3 gp11k (Chapter 4). Mice infected with the E3 null virus, *pm*E314, have a 5-6 log unit higher LD_{50} than do mice infected with wild type MAV-1 (22, 37) indicating that E3 is important in causing MAV-1-induced pathogenesis.

Role of NK cells in MAV-1 pathogenesis

In Chapter 2 of this work we consider the role of NK cells in controlling wild type MAV-1 infection (265). Natural killer cells are an important component of the innate immune response to many viral infections, both for their lytic ability as well as their secretion of IFN-γ and other antiviral cytokines (32, 231, 256). NK cells and CD8 T cells lyse their target cells by secreting the cytolytic, pore-forming molecule perforin (181, 277). Perforin knockout mice are resistant to MAV-1-induced pathogenesis (159), and previous studies suggested that this result could be attributed to the lack of cytolytic activity from CD8 T cells. However, a role for NK cell cytolytic activity in mediating MAV-1 pathogenesis was not eliminated in these studies. Alternatively, NK cell-mediated lysis of infected cells or NK cell cytokine signaling could be important in control of MAV-1 infection. We found no differences in viral load after MAV-1 infection of mice depleted of their NK cells compared to mice not depleted of their NK cells (265). Neither group of mice showed significant signs of disease after infection with a low dose of virus. These results, combined with the undetectable level of NK cells in the brains of mice infected with wild type MAV-1 (Chapter 3), combine to indicate

that NK cells are not important for the early immune response to infection, control of viral replication in the brain or the immunopathology observed after MAV-1 infection. Importantly, the activity of NK cells in MAV-1-infected mice has not been measured, and this analysis could help reveal a subtle role for NK cells in the response to MAV-1 infection that has not yet been detected. Studies of NK cell-depleted mice and other immunodeficient animals, as well as infections with the E3 null virus *pm*E314, all combine to indicate that the inflammatory response to infection, not viral load, is the key determinant of early MAV-1-induced disease.

Effects of MAV-1 infection on the blood brain barrier and pmBECs

To characterize the encephalitis caused by MAV-1 infection of susceptible mouse strains, we examined the inflammatory cells found in the brain and expression levels of cytokine and chemokine transcripts in infected brain endothelial cells (Chapter 3). Wild type MAV-1 infection induced CCL2 expression in a mouse brain microvascular endothelial cell (MBMEC) line and in primary mouse brain endothelial cells (pmBECs), and we investigated the possible role of CCL2 in modulation of BBB integrity of MAV-1 infected mice. Intracranial injection of CCL2 causes breakdown of the BBB in mice (223), and brain endothelial cells exposed to CCL2 lose tight junction protein expression and have decreased transendothelial electrical resistance (219, 223). In HIV-1 infection, CCL2 promotes the transmigration of virus-infected leukocytes across the blood brain barrier (67). Recent work examined the role of cocaine in enhancing HIV-1-induced breakdown of the BBB and found a role for increased CCL2 signaling mediating disruption of tight junction proteins in human brain microvascular endothelial cells

exposed to the drug (58). Combined, these data show that CCL2 is an important signaling molecule in promoting breakdown of the BBB.

We observed that the MAV-1-induced decrease in pmBEC barrier properties was not dependent on CCL2 72 hours after MAV-1 infection. The CCL2 dependence of pmBEC barrier property disruption has not yet been tested at earlier times after MAV-1 infection. While other pathways must be involved in loss of barrier properties at later points in infection, it is possible that CCL2 expression is primarily responsible for BBB breakdown and loss of barrier properties in pmBECs at early points in infection. This hypothesis can be addressed by treating MAV-1-infected pmBEC cultures with neutralizing CCL2 antibody at early times after infection and measuring TEER. Another way to measure the involvement of CCL2 signaling in MAV-1-induced breakdown of the BBB is through the use of $CCL2^{-/-}$ mice. While the *in vitro* data presented in Chapter 3 suggest that $CCL2^{-/-}$ mice will eventually show breakdown of the BBB, it is of interest to determine if this breakdown of the BBB occurs with the same kinetics in $CCL2^{-/-}$ and wild type mice. These studies may reveal a role for CCL2 in MAV-1-induced breakdown of the BBB at early time points and beyond what can be discovered in a tissue culture model.

Other cytokines involved in the integrity of the BBB include interleukin-6 (IL-6) and interleukin-1 (IL-1) (19, 20). Patients with traumatic brain injury showed high levels of IL-6 in their serum, correlating with inflammation, perivascular hemorrhage and altered function of brain endothelial cells (242). In a rat model of acute pancreatitis, BBB permeability was induced in a manner consistent with dependence on either TNF-α or IL-6 (71). More direct evidence of the role of IL-6 in promoting breakdown of the

BBB comes from infection of wt and IL-6 knockout mice with *Streptococcus pneumoniae* (175). Wild type mice showed increased vascular permeability in response to infection whereas IL-6 knockout mice showed significantly less permeability. Wild type mice that were infected and also treated with IL-6 neutralizing antibodies showed reduced breakdown of the BBB compared to control mice, indicating that IL-6 signaling is necessary for vascular permeability during bacterial meningitis. Interestingly there are also reports of IL-6 signaling working to enhance the integrity of the BBB. IL-6 production in the CNS has been shown to result in increased expression of integrin subunits on astrocytes but not endothelial cells (158). An endothelial-astrocyte co-culture system measuring endothelial cell function by TEER demonstrated that IL-6 was important for maintenance of electrical resistance after shear stress was removed from the system (133). In this system the removal of shear stress from the co-culture resulted in an increase in IL-6 production. Anti-IL-6 antibody treatment after the removal of shear stress caused a decrease in TEER, whereas antibody treatment in the presence of shear stress had no effect on TEER levels. Thus the IL-6 produced after the loss of shear stress was important for maintenance of the barrier properties of brain endothelial cells indicating that IL-6 can be necessary for protection of the BBB. Increased IL-1 production is associated with the pathology of CNS diseases including Alzheimer's, multiple sclerosis and stroke (29, 92, 98). IL-1 injection into the CNS results in transient BBB permeability and recruitment of neutrophils (28) as does chronic expression of IL-1 (73). Neither IL-6 nor IL-1 levels have been measured after MAV-1 infection nor it is unknown if these cytokines play a role in mediating MAV-1-induced breakdown of the BBB.

We have shown that MAV-1 infection causes a decrease in expression of the tight junction proteins occludin and claudin-5 on the surface of pmBECs. The mechanism by which this change in expression occurs remains to be determined. Oxidative stress is commonly induced as part of the host cell defense during infections (137, 145), and reactive oxygen species cause increased permeability of brain endothelial cell monolayers and increased ability of monocytes to traffic across these monolayers (96). Addition of matrix metalloproteinase (MMP) inhibitors blocks reactive oxygen species-induced permeability of brain endothelial cells, demonstrating that MMPs are important in BBB disruption. MMP-9 knockout mice are protected from brain injury after cerebral ischemia (12) and show fewer defects in motor function after traumatic brain injury than do wild type mice (255). Wild type mice exposed to transient focal ischemia show markedly reduced ZO-1 expression in the brain (13). In contrast, MMP-9 knockout mice show very little reduction in ZO-1 expression after brain injury, indicating that MMP-9 activity is involved in control of tight junction protein expression. Given these data, it is of interest to study the expression and activity of MMPs after MAV-1 infection. Increased MMP expression following MAV-1 infection would implicate MMPs in mediating MAV-1-induced breakdown of the BBB and indicate the necessity for further studies of this group of proteins.

Infection of MMP-9 knockout mice could reveal a role for MMPs in breakdown of the BBB after MAV-1 infection. To further elucidate a role for MMPs in MAV-1-induced breakdown of the BBB, experiments in pmBECs would be necessary. By adding specific MMP inhibitors to pmBECs infected with MAV-1 and examining cells for expression of tight junction proteins, the role of MMPs in controlling tight junction

protein expression after MAV-1 infection could be determined. Creation of pmBECs from MMP knockout mice, infecting them with
MAV-1 and measuring TEER or levels of tight junction protein expression would also allow examination of the role of these proteins in contributing to breakdown of the BBB after MAV-1 infection.

Other signaling pathways are known to play a role in controlling cell surface expression and function of tight junction proteins by controlling tight junction phosphorylation levels. These include Rho kinase, protein kinase C (PKC), protein kinase A and the mitogen activated kinase (MAP) kinase pathways (reviewed in 88). Tight junction formation and protein function can be regulated by phosphorylation of specific amino acids as well as the overall phosphorylation level of specific proteins. The studies performed in Chapter 3 of this work examined only gross expression levels of tight junction proteins. Effects of MAV-1 infection on tight junction protein phosphorylation have not yet been assessed.

Several PKC isoforms are associated with tight junction proteins at the plasma membrane (15, 101), and herpes simplex virus type 1 infection has been shown to affect the location and activity of PKC isoforms (174). Numerous studies have examined the role of PKC phosphorylation of tight junction proteins in tight junction opening and closing (9, 227). A global understanding of these results is complicated by the fact that activity of the same PKC isoform can cause different effects in different cell types (66). In renal LLC-PK1 cells, nPKCδ decreases tight junction barriers, whereas in MDCK cells nPKCδ activity is necessary for occludin localization to the peripheral cell membrane (9, 167). Thus if PKC is found to be important in MAV-1-induced breakdown of the BBB,

the role of specific PKC isoforms in controlling tight junction formation and tight junction phosphorylation levels must be systematically studied in pmBECs to avoid drawing incorrect conclusions from work performed in other systems. Specific inhibitors of individual PKC isoforms are available and will aid in these studies.

Several studies have highlighted the importance of PKA signaling in control of tight junction formation (53, 110, 146). PKA activity is determined by intracellular cAMP levels (100) which can be perturbed after virus infection (50, 126, 168). cAMP induces phosphorylation of claudin-5 in both PKA-dependent and -independent manners (110). PKA is suspected to directly phosphorylate claudins important for tight junction formation (79), and it is required for cAMP-dependent phosphorylation of tight junction proteins (53, 217). Stimulation of the classical MAP kinase Erk1/2 occurs by sensing oxidative stress, alcohol and viral proteins such as HIV-Tat (7, 88, 123). These stimuli result in decreased expression of tight junction proteins including ZO-1, claudin-5 and occludin on the cell surface. We have not yet examined cAMP levels, PKA signaling or MAPK signaling after MAV-1 infection to determine what signaling molecules and pathways are altered by MAV-1. All of these pathways are potential mediators of MAV-1-induced alterations in tight junction protein expression because they are major regulators of normal cell function and they are perturbed by infection with other viruses.

Infection with West Nile virus causes breakdown of the BBB (254) and the result of West Nile virus infection is contingent upon the host immune response (201, 254), similar to MAV-1 infection (159, Chapter 3 of this work). West Nile virus load in the brain is reduced in MMP9 knockout mice compared to similarly challenged control mice (253). Additionally, MMP9 knockout mice are protected from West Nile virus-induced

breakdown of the BBB as measured by Evans blue dye staining of brain tissue. Additional studies have shown that although West Nile virus infection causes BBB breakdown in C57BL/6 mice, it does not cause BBB breakdown in lethal infections of Balb/c mice, indicating that disruption of the BBB is not necessary for lethal infection (164). $CD8^+$ T cells are important for clearance of West Nile virus from the brain (156) and this function is dependent on CD40-CD40 ligand interaction (214). IFN α/β has been shown to aid in clearance of virus from tissues throughout the infected host (201). Given the overall similarities between West Nile virus- and MAV-1-induced breakdown of the BBB and a similar requirement for T cells in clearance of each virus from CNS tissues, it would be interesting to determine whether if the two viruses cause disruption of the BBB by similar mechanisms.

Mechanism of inflammatory cell recruitment by MAV-1 E3 gp11k

*pm*E314-infected mice showed breakdown of the BBB similar to that in wild type MAV-1 infected mice, but they fail to elicit a strong inflammatory response in the brain as seen in mice infected with wild type MAV-1. Consistent with this finding, *pm*E314 infection caused a decrease in peripheral cell membrane staining of tight junction proteins and a loss of transendothelial electrical resistance in pmBECs. These data support the finding that inflammatory cell mediators are not necessary for breakdown of the BBB but leave unanswered the question of how E3 results in inflammatory cell recruitment and pathogenesis after MAV-1 infection.

E3 gp11k is the only E3 protein product detected after infection with wild type MAV-1. In both inbred and outbred mice *pm*E314 infection caused less lethality than

wild type MAV-1 (data not shown; 37) and less inflammation in the brain than wt infection (Chapter 3, 37). How E3 stimulates and/or recruits inflammatory cells to the site of MAV-1 infection is not clear. Analysis of chemokine mRNA and protein levels after wild type MAV-1 and *pm*E314 infection revealed that endothelial cells infected with wild type MAV-1 expressed higher levels of CCL1, CCL2, CCL5 and CXCL10 than did cells infected with *pm*E314. These chemokines are known to be involved in the recruitment of T cells, neutrophils and macrophages (43), all of which were recruited to the brain after MAV-1 infection.

Interestingly, the majority of inflammatory cells identified in the brains of MAV-1 infected mice were neutrophils, and the number of neutrophils in the brain did not depend on the presence of E3. These data suggest that neutrophils are not involved in the histopathology and pathogenesis observed after infection with wild type MAV-1. Neither the presence of neutrophils in the brain nor circulating levels of neutrophils have been determined in the T cell knockout or perforin knockout mice used as "inflammation deficient" models of MAV-1 infection that were assessed for MAV-1-induced breakdown of the BBB in this work. It is known that histologically no inflammatory cells are observed in the brains of T cell- or perforin-deficient mice after MAV-1 infection (159). However, other assays to determine the presence of inflammatory cells such as flow cytometry have not been performed in these mice. Thus it is a formal possibility, though unlikely due to the lack of inflammatory cells seen in the brains of infected T cell or perforin knockout mice, that MAV-1-induced breakdown of the blood brain barrier is mediated by neutrophils *in vivo*. While an increased presence of neutrophils is unlikely to be responsible for MAV-1-induced opening of the BBB, other studies have shown that

neutrophils can affect BBB permeability (reviewed in 206), making this an important avenue to explore in future work.

It is of interest to determine if the expression of other cell surface proteins is altered after infection of pmBECs with wild type MAV-1 or *pm*E314. Cell surface proteins are important for cell-cell binding, antigen presentation and signaling pathways. Infection by HIV-1 and measles virus can alter the expression of cell surface proteins involved in any or all of these functions in order to evade the host immune response and promote viral replication (46, 274). Alternatively, cells infected with HIV-1, West Nile virus and respiratory syncytial virus can increase expression of adhesion molecules such as ICAM and VCAM, promoting the recruitment of inflammatory cells to the site of infection (11, 57, 209). Human adenoviruses down-regulate MHC class I expression through the action of the E3-gp19k protein (33), but no decrease in MHC class I expression is observed after MAV-1 infection (132). Also, unlike other viruses that infect MHC class II-expressing cells (HIV-1 and cytomegaloviruses) (229, 235), MAV-1 does not alter MHC class II expression. Studies in this work have shown that surface expression of the tight junction proteins occludin and claudin-5 is decreased after MAV-1 infection.

Studies using the J774 macrophage line showed that wild type MAV-1 infection caused an increase in the surface expression of CD40 (Angell and Spindler, unpublished). CD40 is an important co-stimulatory molecule for T cell-induced activation of antigen presenting cells (243). After CD40 binding of its ligand, CD40L, a feedback loop is initiated that results in increased surface expression of CD40 to further augment cell activation (40). CD40 signaling in B cells is important for their activation and ability to

differentiate, produce antibody and isotype switch (reviewed in 52). Previous studies of the adaptive immune response to MAV-1 infection showed that B cells and early T cell-independent antiviral IgM are important for resistance to MAV-1-induced pathogenesis (160). Both antiviral IgM and IgG are produced after MAV-1 infection of wild type mice, indicating a possible role for CD40 expression in isotype switching to protect the host from MAV-1 infection. CD40 expression levels after infection with *pm*E314 have not yet been determined. It is possible that a lack of CD40 upregulation in *pm*E314-infected cells contributes to the low inflammation phenotype seen after infection in comparison to wild type MAV-1 infection.

It is not known what effect MAV-1 infection has on the expression of other cellular adhesion molecules such as intercellular adhesion molecule (ICAM), vascular cell adhesion molecule (VCAM) or junctional adhesion molecules (JAMs). Infection with other viruses including HCMV, influenza A, coxsackie B virus and HIV-1 results in increased expression of adhesion molecules responsible for lymphocyte binding as well as increased invasion of inflammatory cells to the affected tissues (102, 184, 188, 280). Based on our current understanding of MAV-1-induced inflammation and pathogenesis we hypothesize that pmBECs infected with wild type MAV-1 will show increased expression of adhesion molecules involved in inflammatory cell binding. We further predict that *pm*E314 infection of pmBECs will not alter expression (or will have less of an effect on expression) of adhesion molecules such as ICAM, VCAM, endothelial-leukocyte adhesion molecule-1 (ELAM-1) and JAMs based on the lack of inflammation observed after infection with this virus. High levels of these adhesion molecules on the surface of endothelial cells promote the binding of inflammatory cells and aid in their

extravasation to the surrounding tissue (2, 152, 224). ELAM-1 is of particular interest due to the high levels of neutrophils measured in the brains of MAV-1-infected mice. This molecule is important for neutrophil recruitment, activation and adhesion to endothelial cells (147).

Results described in Chapter 4 of this thesis describe potential binding partners for the MAV-1 E3 gp11k protein. Several of these possible interacting proteins could be involved control of protein expression on the cell surface, which could in turn be important for inflammatory cell recruitment. One such protein is Rufy1, also known as Rabip4, which is involved in early endosomal trafficking and cellular mobility (77, 154). Recycling and internalization of transferrin from the early endosome is decreased in cells expressing a dominant negative form of Rabip4 (77). Binding of E3 gp11k to Rabip4 could perturb the normal endosomal recycling pathways used to control cell surface expression of proteins, including those involved in recruiting and binding inflammatory cells. Thus an E3 gp11k-Rufy1 interaction could explain the E3-dependence of MAV-1-induced inflammation. Another potential E3 gp11k binding partner that plays a role in regulating proteins at the plasma membrane is p140 or p140Cap. This protein colocalizes with actin and restricts cell adhesion and mobility when it is overexpressed (59, 60). Thus, E3 gp11k binding with p140 could affect stress fiber formation or expression of cell adhesion molecules, and through these effects, contribute to E3-dependent inflammation after MAV-1 infection.

An alternative possibility for the E3-dependent nature of MAV-1-induced inflammation is that the E3 protein products themselves are highly immunogenic and that presentation of these peptides on the cell surface of infected cells helps to stimulate an

immune response. To test this hypothesis, pmBECs infected with wild type MAV-1 or *pm*E314 could be incubated with carboxyfluorescein succinimidyl ester (CFSE) -labeled CD8 T cells and T cell replication assayed as a surrogate measure for antigen presentation (45). If T cells exposed to cells infected with wild type MAV-1 undergo more rounds of replication than T cells exposed to cells infected with *pm*E314 this would indicate that wild type virus is a better stimulator of the immune response than *pm*E314. Flow cytometry can be used to measure the dilution of CSFE in the T cells to determine the number of cell divisions that occur. It is also possible that the E3 gene products promote presentation of non-E3 viral peptides that are highly recognized by the host immune system. Increased host recognition of viral antigen could involve T cell or B cell responses. The ability of CD8 T cells from infected mice to recognize specific epitopes from viral proteins could be measured by tetramer staining (3), though this assay is complicated by the need to target specific viral epitopes. Currently T cell epitopes of MAV-1 proteins have not been identified. T cell activation levels as well as B cell antibody production from wild type and *pm*E314 infected mice can be measured by ELISPOT (51). While measurement of antibody levels and T cell activation do not directly address the mechanism by which E3 stimulates the host immune response, a further understanding of the differences in immune response to wild type MAV-1 and *pm*E314 could lead to insights about this mechanism.

The studies performed in this work confirm and extend previous findings that inflammation in the brain is essential for MAV-1 pathogenesis and lethality of infection (37, 159). These data demonstrate that MAV-1 causes breakdown of the BBB after wild type MAV-1 infection and also after infection with mutant virus *pm*E314. BBB

disruption was not dependent on inflammation in the brain but instead correlated significantly with the amount of virus present in the brain. While the function of MAV-1 E3 gp11k remains unknown, this work supports the idea of its major role being stimulation of the host inflammatory response. Based on these findings we believe that MAV-1 infection causes disease in a manner dependent on both the amount of virus and the presence of inflammatory cells. After MAV-1 infection, endothelial cells in the brain become infected and this causes a decrease in functional tight junctions due to a loss of tight junction protein expression at the peripheral cell membrane. Infected brain endothelial cells also secrete chemokines that recruit neutrophils, T cells, B cells and macrophages to the site of infection. These inflammatory cells are able to cross the BBB due to the lack of tight junctions between infected endothelial cells. It is the presence of inflammatory cells in the brain that results in pathology and signs of disease in infected animals.

References

1. **Afonso, P. V., S. Ozden, M. C. Prevost, C. Schmitt, D. Seilhean, B. Weksler, P. O. Couraud, A. Gessain, I. A. Romero, and P. E. Ceccaldi.** 2007. Human blood-brain barrier disruption by retroviral-infected lymphocytes: Role of myosin light chain kinase in endothelial tight-junction disorganization. J. Immunol. **179:**2576-2583.
2. **Albelda, S. M., C. W. Smith, and P. A. Ward.** 1994. Adhesion molecules and inflammatory injury. FASEB J. **8:**504-512.
3. **Altman, J. D., P. A. Moss, P. J. Goulder, D. H. Barouch, M. G. McHeyzer-Williams, J. I. Bell, A. J. McMichael, and M. M. Davis.** 1996. Phenotypic analysis of antigen-specific T lymphocytes. Science **274:**94-96.
4. **Alvarez, J. I., and J. M. Teale.** 2006. Breakdown of the blood brain barrier and blood-cerebrospinal fluid barrier is associated with differential leukocyte migration in distinct compartments of the CNS during the course of murine NCC. J. Neuroimmunol. **173:**45-55.
5. **Andersen, I. H., O. Marker, and A. R. Thomsen.** 1991. Breakdown of blood-brain barrier function in the murine lymphocytic choriomeningitis virus infection mediated by virus-specific CD8+ T cells. J. Neuroimmunol. **31:**155-163.
6. **Andersson, M., S. Pääbo, T. Nilsson, and P. A. Peterson.** 1985. Impaired intracellular transport of class I MHC antigens as a possible means for adenoviruses to evade immune surveillance. Cell **43:**215-222.
7. **Andras, I. E., H. Pu, J. Tian, M. A. Deli, A. Nath, B. Hennig, and M. Toborek.** 2005. Signaling mechanisms of HIV-1 Tat-induced alterations of claudin-5 expression in brain endothelial cells. J Cereb Blood Flow Metab **25:**1159-70.
8. **Andreev, J., J. P. Simon, D. D. Sabatini, J. Kam, G. Plowman, P. A. Randazzo, and J. Schlessinger.** 1999. Identification of a new Pyk2 target protein with Arf-GAP activity. Mol. Cell. Biol. **19:**2338-2350.
9. **Andreeva, A. Y., J. Piontek, I. E. Blasig, and D. I. Utepbergenov.** 2006. Assembly of tight junction is regulated by the antagonism of conventional and novel protein kinase C isoforms. Int. J. Biochem. Cell. Biol. **38:**222-233.
10. **Anglen, C. S., M. E. Truckenmiller, T. D. Schell, and R. H. Bonneau.** 2003. The dual role of CD8+ T lymphocytes in the development of stress-induced herpes simplex encephalitis. J. Neuroimmunol. **140:**13-27.
11. **Arnold, R., and W. Konig.** 2005. Respiratory syncytial virus infection of human lung endothelial cells enhances selectively intercellular adhesion molecule-1 expression. J. Immunol. **174:**7359-7367.
12. **Asahi, M., K. Asahi, J. C. Jung, G. J. del Zoppo, M. E. Fini, and E. H. Lo.** 2000. Role for matrix metalloproteinase 9 after focal cerebral ischemia: effects of gene knockout and enzyme inhibition with BB-94. J. Cereb. Blood Flow Metab. **20:**1681-1689.
13. **Asahi, M., X. Wang, T. Mori, T. Sumii, J. C. Jung, M. A. Moskowitz, M. E. Fini, and E. H. Lo.** 2001. Effects of matrix metalloproteinase-9 gene knock-out on the proteolysis of blood-brain barrier and white matter components after cerebral ischemia. J Neurosci **21:**7724-32.

14. **Ashkar, A. A., and K. L. Rosenthal.** 2003. Interleukin-15 and natural killer and NKT cells play a critical role in innate protection against genital herpes simplex virus type 2 infection. J. Virol. **77:**10168-10171.
15. **Avila-Flores, A., E. Rendon-Huerta, J. Moreno, S. Islas, A. Betanzos, M. Robles-Flores, and L. Gonzalez-Mariscal.** 2001. Tight-junction protein zonula occludens 2 is a target of phosphorylation by protein kinase C. Biochem. J. **360:**295-304.
16. **Ball, A. O., C. W. Beard, S. D. Redick, and K. R. Spindler.** 1989. Genome organization of mouse adenovirus type 1 early region 1: A novel transcription map. Virology **170:**523-536.
17. **Ball, A. O., C. W. Beard, P. Villegas, and K. R. Spindler.** 1991. Early region 4 sequence and biological comparison of two isolates of mouse adenovirus type 1. Virology **180:**257-265.
18. **Banks, W. A.** 1999. Physiology and pathology of the blood-brain barrier: Implications for microbial pathogenesis, drug delivery and neurodegenertive disorders. J. Neurovirol. **5:**538-555.
19. **Banks, W. A., and A. J. Kastin.** 1991. Blood to brain transport of interleukin links the immune and central nervous systems. Life Sci. **48:**PL117-121.
20. **Banks, W. A., A. J. Kastin, and E. G. Gutierrez.** 1994. Penetration of interleukin-6 across the murine blood-brain barrier. Neurosci Lett. **179:**53-56.
21. **Beard, C. W., A. O. Ball, E. H. Wooley, and K. R. Spindler.** 1990. Transcription mapping of mouse adenovirus type 1 early region 3. Virology **175:**81-90.
22. **Beard, C. W., and K. R. Spindler.** 1996. Analysis of early region 3 mutants of mouse adenovirus type 1. J. Virol. **70:**5867-5874.
23. **Beard, C. W., and K. R. Spindler.** 1995. Characterization of an 11K protein produced by early region 3 of mouse adenovirus type 1. Virology **208:**457-466.
24. **Becker, T. C., E. J. Wherry, D. Boone, K. Murali-Krishna, R. Antia, A. Ma, and R. Ahmed.** 2002. Interleukin 15 is required for proliferative renewal of virus-specific memory CD8 T cells. J. Exp. Med. **195:**1541-1548.
25. **Bennett, E.M., J. R. Bennink, J. W. Yewdell, and F. M. Brodsky.** 1999. Cutting edge: Adenovirus E19 has two mechanisms for affecting class I MHC expression. J. Immunol. **162:**5049-5052.
26. **Bentz, G. L., M. Jarquin-Pardo, G. Chan, M. S. Smith, C. Sinzger, and A. D. Yurochko.** 2006. Human cytomegalovirus (HCMV) infection of endothelial cells promotes naive monocyte extravasation and transfer of productive virus to enhance hematogenous dissemination of HCMV. J. Virol. **80:**11539-11555.
27. **Biron, C. A., and G. C. Sen.** 2007. Innate responses to viral infections, p. 249-278. *In* D. M. Knipe and P. M. Howley (ed.), Fields Virology, 5th ed, vol. 1. Lippincott Williams & Wilkins, Philadelphia.
28. **Blamire, A. M., D. C. Anthony, B. Rajagopalan, N. R. Sibson, V. H. Perry, and P. Styles.** 2000. Interleukin-1beta -induced changes in blood-brain barrier permeability, apparent diffusion coefficient, and cerebral blood volume in the rat brain: A magnetic resonance study. J. Neurosci. **20:**8153-8159.

29. **Boutin, H., R. A. LeFeuvre, R. Horai, M. Asano, Y. Iwakura, and N. J. Rothwell.** 2001. Role of IL-1alpha and IL-1beta in ischemic brain damage. J. Neurosci. **21:**5528-5534.
30. **Brutkiewicz, R. R., and R. M. Welsh.** 1995. Major histocompatibility complex class I antigens and the control of viral infections by natural killer cells. J. Virol. **69:**3967-3971.
31. **Bryceson, Y. T., M. E. March, H. G. Ljunggren, and E. O. Long.** 2006. Activation, coactivation, and costimulation of resting human natural killer cells. Immunol. Rev. **214:**73-91.
32. **Bukowski, J. F., B. A. Woda, and R. M. Welsh.** 1984. Pathogenesis of murine cytomegalovirus infection in natural killer cell-depleted mice. J. Virol. **52:**119-128.
33. **Burgert, H.-G., and S. Kvist.** 1985. An adenovirus type 2 glycoprotein blocks cell surface expression of human histocompatibility class I antigens. Cell **41:**987-997.
34. **Burns, J. C., T. Friedmann, W. Driever, M. Burrascano, and J. K. Yee.** 1993. Vesicular stomatitis virus G glycoprotein pseudotyped retroviral vectors: Concentration to very high titer and efficient gene transfer into mammalian and nonmammalian cells. Proc. Natl. Acad. Sci. U S A **90:**8033-8037.
35. **Campanella, M., C. Sciorati, G. Tarozzo, and M. Beltramo.** 2002. Flow cytometric analysis of inflammatory cells in ischemic rat brain. Stroke **33:**586-592.
36. **Carson, W. E., J. G. Giri, M. J. Lindemann, M. L. Linett, M. Ahdieh, R. Paxton, D. Anderson, J. Eisenmann, K. Grabstein, and M. A. Caligiuri.** 1994. Interleukin (IL) 15 is a novel cytokine that activates human natural killer cells via components of the IL-2 receptor. J Exp Med **180**.
37. **Cauthen, A. N., C. C. Brown, and K. R. Spindler.** 1999. In vitro and in vivo characterization of a mouse adenovirus type 1 early region 3 mutant. J. Virol. **73:**8640-8646.
38. **Cauthen, A. N., and K. R. Spindler.** 1999. Novel expression of mouse adenovirus type 1 early region 3 gp11K at late times after infection. Virology **259:**119-128.
39. **Cauthen, A. N., A. R. Welton, and K. R. Spindler.** 2007. Construction of mouse adenovirus type 1 mutants. Methods Mol. Med. **130:**41-59.
40. **Chai, H., S. Yan, H. Wang, R. Zhang, P. H. Lin, Q. Yao, and C. Chen.** 2006. CD40 ligand increases expression of its receptor CD40 in human coronary artery endothelial cells. Surgery **140:**236-242.
41. **Charles, P. C., X. Chen, M. S. Horwitz, and C. F. Brosnan.** 1999. Differential chemokine induction by the mouse adenovirus type-1 in the central nervous system of susceptible and resistant strains of mice. J. Neurovirol. **5:**55-64.
42. **Charles, P. C., J. D. Guida, C. F. Brosnan, and M. S. Horwitz.** 1998. Mouse adenovirus type-1 replication is restricted to vascular endothelium in the CNS of susceptible strains of mice. Virology **245:**216-228.
43. **Charo, I. F., and M. B. Taubman.** 2004. Chemokines in the pathogenesis of vascular disease. Circ. Res. **95:**858-866.

44. **Chin, Y. R., and M. S. Horwitz.** 2006. Adenovirus RID complex enhances degradation of internalized tumour necrosis factor receptor 1 without affecting its rate of endocytosis. J. Gen. Virol. **87:**3161-3167.
45. **Cockburn, I. A., S. Chakravarty, M. G. Overstreet, A. Garcia-Sastre, and F. Zavala.** 2008. Memory CD8+ T cell responses expand when antigen presentation overcomes T cell self-regulation. J. Immunol. **180:**64-71.
46. **Collins, K. L., B. K. Chen, S. A. Kalams, B. D. Walker, and D. Baltimore.** 1998. HIV-1 Nef protein protects infected primary cells against killing by cytotoxic T lymphocytes. Nature **391:**397-401.
47. **Cook, J. L., and J. M. Routes.** 2005. Adenovirus E1A gene-induced tumor cell rejection through cellular sensitization to immune and nonimmune apoptotic injuries. Front. Biosci. **10:**1396-1414.
48. **Cormont, M., M. Mari, A. Galmiche, P. Hofman, and Y. Le Marchand-Brustel.** 2001. A FYVE-finger-containing protein, Rabip4, is a Rab4 effector involved in early endosomal traffic. Proc. Natl. Acad. Sci. U S A **98:**1637-1642.
49. **Coutelier, J.-P., J. van Broeck, and S. F. Wolf.** 1995. Interleukin-12 gene expression after viral infection in the mouse. J. Virol. **69:**1955-1958.
50. **Couty, J. P., E. Geras-Raaka, B. B. Weksler, and M. C. Gershengorn.** 2001. Kaposi's sarcoma-associated herpesvirus G protein-coupled receptor signals through multiple pathways in endothelial cells. J. Biol. Chem. **276:**33805-33811.
51. **Czerkinsky, C. C., L. A. Nilsson, H. Nygren, O. Ouchterlony, and A. Tarkowski.** 1983. A solid-phase enzyme-linked immunospot (ELISPOT) assay for enumeration of specific antibody-secreting cells. J. Immunol. Methods **65:**109-121.
52. **D'Orlando, O., G. Gri, G. Cattaruzzi, S. Merluzzi, E. Betto, V. Gattei, and C. Pucillo.** 2007. Outside inside signalling in CD40-mediated B cell activation. J. Biol. Regul. Homeost. Agents **21:**49-62.
53. **D'Souza, T., R. Agarwal, and P. J. Morin.** 2005. Phosphorylation of claudin-3 at threonine 192 by cAMP-dependent protein kinase regulates tight junction barrier function in ovarian cancer cells. J. Biol. Chem. **280:**26233-26240.
54. **Dai, J., P. Wang, F. Bai, T. Town, and E. Fikrig.** 2008. Icam-1 participates in the entry of west nile virus into the central nervous system. J. Virol. **82:**4164-4168.
55. **Dallasta, L. M., L. A. Pisarov, J. E. Esplen, J. V. Werley, A. V. Moses, J. A. Nelson, and C. L. Achim.** 1999. Blood-brain barrier tight junction disruption in human immunodeficiency virus-1 encephalitis. Am. J. Pathol. **155:**1915-1927.
56. **de Vries, H. E., M. C. Blom-Roosemalen, M. van Oosten, A. G. de Boer, T. J. van Berkel, D. D. Breimer, and J. Kuiper.** 1996. The influence of cytokines on the integrity of the blood-brain barrier in vitro. J. Neuroimmunol. **64:**37-43.
57. **Dhawan, S., R. K. Puri, A. Kumar, H. Duplan, J. M. Masson, and B. B. Aggarwal.** 1997. Human immunodeficiency virus-1-tat protein induces the cell surface expression of endothelial leukocyte adhesion molecule-1, vascular cell adhesion molecule-1, and intercellular adhesion molecule-1 in human endothelial cells. Blood **90:**1535-1544.
58. **Dhillon, N. K., F. Peng, S. Bokhari, S. Callen, S. H. Shin, X. Zhu, K. J. Kim, and S. J. Buch.** 2008. Cocaine-mediated alteration in tight junction protein

expression and modulation of CCL2/CCR2 axis across the blood-brain barrier: Implications for HIV-dementia. J. Neuroimmune Pharmacol. **3:**52-56.

59. **Di Stefano, P., S. Cabodi, E. Boeri Erba, V. Margaria, E. Bergatto, M. G. Giuffrida, L. Silengo, G. Tarone, E. Turco, and P. Defilippi.** 2004. P130Cas-associated protein (p140Cap) as a new tyrosine-phosphorylated protein involved in cell spreading. Mol. Biol. Cell **15:**787-800.
60. **Di Stefano, P., L. Damiano, S. Cabodi, S. Aramu, L. Tordella, A. Praduroux, R. Piva, F. Cavallo, G. Forni, L. Silengo, G. Tarone, E. Turco, and P. Defilippi.** 2007. p140Cap protein suppresses tumour cell properties, regulating Csk and Src kinase activity. EMBO J **26:**2843-2855.
61. **Dobrogowska, D. H., and A. W. Vorbrodt.** 2004. Immunogold localization of tight junctional proteins in normal and osmotically-affected rat blood-brain barrier. J. Mol. Histol. **35:**529-539.
62. **Doronin, K., K. Toth, M. Kuppuswamy, P. Krajcsi, A. E. Tollefson, and W. S. Wold.** 2003. Overexpression of the ADP (E3-11.6K) protein increases cell lysis and spread of adenovirus. Virology **305:**378-387.
63. **Dragulev, B. P., S. Sira, M. G. AbouHaidar, and J. B. Campbell.** 1991. Sequence analysis of putative E3 and fiber genomic regions of two strains of canine adenovirus type 1. Virology **183:**298-305.
64. **Dubberke, E. R., B. Tu, D. J. Rivet, G. A. Storch, A. Apisarnthanarak, R. E. Schmidt, S. Weiss, and L. B. Polish.** 2006. Acute meningoencephalitis caused by adenovirus serotype 26. J Neurovirol **12:**235-40.
65. **Ehrlich, P. E.** 1885. Das Sauerstoff-Bedurfnis des Organismus. Eine Farbenanalytishe Studie.**:**4.
66. **Ellis, B., E. E. Schneeberger, and C. A. Rabito.** 1992. Cellular variability in the development of tight junctions after activation of protein kinase C. Am J Physiol **263:**F293-300.
67. **Eugenin, E. A., K. Osiecki, L. Lopez, H. Goldstein, T. M. Calderon, and J. W. Berman.** 2006. CCL2/monocyte chemoattractant protein-1 mediates enhanced transmigration of human immunodeficiency virus (HIV)-infected leukocytes across the blood-brain barrier: A potential mechanism of HIV-CNS invasion and NeuroAIDS. J. Neurosci. **26:**1098-1106.
68. **Fang, L., and K. R. Spindler.** 2005. E1A-CR3 interaction-dependent and -independent functions of mSur2 in viral replication of early region 1A mutants of mouse adenovirus type 1. J. Virol. **79:**3267-3276.
69. **Fang, L., J. L. Stevens, A. J. Berk, and K. R. Spindler.** 2004. Requirement of Sur2 for efficient replication of mouse adenovirus type 1. J. Virol. **78:**12888-12900.
70. **Fanning, A. S., B. J. Jameson, L. A. Jesaitis, and J. M. Anderson.** 1998. The tight junction protein ZO-1 establishes a link between the transmembrane protein occludin and the actin cytoskeleton. J. Biol. Chem. **273:**29745-29753.
71. **Farkas, G., J. Marton, Z. Nagy, Y. Mandi, T. Takacs, M. A. Deli, and C. S. Abraham.** 1998. Experimental acute pancreatitis results in increased blood-brain barrier permeability in the rat: A potential role for tumor necrosis factor and interleukin 6. Neurosci. Lett. **242:**147-150.

72. **Fauci, A. S., D. Mavilio, and S. Kottilil.** 2005. NK cells in HIV infection: paradigm for protection or targets for ambush. Nat. Rev. Immunol. **5:**835-843.
73. **Ferrari, C. C., A. M. Depino, F. Prada, N. Muraro, S. Campbell, O. Podhajcer, V. H. Perry, D. C. Anthony, and F. J. Pitossi.** 2004. Reversible demyelination, blood-brain barrier breakdown, and pronounced neutrophil recruitment induced by chronic IL-1 expression in the brain. Am. J. Pathol. **165:**1827-1837.
74. **Fischer, S., M. Wiesnet, D. Renz, and W. Schaper.** 2005. H2O2 induces paracellular permeability of porcine brain-derived microvascular endothelial cells by activation of the p44/42 MAP kinase pathway. Eur. J. Cell. Biol. **84:**687-697.
75. **Flomenberg, P., J. Babbitt, W. R. Drobyski, R. C. Ash, D. R. Carigan, G. V. Sedmak, T. McAuliffe, B. Camitta, M. M. Horowitz, N. Bunin, and J. T. Casper.** 1994. Increasing incidence of adenovirus disease in bone marrow transplant recipients. J. Inf. Dis. **169:**775-781.
76. **Flomenberg, P. R., M. Chen, and M. S. Horwitz.** 1988. Sequence and genetic organization of adenovirus type 35 early region 3. J. Virol. **62:**4431-4437.
77. **Fouraux, M. A., M. Deneka, V. Ivan, A. van der Heijden, J. Raymackers, D. van Suylekom, W. J. van Venrooij, P. van der Sluijs, and G. J. Pruijn.** 2004. Rabip4' is an effector of rab5 and rab4 and regulates transport through early endosomes. Mol. Biol. Cell **15:**611-624.
78. **Francis, K., J. van Beek, C. Canova, J. W. Neal, and P. Gasque.** 2003. Innate immunity and brain inflammation: The key role of complement. Expert Rev. Mol. Med. **5:**1-19.
79. **Fujibe, M., H. Chiba, T. Kojima, T. Soma, T. Wada, T. Yamashita, and N. Sawada.** 2004. Thr203 of claudin-1, a putative phosphorylation site for MAP kinase, is required to promote the barrier function of tight junctions. Exp. Cell. Res. **295:**36-47.
80. **Fukao, T., and S. Koyasu.** 2000. Expression of functional IL-2 receptors on mature splenic dendritic cells. Eur. J. Immunol. **30:**1453-1457.
81. **Fukao, T., S. Matsuda, and S. Koyasu.** 2000. Synergistic effects of IL-4 and IL-18 on IL-12-dependent IFN-gamma production by dendritic cells. J. Immunol. **164:**64-71.
82. **Gaillard, P. J., L. H. Voorwinden, J. L. Nielsen, A. Ivanov, R. Atsumi, H. Engman, C. Ringbom, A. G. de Boer, and D. D. Breimer.** 2001. Establishment and functional characterization of an in vitro model of the blood-brain barrier, comprising a co-culture of brain capillary endothelial cells and astrocytes. Eur. J. Pharm. Sci. **12:**215-222.
83. **Gallin, J. I., J. S. Bujak, E. Patten, and S. M. Wolff.** 1974. Granulocyte function in the Chediak-Higashi syndrome of mice. Blood **43:**201-206.
84. **Garnett, C. T., D. Erdman, W. Xu, and L. R. Gooding.** 2002. Prevalence and quantitation of species C adenovirus DNA in human mucosal lymphocytes. J. Virol. **76:**10608-10616.
85. **Ginsberg, H. S.** 1999. The life and times of adenoviruses. Adv. Virus Res. **54:**1-13.
86. **Glaser, C. A., S. Honarmand, L. J. Anderson, D. P. Schnurr, B. Forghani, C. K. Cossen, F. L. Schuster, L. J. Christie, and J. H. Tureen.** 2006. Beyond

viruses: clinical profiles and etiologies associated with encephalitis. Clin Infect Dis **43:**1565-77.

87. **Goldrath, A. W., P. V. Sivakumar, M. Glaccum, M. K. Kennedy, M. J. Bevan, C. Benoist, D. Mathis, and E. A. Butz.** 2002. Cytokine requirements for acute and basal homeostatic proliferation of naive and memory CD8+ T cells. J. Exp. Med. **195:**1515-1522.
88. **Gonzalez-Mariscal, L., R. Tapia, and D. Chamorro.** 2008. Crosstalk of tight junction components with signaling pathways. Biochim. Biophys. Acta. **1778:**729-756.
89. **Gopalakrishnan, S., N. Raman, S. J. Atkinson, and J. A. Marrs.** 1998. Rho GTPase signaling regulates tight junction assembly and protects tight junctions during ATP depletion. Am J Physiol **275:**C798-809.
90. **Gottardi, C. J., M. Arpin, A. S. Fanning, and D. Louvard.** 1996. The junction-associated protein, zonula occludens-1, localizes to the nucleus before the maturation and during the remodeling of cell-cell contacts. Proc. Natl. Acad. Sci. U S A **93:**10779-10784.
91. **Grabner, R., U. Till, and R. Heller.** 2000. Flow cytometric determination of E-selectin, vascular cell adhesion molecule-1, and intercellular cell adhesion molecule-1 in formaldehyde-fixed endothelial cell monolayers. Cytometry **40:**238-244.
92. **Griffin, W. S., and R. E. Mrak.** 2002. Interleukin-1 in the genesis and progression of and risk for development of neuronal degeneration in Alzheimer's disease. J. Leukoc. Biol. **72:**233-238.
93. **Grubor-Bauk, B., A. Simmons, G. Mayrhofer, and P. G. Speck.** 2003. Impaired clearance of herpes simplex virus type 1 from mice lacking CD1d or NKT cells expressing the semivariant Vα14-Jα281 TCR. J. Immunol. **170:**1430-1434.
94. **Guida, J. D., G. Fejer, L.-A. Pirofski, C. F. Brosnan, and M. S. Horwitz.** 1995. Mouse adenovirus type 1 causes a fatal hemorrhagic encephalomyelitis in adult C57BL/6 but not BALB/c mice. J. Virol. **69:**7674-7681.
95. **Hakim, F. A., and I. M. Tleyjeh.** 2008. Severe adenovirus pneumonia in immunocompetent adults: a case report and review of the literature. Eur J Clin Microbiol Infect Dis **27:**153-8.
96. **Haorah, J., S. H. Ramirez, K. Schall, D. Smith, R. Pandya, and Y. Persidsky.** 2007. Oxidative stress activates protein tyrosine kinase and matrix metalloproteinases leading to blood-brain barrier dysfunction. J. Neurochem. **101:**566-576.
97. **Hartley, J. W., and W. P. Rowe.** 1960. A new mouse virus apparently related to the adenovirus group. Virology **11:**645-647.
98. **Hauser, S. L., T. H. Doolittle, R. Lincoln, R. H. Brown, and C. A. Dinarello.** 1990. Cytokine accumulations in CSF of multiple sclerosis patients: Frequent detection of interleukin-1 and tumor necrosis factor but not interleukin-6. Neurology **40:**1735-1739.
99. **Hawkins, B. T., and T. P. Davis.** 2005. The blood-brain barrier/neurovascular unit in health and disease. Pharmacol. Rev. **57:**173-185.

100. **Hayes, J. S., and S. E. Mayer.** 1981. Regulation of guinea pig heart phosphorylase kinase by cAMP, protein kinase, and calcium. Am J Physiol **240:**E340-9.
101. **Helfrich, I., A. Schmitz, P. Zigrino, C. Michels, I. Haase, A. le Bivic, M. Leitges, and C. M. Niessen.** 2007. Role of aPKC isoforms and their binding partners Par3 and Par6 in epidermal barrier formation. J. Invest. Dermatol. **127:**782-791.
102. **Herold, S., W. von Wulffen, M. Steinmueller, S. Pleschka, W. A. Kuziel, M. Mack, M. Srivastava, W. Seeger, U. A. Maus, and J. Lohmeyer.** 2006. Alveolar epithelial cells direct monocyte transepithelial migration upon influenza virus infection: impact of chemokines and adhesion molecules. J. Immunol. **177:**1817-1824.
103. **Hierholzer, J. C., R. Wigand, L. J. Anderson, T. Adrian, and J. W. M. Gold.** 1988. Adenoviruses from patients with AIDS: a plethora of serotypes and a description of five new serotypes of subgenus D (types 43-47). J. Inf. Dis. **158:**804-813.
104. **Hirase, T., J. M. Staddon, M. Saitou, Y. Ando-Akatsuka, M. Itoh, M. Furuse, K. Fujimoto, S. Tsukita, and L. L. Rubin.** 1997. Occludin as a possible determinant of tight junction permeability in endothelial cells. J Cell Sci **110 (Pt 14):**1603-13.
105. **Hollander, G. A., S. J. Simpson, E. Mizoguchi, A. Nichogiannopoulou, J. She, J. C. Gutierrez-Ramos, A. K. Bhan, S. J. Burakoff, B. Wang, and C. Terhorst.** 1995. Severe colitis in mice with aberrant thymic selection. Immunity **3:**27-38.
106. **Horvath, J., L. Palkonyay, and J. Weber.** 1986. Group C adenovirus DNA sequences in human lymphoid cells. J. Virol. **59:**189-192.
107. **Horwitz, M. S.** 2001. Adenovirus immunoregulatory genes and their cellular targets. Virology **279:**1-8.
108. **Horwitz, M. S.** 1990. Adenoviruses, p. 1723-1740. *In* B. N. Fields and D. M. Knipe (ed.), Virology, 2d ed. Raven Press, New York.
109. **Horwitz, M. S., G. Valderrama, V. Hatcher, R. Korn, P. deJong, and I. Spigland.** 1984. Characterization of adenovirus isolates from AIDS patients. Ann N Y Acad Sci **437:**161-74.
110. **Ishizaki, T., H. Chiba, T. Kojima, M. Fujibe, T. Soma, H. Miyajima, K. Nagasawa, I. Wada, and N. Sawada.** 2003. Cyclic AMP induces phosphorylation of claudin-5 immunoprecipitates and expression of claudin-5 gene in blood-brain-barrier endothelial cells via protein kinase A-dependent and -independent pathways. Exp. Cell Res. **290:**275-288.
111. **Jain, S. K., M. Paul-Satyaseela, G. Lamichhane, K. S. Kim, and W. R. Bishai.** 2006. Mycobacterium tuberculosis invasion and traversal across an in vitro human blood-brain barrier as a pathogenic mechanism for central nervous system tuberculosis. J. Infec. Dis. **193:**1287-1295.
112. **Jou, T. S., E. E. Schneeberger, and W. J. Nelson.** 1998. Structural and functional regulation of tight junctions by RhoA and Rac1 small GTPases. J Cell Biol **142:**101-15.

113. **Kajon, A. E., C. C. Brown, and K. R. Spindler.** 1998. Distribution of mouse adenovirus type 1 in intraperitoneally and intranasally infected adult outbred mice. J. Virol. **72:**1219-1223.
114. **Kajon, A. E., and K. R. Spindler.** 2000. Mouse adenovirus type 1 replication *in vitro* is resistant to interferon. Virology **274:**213-219.
115. **Kalvakolanu, D. V. R., S. K. Bandyopadhyay, M. L. Harter, and G. C. Sen.** 1991. Inhibition of interferon-inducible gene expression by adenovirus E1A proteins - block in transcriptional complex formation. Proc. Natl. Acad. Sci. USA **88:**7459-7463.
116. **Kaminsky, S. G., I. Nakamura, and G. Cudkowicz.** 1983. Selective defect of natural killer and killer cell activity against lymphomas in SJL mice: low responsiveness to interferon inducers. J. Immunol. **130:**1980-1984.
117. **Kampmann, B., D. Cubitt, T. Walls, P. Naik, M. Depala, S. Samarasinghe, D. Robson, A. Hassan, K. Rao, H. Gaspar, G. Davies, A. Jones, C. Cale, K. Gilmour, M. Real, M. Foo, N. Bennett-Rees, A. Hewitt, P. Amrolia, and P. Veys.** 2005. Improved outcome for children with disseminated adenoviral infection following allogeneic stem cell transplantation. Br J Haematol **130:**595-603.
118. **Kanmogne, G. D., C. Primeaux, and P. Grammas.** 2005. HIV-1 gp120 proteins alter tight junction protein expression and brain endothelial cell permeability: Implications for the pathogenesis of HIV-associated dementia. J. Neuropathol. Exp. Neurol. **64:**498-505.
119. **Karpus, W. J., K. J. Kennedy, B. T. Fife, J. L. Bennett, M. C. Dal Canto, S. L. Kunkel, and N. W. Lukacs.** 2006. Anti-CCL2 treatment inhibits Theiler's murine encephalomyelitis virus-induced demyelinating disease. J. Neurovirol. **12:**251-261.
120. **Kärre, K., G. O. Klein, R. Kiessling, G. Klein, and J. C. Roder.** 1980. In vitro NK-activity and in vivo resistance to leukemia: Studies of beige, beige//nude and wild-type hosts on C57BL background. Int. J. Cancer **26:**789-797.
121. **Kawakami, K., N. Yamamoto, Y. Kinjo, K. Miyagi, C. Nakasone, K. Uezu, T. Kinjo, T. Nakayama, M. Taniguchi, and A. Saito.** 2003. Critical role of Vα14+ natural killer T cells in the innate phase of host protection against *Streptococcus pneumoniae* infection. Eur. J. Immunol. **33:**3322-3330.
122. **Kennedy, M. K., M. Glaccum, S. N. Brown, E. A. Butz, J. L. Viney, M. Embers, N. Matsuki, K. Charrier, L. Sedger, C. R. Willis, K. Brasel, P. J. Morrissey, K. Stocking, J. C. Schuh, S. Joyce, and J. J. Peschon.** 2000. Reversible defects in natural killer and memory CD8 T cell lineages in interleukin 15-deficient mice. J. Exp. Med. **191:**771-780.
123. **Kevil, C. G., T. Oshima, B. Alexander, L. L. Coe, and J. S. Alexander.** 2000. H(2)O(2)-mediated permeability: Role of MAPK and occludin. Am. J. Physiol. Cell. Physiol. **279:**C21-30.
124. **Khan, W. N., F. W. Alt, R. M. Gerstein, B. A. Malynn, I. Larsson, G. Rathbun, L. Davidson, S. Muller, A. B. Kantor, L. A. Herzenberg, F. S. Rosen, and P. Sideras.** 1995. Defective B cell development and function in Btk-deficient mice. Immunity **3:**283-299.

125. **Khan, W. N., P. Sideras, F. S. Rosen, and F. W. Alt.** 1995. The role of Bruton's tyrosine kinase in B-cell development and function in mice and man. Ann. N.Y. Acad. Sci. **764:**27-38.
126. **Kim, K. M., S. N. Kwon, J. I. Kang, S. H. Lee, S. K. Jang, B. Y. Ahn, and Y. K. Kim.** 2007. Hepatitis C virus NS2 protein activates cellular cyclic AMP-dependent pathways. Biochem. Biophys. Res. Commun. **356:**948-954.
127. **Kjems, J., M. Brown, D. D. Chang, and P. A. Sharp.** 1991. Structural analysis of the interaction between the human immunodeficiency virus Rev protein and the Rev response element. Proc. Natl. Acad. Sci. U S A **88:**683-687.
128. **Knuesel, M., Y. Wan, Z. Xiao, E. Holinger, N. Lowe, W. Wang, and X. Liu.** 2003. Identification of novel protein-protein interactions using a versatile mammalian tandem affinity purification expression system. Mol. Cell. Proteomics **2:**1225-1233.
129. **Koneru, B., R. Jaffe, C. O. Esquivel, R. Kunz, S. Todo, S. Iwatsuki, and T. E. Starzl.** 1987. Adenoviral infections in pediatric liver transplant recipients. JAMA **258:**489-492.
130. **Kozak, M.** 1986. Point mutations define a sequence flanking the AUG initiator codon that modulates translation by eukaryotic ribosomes. Cell **44:**283-292.
131. **Kring, S. C., C. S. King, and K. R. Spindler.** 1995. Susceptibility and signs associated with mouse adenovirus type 1 infection of adult outbred Swiss mice. J. Virol. **69:**8084-8088.
132. **Kring, S. C., and K. R. Spindler.** 1996. Lack of effect of mouse adenovirus type 1 infection on the cell surface expression of major histocompatibility complex class I antigens. J. Virol. **70:**5495-5502.
133. **Krizanac-Bengez, L., M. Kapural, F. Parkinson, L. Cucullo, M. Hossain, M. R. Mayberg, and D. Janigro.** 2003. Effects of transient loss of shear stress on blood-brain barrier endothelium: Role of nitric oxide and IL-6. Brain Res. Brain Res. Rev. **977:**239-246.
134. **Krizbai, I. A., and M. A. Deli.** 2003. Signalling pathways regulating the tight junction permeability in the blood-brain barrier. Cell. Mol. Biol. (Noisy-le-grand) **49:**23-31.
135. **Lai, C. H., K. H. Kuo, and J. M. Leo.** 2005. Critical role of actin in modulating BBB permeability. Brain Res. Brain Res. Rev. **50:**7-13.
136. **Larsen, S. H., and D. Nathans.** 1977. Mouse adenovirus: growth of plaque-purified FL virus in cell lines and characterization of viral DNA. Virology **82:**182-195.
137. **Lassoued, S., R. Ben Ameur, W. Ayadi, B. Gargouri, R. Ben Mansour, and H. Attia.** 2008. Epstein-Barr virus induces an oxidative stress during the early stages of infection in B lymphocytes, epithelial, and lymphoblastoid cell lines. Mol. Cell. Biochem. **313:**179-186.
138. **Lauer, K. P., I. Llorente, E. Blair, J. Seto, V. Krasnov, A. Purkayastha, S. E. Ditty, T. L. Hadfield, C. Buck, C. Tibbetts, and D. Seto.** 2004. Natural variation among human adenoviruses: genome sequence and annotation of human adenovirus serotype 1. J Gen Virol **85:**2615-25.

139. **Lee, J. D., L. Y. Tsai, C. H. Chen, J. J. Wang, J. K. Hsiao, and C. M. Yen.** 2006. Blood-brain barrier dysfunction occurring in mice infected with Angiostrongylus cantonensis. Acta. Trop. **97:**204-211.
140. **Lee, Y. R., M. T. Liu, H. Y. Lei, C. C. Liu, J. M. Wu, Y. C. Tung, Y. S. Lin, T. M. Yeh, S. H. Chen, and H. S. Liu.** 2006. MCP-1, a highly expressed chemokine in dengue haemorrhagic fever/dengue shock syndrome patients, may cause permeability change, possibly through reduced tight junctions of vascular endothelium cells. J. Gen. Virol. **87:**3623-3630.
141. **Lenaerts, L., E. Verbeken, E. De Clercq, and L. Naesens.** 2005. Mouse adenovirus type 1 infection in SCID mice: An experimental model for antiviral therapy of systemic adenovirus infections. Antimicrob. Agents Chemother. **49:**4689-4699.
142. **Leonard, G. T., and G. C. Sen.** 1996. Effects of adenovirus E1A protein on interferon-signaling. Virology **224:**25-33.
143. **Li, Y., J. Kang, and M. S. Horowitz.** 1998. Interaction of an adenovirus E3 14.7-kilodalton protein with a novel tumor necrosis factor alpha-inducible cellular protein containing leucine zipper domains. Molec. Cell. Bio. **18:**1601-1610.
144. **Liebner, S., U. Kniesel, H. Kalbacher, and H. Wolburg.** 2000. Correlation of tight junction morphology with the expression of tight junction proteins in blood-brain barrier endothelial cells. Eur. J. Cell Biol. **79:**707-717.
145. **Lindgren, H., S. Stenmark, W. Chen, A. Tarnvik, and A. Sjostedt.** 2004. Distinct roles of reactive nitrogen and oxygen species to control infection with the facultative intracellular bacterium Francisella tularensis. Infect. Immun. **72:**7172-7182.
146. **Liu, L. B., Y. X. Xue, Y. H. Liu, and Y. B. Wang.** 2008. Bradykinin increases blood-tumor barrier permeability by down-regulating the expression levels of ZO-1, occludin, and claudin-5 and rearranging actin cytoskeleton. J. Neurosci. Res. **86:**1153-1168.
147. **Lo, S. K., S. Lee, R. A. Ramos, R. Lobb, M. Rosa, G. Chi-Rosso, and S. D. Wright.** 1991. Endothelial-leukocyte adhesion molecule 1 stimulates the adhesive activity of leukocyte integrin CR3 (CD11b/CD18, Mac-1, alpha m beta 2) on human neutrophils. J Exp Med **173:**1493-500.
148. **Lodoen, M. B., and L. L. Lanier.** 2006. Natural killer cells as an initial defense against pathogens. Curr. Opin. Immunol. **18:**391-398.
149. **Lois, C., E. J. Hong, S. Pease, E. J. Brown, and D. Baltimore.** 2002. Germline transmission and tissue-specific expression of transgenes delivered by lentiviral vectors. Science **295:**868-872.
150. **Lukashok, S. A., and M. S. Horwitz.** 1999. Adenovirus, p. 147-164. *In* R. Ahmed and I. Chen (ed.), Persistent Viral Infections. John Wiley & Sons, New York.
151. **Lukashok, S. A., L. Tarassishin, Y. Li, and M. Horwitz.** 2000. An adenovirus inhibitor of tumor necrosis factor alpha-induced apoptosis complexes with dynein and a small GTPase. J. Virol. **74:**4705-4709.
152. **Luscinskas, F. W., and M. A. Gimbrone, Jr.** 1996. Endothelial-dependent mechanisms in chronic inflammatory leukocyte recruitment. Annu. Rev. Med. **47:**413-421.

153. **Mahad, D., M. K. Callahan, K. A. Williams, E. E. Ubogu, P. Kivisakk, B. Tucky, G. Kidd, G. A. Kingsbury, A. Chang, R. J. Fox, M. Mack, M. B. Sniderman, R. Ravid, S. M. Staugaitis, M. F. Stins, and R. M. Ransohoff.** 2006. Modulating CCR2 and CCL2 at the blood-brain barrier: Relevance for multiple sclerosis pathogenesis. Brain **129:**212-223.

154. **Mari, M., P. Monzo, V. Kaddai, F. Keslair, T. Gonzalez, Y. Le Marchand-Brustel, and M. Cormont.** 2006. The Rab4 effector Rabip4 plays a role in the endocytotic trafficking of Glut 4 in 3T3-L1 adipocytes. J. Cell. Sci. **119:**1297-1306.

155. **Mark, K. S., and D. W. Miller.** 1999. Increased permeability of primary cultured brain microvessel endothelial cell monolayers following TNF-alpha exposure. Life Sci. **64:**1941-1953.

156. **McCandless, E. E., B. Zhang, M. S. Diamond, and R. S. Klein.** 2008. CXCR4 antagonism increases T cell trafficking in the central nervous system and improves survival from West Nile virus encephalitis. Proc. Natl. Acad. Sci. U S A **105:**11270-11275.

157. **McSharry, B. P., H. G. Burgert, D. P. Owen, R. J. Stanton, V. Prod'homme, M. Sester, K. Koebernick, V. Groh, T. Spies, S. Cox, A. M. Little, E. C. Wang, P. Tomasec, and G. W. Wilkinson.** 2008. Adenovirus E3/19K promotes evasion of NK cell recognition by intracellular sequestration of the NKG2D ligands major histocompatibility complex class I chain-related proteins A and B. J Virol **82:**4585-94.

158. **Milner, R., and I. L. Campbell.** 2006. Increased expression of the beta4 and alpha5 integrin subunits in cerebral blood vessels of transgenic mice chronically producing the pro-inflammatory cytokines IL-6 or IFN-alpha in the central nervous system. Mol. Cell. Neurosci. **33:**429-440.

159. **Moore, M. L., C. C. Brown, and K. R. Spindler.** 2003. T cells cause acute immunopathology and are required for long-term survival in mouse adenovirus type 1-induced encephalomyelitis. J. Virol. **77:**10060-10070.

160. **Moore, M. L., E. L. McKissic, C. C. Brown, J. E. Wilkinson, and K. R. Spindler.** 2004. Fatal disseminated mouse adenovirus type 1 infection in mice lacking B cells or Bruton's tyrosine kinase. *J. Virol.* **78:**5584-5590.

161. **Morgan, L., B. Shah, L. E. Rivers, L. Barden, A. J. Groom, R. Chung, D. Higazi, H. Desmond, T. Smith, and J. M. Staddon.** 2007. Inflammation and dephosphorylation of the tight junction protein occludin in an experimental model of multiple sclerosis. Neuroscience **147:**664-73.

162. **Morganti-Kossmann, M. C., M. Rancan, P. F. Stahel, and T. Kossmann.** 2002. Inflammatory response in acute traumatic brain injury: a double-edged sword. Curr. Opin. Crit. Care **8:**101-105.

163. **Morita, K., M. Furuse, K. Fujimoto, and S. Tsukita.** 1999. Claudin multigene family encoding four-transmembrane domain protein components of tight junction strands. Proc Natl Acad Sci U S A **96:**511-6.

164. **Morrey, J. D., A. L. Olsen, V. Siddharthan, N. E. Motter, H. Wang, B. S. Taro, D. Chen, D. Ruffner, and J. O. Hall.** 2008. Increased blood-brain barrier permeability is not a primary determinant for lethality of West Nile virus infection in rodents. J. Gen. Virol. **89:**467-473.

165. **Morrison, M. D., D. Reid, D. Onions, N. Spibey, and L. Nicolson.** 2002. Generation of E3-deleted canine adenoviruses expressing canine parvovirus capsid by homologous recombination in bacteria. Virology **293:**26-30.
166. **Mühlen, K. A., J. Schumann, F. Wittke, S. Stenger, N. Van Rooijen, L. Van Kaer, and G. Tiegs.** 2004. NK cells, but not NKT cells, are involved in *Pseudomonas aeruginosa* exotoxin A-induced hepatotoxicity in mice. J. Immunol. **172:**3034-3041.
167. **Mullin, J. M., J. A. Kampherstein, K. V. Laughlin, C. E. Clarkin, R. D. Miller, Z. Szallasi, B. Kachar, A. P. Soler, and D. Rosson.** 1998. Overexpression of protein kinase C-delta increases tight junction permeability in LLC-PK1 epithelia. Am. J. Physiol. **275:**C544-554.
168. **Nokta, M., and R. Pollard.** 1991. Human immunodeficiency virus infection: Association with altered intracellular levels of cAMP and cGMP in MT-4 cells. Virology **181:**211-217.
169. **Nusrat, A., M. Giry, J. R. Turner, S. P. Colgan, C. A. Parkos, D. Carnes, E. Lemichez, P. Boquet, and J. L. Madara.** 1995. Rho protein regulates tight junctions and perijunctional actin organization in polarized epithelia. Proc. Natl. Acad. Sci. U S A **92:**10629-10633.
170. **Obar, J. J., S. G. Crist, E. K. Leung, and E. J. Usherwood.** 2004. IL-15-independent proliferative renewal of CD8+ T cells in latent gammaherpesvirus infection. J. Immunol. **173:**2705-2714.
171. **Ohteki, T., T. Fukao, K. Suzue, C. Maki, M. Ito, M. Nakamura, and S. Koyasu.** 1999. Interleukin 12-dependent interferon gamma production by CD8alpha+ lymphoid dendritic cells. J. Exp. Med. **189:**1981-1986.
172. **Ono, S. J., T. Nakamura, D. Miyazaki, M. Ohbayashi, M. Dawson, and M. Toda.** 2003. Chemokines: Roles in leukocyte development, trafficking, and effector function. J. Allergy Clin. Immunol. **111:**1185-1199.
173. **Orange, J. S., M. S. Fassett, L. A. Koopman, J. E. Boyson, and J. L. Strominger.** 2002. Viral evasion of natural killer cells. Nat. Immunol. **3:**1006-1012.
174. **Park, R., and J. D. Baines.** 2006. Herpes simplex virus type 1 infection induces activation and recruitment of protein kinase C to the nuclear membrane and increased phosphorylation of lamin B. J. Virol. **80:**494-504.
175. **Paul, R., U. Koedel, F. Winkler, B. C. Kieseier, A. Fontana, M. Kopf, H. P. Hartung, and H. W. Pfister.** 2003. Lack of IL-6 augments inflammatory response but decreases vascular permeability in bacterial meningitis. Brain **126:**1873-1882.
176. **Peng, Y., E. Falck-Pedersen, and K. B. Eikon.** 2001. Variation in adenovirus transgene expression between BALB/c and C57BL/6 mice is associated with differences in interleukin-12 and gamma interferon production and NK cell activation. J. Virol. **75:**4540-4550.
177. **Persidsky, Y., D. Heilman, J. Haorah, M. Zelivyanskaya, R. Persidsky, G. A. Weber, H. Shimokawa, K. Kaibuchi, and T. Ikezu.** 2006. Rho-mediated regulation of tight junctions during monocyte migration across the blood-brain barrier in HIV-1 encephalitis (HIVE). Blood **107:**4770-80.

178. **Persidsky, Y., S. H. Ramirez, J. Haorah, and G. D. Kanmogne.** 2006. Blood-brain barrier: Structural components and function under physiologic and pathologic conditions. J. Neuroimmune Pharmacol. **1:**223-236.
179. **Phares, T. W., R. B. Kean, T. Mikheeva, and D. C. Hooper.** 2006. Regional differences in blood-brain barrier permeability changes and inflammation in the apathogenic clearance of virus from the central nervous system. J. Immunol. **176:**7666-7675.
180. **Pirofski, L., M. S. Horwitz, M. D. Scharff, and S. M. Factor.** 1991. Murine adenovirus infection of SCID mice induces hepatic lesions that resemble human Reye syndrome. Proc. Natl. Acad. Sci. USA **88:**4358-4362.
181. **Podack, E. R., J. D. Young, and Z. A. Cohn.** 1985. Isolation and biochemical and functional characterization of perforin 1 from cytolytic T-cell granules. Proc. Natl. Acad. Sci. U S A **82:**8629-8633.
182. **Prlic, M., L. Lefrancois, and S. C. Jameson.** 2002. Multiple choices: regulation of memory CD8 T cell generation and homeostasis by interleukin (IL)-7 and IL-15. J. Exp. Med. **195:**F49-52.
183. **Pu, H., J. Tian, I. E. Andras, K. Hayashi, G. Flora, B. Hennig, and M. Toborek.** 2005. HIV-1 Tat protein-induced alterations of ZO-1 expression are mediated by redox-regulated ERK 1/2 activation. J. Cereb. Blood Flow Metab. **25:**1325-1335.
184. **Pu, H., J. Tian, G. Flora, Y. W. Lee, A. Nath, B. Hennig, and M. Toborek.** 2003. HIV-1 Tat protein upregulates inflammatory mediators and induces monocyte invasion into the brain. Mol. Cell. Neurosci. **24:**224-237.
185. **Puddu, P., L. Fantuzzi, P. Borghi, B. Varano, G. Rainaldi, E. Guillemard, W. Malorni, P. Nicaise, S. F. Wolf, F. Belardelli, and S. Gessani.** 1997. IL-12 induces IFN-gamma expression and secretion in mouse peritoneal macrophages. J. Immunol. **159:**3490-3497.
186. **Puig, O., F. Caspary, G. Rigaut, B. Rutz, E. Bouveret, E. Bragado-Nilsson, M. Wilm, and B. Seraphin.** 2001. The tandem affinity purification (TAP) method: A general procedure of protein complex purification. Methods **24:**218-229.
187. **Qin, X. F., D. S. An, I. S. Chen, and D. Baltimore.** 2003. Inhibiting HIV-1 infection in human T cells by lentiviral-mediated delivery of small interfering RNA against CCR5. Proc. Natl. Acad. Sci. U S A **100:**183-188.
188. **Rahbar, A., and C. Soderberg-Naucler.** 2005. Human cytomegalovirus infection of endothelial cells triggers platelet adhesion and aggregation. J. Virol. **79:**2211-2220.
189. **Raub, T. J.** 1996. Signal transduction and glial cell modulation of cultured brain microvessel endothelial cell tight junctions. Am J Physiol **271:**C495-503.
190. **Raviprakash, K. S., A. Grunhaus, M. A. El Kholy, and M. S. Horwitz.** 1989. The mouse adenovirus type 1 contains an unusual E3 region. J. Virol. **63:**5455-5458.
191. **Reddy, P. S., N. Idamakanti, J. B. Derbyshire, and E. Nagy.** 1996. Porcine adenoviruses types 1, 2 and 3 have short and simple early E-3 regions. Virus Res. **43:**99-109.

192. **Reich, N. C., R. Pine, D. Levy, and J. E. Darnell.** 1988. Transcription of interferon-stimulated genes is induced by adenovirus particles but is suppressed by E1A gene products. J. Virol. **62:**114-119.
193. **Rigaut, G., A. Shevchenko, B. Rutz, M. Wilm, M. Mann, and B. Seraphin.** 1999. A generic protein purification method for protein complex characterization and proteome exploration. Nat. Biotechnol. **17:**1030-1032.
194. **Roder, J., and A. Duwe.** 1979. The *beige* mutation in the mouse selectively impairs natural killer cell function. Nature **278:**451-453.
195. **Rowe, P. W., and J. W. Hartley.** 1962. A general review of the adenoviruses. Ann. New York Acad. Sci. **101:**466-474.
196. **Rubin, L. L., and J. M. Staddon.** 1999. The cell biology of the blood-brain barrier. Annu. Rev. Neurosci. **22:**11-28.
197. **Russell, W. C.** 2000. Update on adenovirus and its vectors. J. Gen. Virol. **81:**2573-2604.
198. **Ruzek, M. C., B. F. Kavanagh, A. Scaria, S. M. Richards, and R. D. Garman.** 2002. Adenoviral vectors stimulate murine natural killer cell responses and demonstrate antitumor activities in the absence of transgene expression. Molec. Ther. **5:**115-124.
199. **Sadowski, M., J. Pankiewicz, H. Scholtzova, Y. S. Li, D. Quartermain, K. Duff, and T. Wisniewski.** 2004. Links between the pathology of Alzheimer's disease and vascular dementia. Neurochem. Res. **29:**1257-1266.
200. **Sakakibara, A., M. Furuse, M. Saitou, Y. Ando-Akatsuka, and S. Tsukita.** 1997. Possible involvement of phosphorylation of occludin in tight junction formation. J. Cell Biol. **137:**1393-1401.
201. **Samuel, M. A., and M. S. Diamond.** 2005. Alpha/beta interferon protects against lethal West Nile virus infection by restricting cellular tropism and enhancing neuronal survival. J Virol **79:**13350-61.
202. **Sauty, A., M. Dziejman, R. A. Taha, A. S. Iarossi, K. Neote, E. A. Garcia-Zepeda, Q. Hamid, and A. D. Luster.** 1999. The T cell-specific CXC chemokines IP-10, Mig, and I-TAC are expressed by activated human bronchial epithelial cells. J. Immunol. **162:**3549-3558.
203. **Saxena, R. K., Q. B. Saxena, and W. H. Adler.** 1982. Defective T-cell response in beige mutant mice. Nature **295:**240-241.
204. **Schluns, K. S., K. Williams, A. Ma, X. X. Zheng, and L. Lefrancois.** 2002. Cutting edge: Requirement for IL-15 in the generation of primary and memory antigen-specific CD8 T cells. J. Immunol. **168:**4827-4831.
205. **Schneider-Brachert, W., V. Tchikov, O. Merkel, M. Jakob, C. Hallas, M. L. Kruse, P. Groitl, A. Lehn, E. Hildt, J. Held-Feindt, T. Dobner, D. Kabelitz, M. Kronke, and S. Schutze.** 2006. Inhibition of TNF receptor 1 internalization by adenovirus 14.7K as a novel immune escape mechanism. J, Clin, Invest, **116:**2901-2913.
206. **Scholz, M., J. Cinatl, M. Schadel-Hopfner, and J. Windolf.** 2007. Neutrophils and the blood-brain barrier dysfunction after trauma. Med. Res. Rev. **27:**401-416.
207. **Seth, A., P. Sheth, B. C. Elias, and R. Rao.** 2007. Protein phosphatases 2A and 1 interact with occludin and negatively regulate the assembly of tight junctions in the CACO-2 cell monolayer. J Biol Chem **282:**11487-98.

208. **Sheibani, N.** 1999. Prokaryotic gene fusion expression systems and their use in structural and functional studies of proteins. Prep. Biochem. Biotechnol. **29:**77-90.
209. **Shen, J., T. T. SS, L. Schrieber, and N. J. King.** 1997. Early E-selectin, VCAM-1, ICAM-1, and late major histocompatibility complex antigen induction on human endothelial cells by flavivirus and comodulation of adhesion molecule expression by immune cytokines. J. Virol. **71:**9323-9332.
210. **Shevchenko, A., D. Schaft, A. Roguev, W. W. Pijnappel, and A. F. Stewart.** 2002. Deciphering protein complexes and protein interaction networks by tandem affinity purification and mass spectrometry: Analytical perspective. Mol. Cell. Proteomics **1:**204-212.
211. **Shrestha, B., B. Zhang, W. E. Purtha, R. S. Klein, and M. S. Diamond.** 2008. Tumor necrosis factor alpha protects against lethal West Nile virus infection by promoting trafficking of mononuclear leukocytes into the central nervous system. J. Virol. **82:**8956-8964.
212. **Sikorski, E. E., R. Hallmann, E. L. Berg, and E. C. Butcher.** 1993. The Peyer's patch high endothelial receptor for lymphocytes, the mucosal vascular addressin, is induced on a murine endothelial cell line by tumor necrosis factor-alpha and IL-1. J. Immunol. **151:**5239-5250.
213. **Singh, C. R., and K. Asano.** 2007. Localization and characterization of protein-protein interaction sites. Methods Enzymol. **429:**139-161.
214. **Sitati, E., E. E. McCandless, R. S. Klein, and M. S. Diamond.** 2007. CD40-CD40 ligand interactions promote trafficking of CD8+ T cells into the brain and protection against West Nile virus encephalitis. J. Virol. **81:**9801-9811.
215. **Slifka, M. K., R. R. Pagarigan, and J. L. Whitton.** 2000. NK markers are expressed on a high percentage of virus-specific CD8+ and CD4+ T cells. J. Immunol. **164:**2009-2015.
216. **Smith, K., C. C. Brown, and K. R. Spindler.** 1998. The role of mouse adenovirus type 1 early region 1A in acute and persistent infections in mice. J. Virol. **72:**5699-5706.
217. **Soma, T., H. Chiba, Y. Kato-Mori, T. Wada, T. Yamashita, T. Kojima, and N. Sawada.** 2004. Thr(207) of claudin-5 is involved in size-selective loosening of the endothelial barrier by cyclic AMP. Exp. Cell. Res. **300:**202-212.
218. **Song, L., and J. S. Pachter.** 2003. Culture of murine brain microvascular endothelial cells that maintain expression and cytoskeletal association of tight junction-associated proteins. In Vitro Cell. Dev. Bio.l Anim. **39:**313-320.
219. **Song, L., and J. S. Pachter.** 2004. Monocyte chemoattractant protein-1 alters expression of tight junction-associated proteins in brain microvascular endothelial cells. Microvasc. Res. **67:**78-89.
220. **Spindler, K. R., L. Fang, M. L. Moore, C. C. Brown, G. N. Hirsch, and A. K. Kajon.** 2001. SJL/J mice are highly susceptible to infection by mouse adenovirus type 1. J. Virol. **75:**12039-12046.
221. **Spindler, K. R., M. L. Moore, and A. N. Cauthen.** 2007. Mouse adenoviruses, p. 49-65, The mouse in biomedical research, 2nd ed, vol. 2. Academic Press, New York.

222. **Stamatovic, S. M., R. F. Keep, S. L. Kunkel, and A. V. Andjelkovic.** 2003. Potential role of MCP-1 in endothelial cell tight junction 'opening' signaling via Rho and Rho kinase. J. Cell Sci. **116:**4615-4628.
223. **Stamatovic, S. M., P. Shakui, R. F. Keep, B. B. Moore, S. L. Kunkel, N. Van Rooijen, and A. V. Andjelkovic.** 2005. Monocyte chemoattractant protein-1 regulation of blood-brain barrier permeability. J. Cereb. Blood Flow Metab. **25:**593-606.
224. **Steeber, D. A., and T. F. Tedder.** 2000. Adhesion molecule cascades direct lymphocyte recirculation and leukocyte migration during inflammation. Immunol. Res. **22:**299-317.
225. **Steurbaut, S., E. Merckx, B. Rombaut, and R. Vrijsen.** 2008. Modulation of viral replication in macrophages persistently infected with the DA strain of Theiler's murine encephalomyelitis virus. Virol. J. **5:**89.
226. **Stevenson, B. R., J. M. Anderson, I. D. Braun, and M. S. Mooseker.** 1989. Phosphorylation of the tight-junction protein ZO-1 in two strains of Madin-Darby canine kidney cells which differ in transepithelial resistance. Biochem. J. **263:**597-599.
227. **Stewart, A. R., A. E. Tollefson, P. Krajcsi, S.-P. Yei, and W. S. M. Wold.** 1995. The adenovirus E3 10.4K and 14.5K proteins, which function to prevent cytolysis by tumor necrosis factor and to down-regulate the epidermal growth factor receptor, are localized in the plasma membrane. J. Virol. **69:**172-181.
228. **Stewart, P. A., and M. J. Wiley.** 1981. Developing nervous tissue induces formation of blood-brain barrier characteristics in invading endothelial cells: A study using quail--chick transplantation chimeras. Dev. Biol. **84:**183-192.
229. **Stumptner-Cuvelette, P., S. Morchoisne, M. Dugast, S. Le Gall, G. Raposo, O. Schwartz, and P. Benaroch.** 2002. HIV-1 Nef impairs MHC class II antigen presentation and surface expression. Proc. Natl. Acad. Sci. USA **98:**12144-12149.
230. **Szomolanyi-Tsuda, E., J. D. Brien, J. E. Dorgan, R. L. Garcea, R. T. Woodland, and R. M. Welsh.** 2001. Antiviral T-cell-independent type 2 antibody responses induced *in vivo* in the absence of T and NK cells. Virology **280:**160-168.
231. **Tay, C. H., and R. M. Welsh.** 1997. Distinct organ-dependent mechanisms for the control of murine cytomegalovirus infection by natural killer cells. J. Virol. **71:**267-275.
232. **Toborek, M., Y. W. Lee, G. Flora, H. Pu, I. E. Andras, E. Wylegala, B. Hennig, and A. Nath.** 2005. Mechanisms of the blood-brain barrier disruption in HIV-1 infection. Cell. Mol. Neurobiol. **25:**181-199.
233. **Tollefson, A. E., T. E. Hermiston, D. L. Lichtenstein, C. F. Colle, R. A. Tripp, T. Dimitrov, K. Toth, C. E. Wells, P. C. Doherty, and W. S. M. Wold.** 1998. Forced degradation of Fas inhibits apoptosis in adenovirus-infected cells. Nature **392:**726-730.
234. **Tollefson, A. E., A. Scaria, T. W. Hermiston, J. S. Ryerse, L. J. Wold, and W. S. Wold.** 1996. The adenovirus death protein (E3-11.6K) is required at very late stages of infection for efficient cell lysis and release of adenovirus from infected cells. J. Virol. **70:**2296-2306.

235. **Tomazin, R., J. Boname, N. R. Hedge, D. M. Lewinsohn, Y. Altshuler, T. R. Jones, P. Cresswell, J. A. Nelson, S. R. Riddell, and D. C. Johnson.** 1999. Cytomegalovirus US2 destroys two components of the MHC class II pathway, preventing recognition by CD4+ T cells. Nature Medicine **5:**1039-1043.
236. **Toth, K., K. Doronin, A. E. Tollefson, and W. S. Wold.** 2003. A multitasking oncolytic adenovirus vector. Mol. Ther. **7:**435-437.
237. **Traweger, A., R. Fuchs, I. A. Krizbai, T. M. Weiger, H. C. Bauer, and H. Bauer.** 2003. The tight junction protein ZO-2 localizes to the nucleus and interacts with the heterogeneous nuclear ribonucleoprotein scaffold attachment factor-B. J. Biol. Chem. **278:**2692-2700.
238. **Tsao, N., H. P. Hsu, C. M. Wu, C. C. Liu, and H. Y. Lei.** 2001. Tumour necrosis factor-alpha causes an increase in blood-brain barrier permeability during sepsis. J. Med. Microbiol. **50:**812-821.
239. **Tuboly, T., and E. Nagy.** 2000. Sequence analysis and deletion of porcine adenovirus serotype 5 E3 region. Virus Res. **68:**109-117.
240. **Umeda, K., T. Matsui, M. Nakayama, K. Furuse, H. Sasaki, M. Furuse, and S. Tsukita.** 2004. Establishment and characterization of cultured epithelial cells lacking expression of ZO-1. J. Biol. Chem. **279:**44785-44794.
241. **Usherwood, E. J., S. K. Meadows, S. G. Crist, S. C. Bellfy, and C. L. Sentman.** 2005. Control of murine gammaherpesvirus infection is independent of NK cells. Eur. J. Immunol. **35:**2956-2961.
242. **Vajtr, D., O. Benada, J. Kukacka, R. Prusa, L. Houstava, P. Toupalik, and R. Kizek.** 2008. Correlation of ultrastructural changes of endothelial cells and astrocytes occuring during blood brain barrier damage after traumatic brain injury with biochemical markers of BBB leakage and inflammatory response. Physiol. Res.
243. **Valle, A., C. E. Zuber, T. Defrance, O. Djossou, M. De Rie, and J. Banchereau.** 1989. Activation of human B lymphocytes through CD40 and interleukin 4. Eur. J. Immunol. **19:**1463-1467.
244. **Van Dommelen, S. L., and M. A. Degli-Esposti.** 2004. NKT cells and viral immunity. Immunol. Cell Biol. **82:**332-341.
245. **van Hinsbergh, V. W., L. Havekes, J. J. Emeis, E. van Corven, and M. Scheffer.** 1983. Low density lipoprotein metabolism by endothelial cells from human umbilical cord arteries and veins. Arteriosclerosis **3:**547-559.
246. **Veraksa, A., A. Bauer, and S. Artavanis-Tsakonas.** 2005. Analyzing protein complexes in Drosophila with tandem affinity purification-mass spectrometry. Dev. Dyn. **232:**827-834.
247. **Vorbrodt, A. W., and D. H. Dobrogowska.** 2004. Molecular anatomy of interendothelial junctions in human blood-brain barrier microvessels. Folia Histochem. Cytobiol. **42:**67-75.
248. **Vukmirica, J., P. Monzo, Y. Le Marchand-Brustel, and M. Cormont.** 2006. The Rab4A effector protein Rabip4 is involved in migration of NIH 3T3 fibroblasts. J. Biol. Chem. **281:**36360-36368.
249. **Walczak, H., and T. L. Haas.** 2008. Biochemical analysis of the native TRAIL death-inducing signaling complex. Methods Mol Biol **414:**221-39.

250. **Walls, T., A. G. Shankar, and D. Shingadia.** 2003. Adenovirus: An increasingly important pathogen in paediatric bone marrow transplant patients. Lancet Infect. Dis. **3:**79-86.
251. **Wang, B., C. Biron, J. She, K. Higgins, M.-J. Sunshine, E. Lacy, N. Lonberg, and C. Terhorst.** 1994. A block in both early T lymphocyte and natural killer cell development in transgenic mice with high-copy numbers of the human *CD3E* gene. Proc. Natl. Acad. Sci. USA **91:**9402-9406.
252. **Wang, M., C. A. Ellison, J. G. Gartner, and K. T. HayGlass.** 1998. Natural killer cell depletion fails to influence initial CD4 T cell commitment in vivo in exogenous antigen-stimulated cytokine and antibody responses. J. Immunol. **160:**1098-1105.
253. **Wang, P., J. Dai, F. Bai, K. F. Kong, S. J. Wong, R. R. Montgomery, J. A. Madri, and E. Fikrig.** 2008. Matrix metalloproteinase 9 facilitates West Nile virus entry into the brain. J. Virol. **82:**8978-8985.
254. **Wang, T., T. Town, L. Alexopoulou, J. F. Anderson, E. Fikrig, and R. A. Flavell.** 2004. Toll-like receptor 3 mediates West Nile virus entry into the brain causing lethal encephalitis. Nat Med **10:**1366-1373.
255. **Wang, X., J. Jung, M. Asahi, W. Chwang, L. Russo, M. A. Moskowitz, C. E. Dixon, M. E. Fini, and E. H. Lo.** 2000. Effects of matrix metalloproteinase-9 gene knock-out on morphological and motor outcomes after traumatic brain injury. J. Neurosci. **20:**7037-7042.
256. **Warfield, K. L., J. G. Perkins, D. L. Swenson, E. M. Deal, C. M. Bosio, M. J. Aman, W. M. Yokoyama, H. A. Young, and S. Bavari.** 2004. Role of natural killer cells in innate protection against lethal ebola virus infection. J. Exp. Med. **200:**169-179.
257. **Weinberg, J. B., D. R. Jensen, L. E. Gralinski, A. R. Lake, G. S. Stempfle, and K. R. Spindler.** 2007. Contributions of E1A to mouse adenovirus type 1 pathogenesis following intranasal inoculation. Virology **357:**54-67.
258. **Weinberg, J. B., G. S. Stempfle, J. E. Wilkinson, J. G. Younger, and K. R. Spindler.** 2005. Acute respiratory infection with mouse adenovirus type 1. Virology **340:**245-254.
259. **Weiss, J. M., S. A. Downie, W. D. Lyman, and J. W. Berman.** 1998. Astrocyte-derived monocyte-chemoattractant protein-1 directs the transmigration of leukocytes across a model of the human blood-brain barrier. J. Immunol. **161:**6896-6903.
260. **Welsh, R. M.** 1986. Regulation of virus infections by natural killer cells. A review. Nat. Immun. Cell Growth Regul. **5:**169-199.
261. **Welsh, R. M., P. L. Dundon, E. E. Eynon, J. O. Brubaker, G. C. Koo, and C. L. O'Donnell.** 1990. Demonstration of the antiviral role of natural killer cells in vivo with a natural killer cell-specific monoclonal antibody (NK1.1). Nat. Immun. Cell Growth Regul. **9:**112-120.
262. **Welsh, R. M., Jr.** 1978. Cytotoxic cells induced during lymphocytic choriomeningitis virus infection of mice. I. Characterization of natural killer cell induction. J. Exp. Med. **148:**163-181.

263. **Welsh, R. M., Jr., and R. W. Kiessling.** 1980. Natural killer cell response to lymphocytic choriomeningitis virus in beige mice. Scand. J. Immunol. **11:**363-367.
264. **Welton, A. R., E. J. Chesler, C. Sturkie, A. U. Jackson, G. N. Hirsch, and K. R. Spindler.** 2005. Identification of quantitative trait loci for susceptibility to mouse adenovirus type 1. J. Virol. **79:**11517-11522.
265. **Welton, A. R., L. E. Gralinski, and K. R. Spindler.** 2008. Mouse adenovirus infection of natural killer cell-deficient mice. Virol. **373:**163-170.
266. **Welton, A. R., and K. R. Spindler.** 2007. Capture ELISA quantitation of mouse adenovirus type 1 in infected organs. Methods. Mol. Biol. **130:**215-221.
267. **Whitton, J. L., and M. B. A. Oldstone.** 2001. The immune response to viruses, p. 285-320. *In* D. K. Knipe and P. M. Howley (ed.), Fields Virology, 4th ed, vol. 1. Lippincott Williams and Wilkins, Philadelphia.
268. **Wolburg, H., J. Neuhaus, U. Kniesel, B. Krauss, E. M. Schmid, M. Ocalan, C. Farrell, and W. Risau.** 1994. Modulation of tight junction structure in blood-brain barrier endothelial cells. Effects of tissue culture, second messengers and cocultured astrocytes. J. Cell. Sci. **107 (Pt 5):**1347-1357.
269. **Wolman, M., I. Klatzo, E. Chui, F. Wilmes, K. Nishimoto, K. Fujiwara, and M. Spatz.** 1981. Evaluation of the dye-protein tracers in pathophysiology of the blood-brain barrier. Acta. Neuropathol. **54:**55-61.
270. **Wong, D., K. Dorovini-Zis, and S. R. Vincent.** 2004. Cytokines, nitric oxide, and cGMP modulate the permeability of an in vitro model of the human blood-brain barrier. Exp. Neurol. **190:**446-455.
271. **Yamamoto, M., S. H. Ramirez, S. Sato, T. Kiyota, R. L. Cerny, K. Kaibuchi, Y. Persidsky, and T. Ikezu.** 2008. Phosphorylation of claudin-5 and occludin by rho kinase in brain endothelial cells. Am. J. Pathol. **172:**521-33.
272. **Yang, J., O. Kim, J. Wu, and Y. Qiu.** 2002. Interaction between tyrosine kinase Etk and a RUN domain- and FYVE domain-containing protein RUFY1. A possible role of ETK in regulation of vesicle trafficking. J. Biol. Chem. **277:**30219-30226.
273. **Yepes, M., M. Sandkvist, E. G. Moore, T. H. Bugge, D. K. Strickland, and D. A. Lawrence.** 2003. Tissue-type plasminogen activator induces opening of the blood-brain barrier via the LDL receptor-related protein. J. Clin. Invest. **112:**1533-1540.
274. **Yilla, M., C. Hickman, M. McGrew, E. Meade, and W. J. Bellini.** 2003. Edmonston measles virus prevents increased cell surface expression of peptide-loaded major histocompatibility complex class II proteins in human peripheral monocytes. J. Virol. **77:**9412-9421.
275. **Yokoyama, W. M.** 2005. Natural killer cell immune responses. Immunol. Res. **32:**317-325.
276. **Yokoyama, W. M., and S. Kim.** 2006. Licensing of natural killer cells by self-major histocompatibility complex class I. Immunol. Rev. **214:**143-154.
277. **Young, J. D., H. Hengartner, E. R. Podack, and Z. A. Cohn.** 1986. Purification and characterization of a cytolytic pore-forming protein from granules of cloned lymphocytes with natural killer activity. Cell **44:**849-859.

278. **Zahradnik, J. M., M. J. Spencer, and D. D. Porter.** 1980. Adenovirus infection in the immunocompromised patient. Am. J. Med. **68:**725-732.
279. **Zakhartchouk, A. N., D. L. Godson, L. A. Babiuk, and S. K. Tikoo.** 2001. 121R protein from the E3 region of bovine adenovirus-3 inhibits cytolysis of mouse cells by human tumor necrosis factor. Intervirology **44:**29-35.
280. **Zanone, M. M., E. Favaro, P. G. Conaldi, J. Greening, A. Bottelli, P. C. Perin, N. J. Klein, M. Peakman, and G. Camussi.** 2003. Persistent infection of human microvascular endothelial cells by coxsackie B viruses induces increased expression of adhesion molecules. J Immunol **171:**438-46.
281. **Zhang, L., S. Gomis, and S. K. Tikoo.** 2005. Evaluation of promoters for foreign gene expression in the E3 region of bovine adenovirus type-3. Virus Res. **110:**169-176.
282. **Zhang, Y., D. Feigenblum, and R. J. Schneider.** 1994. A late adenovirus factor induces eIF-4E dephosphorylation and inhibition of cell protein synthesis. J. Virol. **68:**7040-7050.
283. **Zhu, S., W. Wang, D. C. Clarke, and X. Liu.** 2007. Activation of Mps1 promotes transforming growth factor-beta-independent Smad signaling. J. Biol. Chem. **282:**18327-18338.
284. **Zuo, J., S. A. Stohlman, and C. C. Bergmann.** 2005. IL-15-independent antiviral function of primary and memory CD8+ T cells. Virology **331:**338-348.